

FINAL REPORT

Evaluation of Washington Hydraulic Fracture Test (SHRP) for D-Cracking Aggregate

Project IA-H2, 1995/96

Report No. ITRC FR 95/96-5

Prepared by

Co-Principal Investigators

Mohsen A. Issa, Mahmoud A. Issa, and Mark Bendok

Department of Civil and Materials Engineering

University of Illinois at Chicago

Chicago, Illinois

June 1999

Illinois Transportation Research Center
Illinois Department of Transportation

ILLINOIS TRANSPORTATION RESEARCH CENTER

This research project was sponsored by the State of Illinois, acting by and through its Department of Transportation, according to the terms of the Memorandum of Understanding established with the Illinois Transportation Research Center. The Illinois Transportation Research Center is a joint Public-Private-University cooperative transportation research unit underwritten by the Illinois Department of Transportation. The purpose of the Center is the conduct of research in all modes of transportation to provide the knowledge and technology base to improve the capacity to meet the present and future mobility needs of individuals, industry and commerce of the State of Illinois.

Research reports are published throughout the year as research projects are completed. The contents of these reports reflect the views of the authors who are responsible for the facts and the accuracy of the data presented herein. The contents do not necessarily reflect the official views or policies of the Illinois Transportation Research Center or the Illinois Department of Transportation. This report does not constitute a standard, specification, or regulation.

Neither the United States Government nor the State of Illinois endorses products or manufacturers. Trade or manufacturers' names appear in the reports solely because they are considered essential to the object of the reports.

Illinois Transportation Research Center Members

**Bradley University
DePaul University
Eastern Illinois University
Illinois Department of Transportation
Illinois Institute of Technology
Lewis University
Northern Illinois University
Northwestern University
Southern Illinois University at Carbondale
Southern Illinois University at Edwardsville
University of Illinois at Chicago
University of Illinois at Urbana-Champaign
Western Illinois University**

Reports may be obtained by writing to the administrative offices of the Illinois Transportation Research Center at 200 University Park, Edwardsville, IL 62025 [telephone (618) 650-2972], or you may contact the Engineer of Physical Research, Illinois Department of Transportation, at (217) 782-6732.

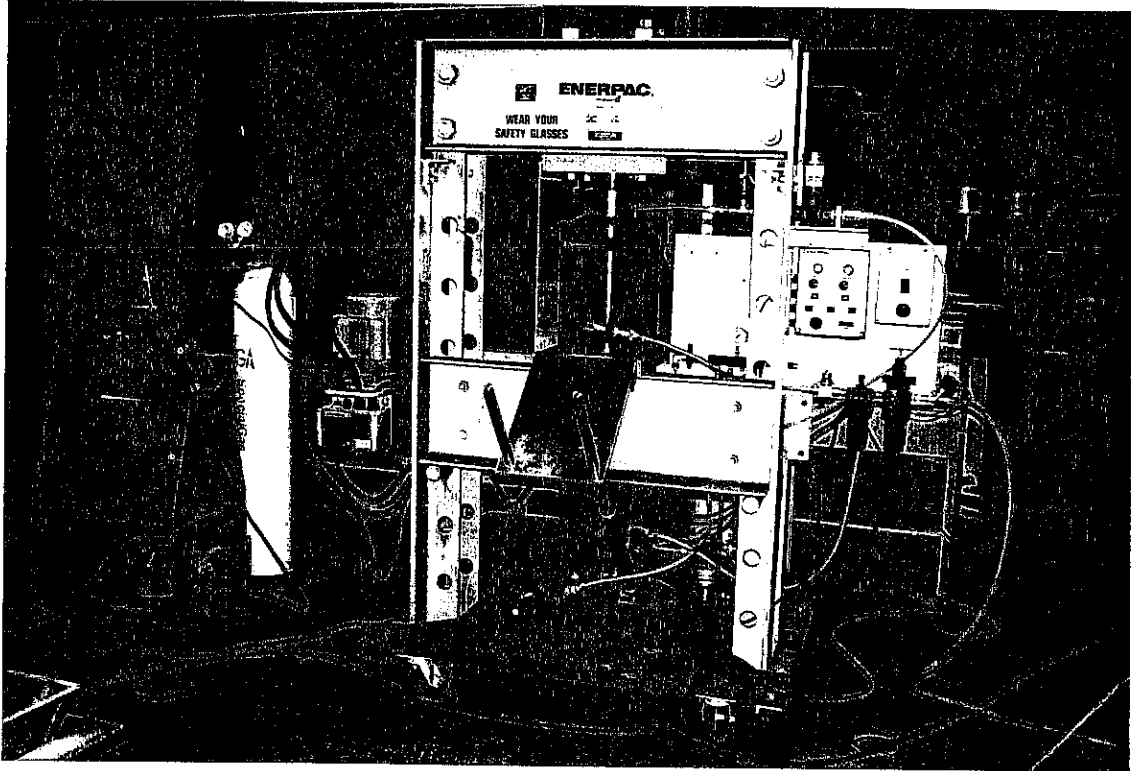
1. Report No. ITRC FR 95/96-5		2. Government Accession No.		3. Recipient's Catalog No.	
4. Title and Subtitle Evaluation of Washington Hydraulic Fracture Test (SHRP) for D-Cracking Aggregates				5. Report Date June 1999	
				6. Performing Organization Code	
				8. Performing Organization Report No.	
7. Author(s) Mohsen A. Issa, Mahmoud A. Issa, and Mark Bendok				10. Work Unit No. (TRAIS)	
9. Performing Organization Name and Address University of Illinois at Chicago Department of Civil and Materials Engineering 2095 ERF, M/C 246, 842 West Taylor Street Chicago, IL 60607				11. Contract or Grant No. IA-H2, 1995/96	
				13. Type of Report and Period Covered Final Report April 1997 through April 1999	
12. Sponsoring Agency Name and Address Illinois Transportation Research Center 200 University Park, Room 2210 Edwardsville, IL 62025				14. Sponsoring Agency Code	
				15. Supplementary Notes	
16. Abstract <p>An evaluation was funded by the Illinois Department of Transportation (ILDOT) to investigate the ability of the Washington Hydraulic Fracture Test to identify D-cracking susceptible aggregate. Two machines were used for testing: the large (WHFT 97) which was fabricated at UIC and the smaller chamber (WHFT 94). The WHFT 97 is completely automated in terms of controlling the entire testing procedure for each respective 10 cycles of operation, and requires minimal manual labor.</p> <p>Twenty-one different aggregate samples, with different degrees of freeze-thaw susceptibility, were tested according to the WHFT test procedure on both machines to establish a direct correlation, if possible, between the results of the proposed WHFT test and those reported for the ASTM C 666 Method B as modified by ILDOT. In addition, a petrographic analysis was conducted on each aggregate sample in order to determine its percentage of air voids, pore size, and pore size distribution. The pore size distribution, as well as the durability factor of all the aggregates, were also determined. Unfortunately, a comparison of WHFT to ASTM C 666 Method B (ILDOT modified) test results showed a lack of direct correlation across the vast majority of the 21 test samples. This lack of direct correlation precludes the use of the WHFT test as a direct replacement for the ASTM C 666 Method B test procedure. Since a direct correlation was not established, the test data was compared using the two test methods failure modes to establish the WHFT 97's potential as a screening test. All the aggregate types (dolomite, gravel, ACBF slag) were successfully classified using these failure modes with the exception of one aggregate type, limestone. It appears, based on this comparison, the WHFT 97 test may have the potential to be used as a screening test prior to the ASTM freeze-thaw test. In addition, the percentage of air voids test showed potential in rating limestone aggregate as to what other testing would have to be run to identify D-cracking susceptible aggregate. Additional research is recommended to increase reliability for both the WHFT 97 test as a screening procedure and use of the percentage of air voids test to identify testing necessary on limestones. A wider range of durable and non-durable sources for each aggregate type will have to be investigated.</p>					
17. Key Words D-cracking, aggregates, porosity, Washington Hydraulic Fracture test (WHFT), petrographic analysis, correlation, freeze-thaw, limestone			18. Distribution Statement No Restrictions. This document is available to the public through the National Technical Information Service (NTIS), Springfield, Virginia 22161		
19. Security Classif. (of this report) Unclassified		20. Security Classif. (of this page) Unclassified		21. No. of Pages 152	22. Price



FINAL REPORT

**EVALUATION OF WASHINGTON HYDRAULIC FRACTURE
TEST (SHRP) FOR D-CRACKING AGGREGATE**

Project IA-H2, FY 1995/6



Prepared by

**Mohsen A. Issa, Mahmoud A. Issa, and Mark Bendok
Department of Civil and Materials Engineering
University of Illinois at Chicago
Chicago, Illinois**

June 1999

**Illinois Transportation Research Center
Illinois Department of Transportation**



DISCLAIMER

This document is disseminated under the sponsorship of the Department of Transportation and Illinois Department of Transportation in the interest of information exchange. Neither the United States Government nor the State of Illinois assumes liability for its contents or use thereof. The contents of this report reflect the views of the authors who are responsible for the facts and the accuracy of the data presented herein. The contents do not necessarily reflect the policy of the Department of Transportation or the Illinois Department of Transportation. This report does not constitute a standard, specification, or regulation. Neither the United States Government nor the State of Illinois endorses products or manufacturers. Trade or manufacturers' names appear herein only because they are considered essential to the objective of this document.

CONVERSION FACTORS, US CUSTOMARY TO METRIC UNITS

Multiply	by	to obtain
in.	25.4	mm
ft	0.3048	m
in. ²	645	mm ²
yd ³	0.765	m ³
pound (lb)	4.448	newtons (N)
kip (1000 lb)	4.448	kilo newtons (kN)
kip/ft	14.59	kN/m
psi	0.0069	MPa
ksi	6.895	MPa
ft-kip	1.356	kN·m
in.-kip	0.113	kN·m

PREFACE

This study was funded by a contract awarded to the University of Illinois at Chicago (UIC) by the Illinois Transportation Research Center (ITRC) and the Illinois Department of Transportation (ILDOT). Their financial support is gratefully acknowledged. Thanks are due to the members of the Technical Review Panel, Eric Harm, William Sheftick, and Marshall Metcalf. The authors acknowledge the continuous support of Dr. Steven Hanna of ITRC.

Thanks are due to the Illinois Department of Transportation for providing the aggregate samples and for providing helpful technical information. Thanks are due to the staff at Purdue University where the mercury intrusion tests were performed. Also thanks are due to Mohamad Nagi and CTL for providing the 1994 WHFT machine for testing.

We are indebted to Dr. Chien H. Wu, Chairman of the Department of Civil and Materials Engineering at UIC for the financial support for the students working on the project. Thanks are due to John Gramsas for helping in the fabrication of the 1997 WHFT machine as well as modification and continuous maintenance of the 1994 WHFT machine. Also thanks are due to Boris Itkis for assisting in developing the controller interface. Thanks are due to Alfred Yousif and graduate students MD Shahidul Islam, Cyro Luiz Ribeiro do Valle, and Mohamad Faraj for their valuable contributions.

EXECUTIVE SUMMARY

Evaluation of Washington Hydraulic Fracture Test (SHRP) for D-cracking Aggregate

Project IA-H2, FY 1995/6

Mohsen A. Issa, Mahmoud A. Issa, and Mark Bendok

June 1999

In the Strategic Highway Research Program (SHRP) a test method, apparently capable of identifying D-cracking susceptible aggregates in approximately 8 days, was developed to replace the widely used but time-consuming Rapid Freeze-thaw test using ASTM C666 test methods. The basic assumption in this new method is that the hydraulic pressure expected in concrete aggregates during freezing and thawing can be simulated by subjecting sample aggregates, submerged in water, to high pressures and the extreme rapid release of the pressure. The percent fracture, percent mass loss, and hydraulic fracture index are the parameters calculated as a result of the test, which is commonly called the Washington Hydraulic Fracture Test (WHFT). A number of states have conducted tests using this apparatus on the same aggregate source, and have found a scatter in the results (Whiting and Nagi). These reports have prompted research on a newer modified apparatus that accounts for this variability by allowing for a larger specimen size and also introducing a computer interface to control every phase of the machine and data recording.

An evaluation was funded by the Illinois Department of Transportation (ILDOT) to investigate the ability of the Washington Hydraulic Fracture Test to identify D-cracking susceptible aggregate. Two machines were used for testing: the large (WHFT 97) which was fabricated at UIC and the smaller chamber (WHFT 94) which was provided by Construction Technology Laboratories (CTL), Skokie, Illinois. The WHFT 97 is a modified version of the WHFT 94 apparatus. The WHFT 97 is completely automated in terms of controlling the entire testing procedure for each respective 10 cycles of operation, and requires minimal manual labor. A controlled interface is connected to the machine which provides a plot of the release for each cycle, hence good quality control of the system and much better results are expected. The controller interface included data acquisition and control components of the D-cracking apparatus.

Twenty-one different aggregate samples, with different degrees of freeze-thaw susceptibility, were tested according to the WHFT test procedure on both machines to establish a direct correlation, if possible, between the results of the proposed WHFT test and those reported for the ASTM C 666 Method B as modified by ILDOT. In addition, a petrographic analysis was conducted on each aggregate sample in order to determine its percentage of air voids, pore size, and pore size distribution. The pore size distribution, as well as the durability factor of all the aggregates, were also determined by performing the mercury intrusion porosimeter test at Purdue University, Indiana.

Unfortunately, a comparison of WHFT to ASTM C 666 Method B (ILDOT modified) test results showed a lack of direct correlation across the vast majority of the 21 test samples. This lack of direct correlation precludes the use of the WHFT test as a direct replacement for the ASTM C 666 Method B test procedure.

Since a direct correlation was not established, the test data was compared using the two test methods failure modes to establish the WHFT 97's potential as a screening test. The failure criteria presented by the percent fracture (2%) from the WHFT 97 test and 0.060% maximum expansion from the ILDOT freeze-thaw test were used. This comparison indicated 67% of the test results on the WHFT 94 and 76% on the WHFT 97 are identified correctly based on the ILDOT criteria.

All the aggregate types (dolomite, gravel, ACBF slag) were successfully classified using these failure modes with the exception of one aggregate type, limestone. It appears, based on this comparison, the WHFT 97 test may have the potential to be used as a screening test prior to the ASTM freeze-thaw test. In addition, the percentage of air voids test showed potential in rating limestone aggregate as to what other testing would have to be run to identify D-cracking susceptible aggregate.

Additional research is recommended to increase reliability for both the WHFT 97 test as a screening procedure and use of the percentage of air voids test to identify testing necessary on limestones. A wider range of durable and non-durable sources for each aggregate type will have to be investigated. Accuracy of the WHFT 97 machine could possibly be enhanced by conducting additional sensitivity testing by increasing the pressurization time under each cycle and number of cycles. Other methods would look at increasing the cycle pressure, but keep the same release rate.

TABLE OF CONTENTS

	Page
PREFACE	iii
EXECUTIVE SUMMARY	iv
TABLE OF CONTENTS	vi
LIST OF TABLES	ix
LIST OF FIGURES	x
1. INTRODUCTION	1
1.1 General	1
1.2 Objectives of Study	2
2. LITERATURE REVIEW	4
3. DESIGN AND FABRICATION OF CHAMBER	14
3.1 Finite Element Analysis	14
3.2 Results	15
3.3 Chamber Testing	15
3.4 Release Valve	19
4. MERCURY INTRUSION POROSIMETRY	21
4.1 Introduction	21
4.2 Apparatus	23
4.3 Results	25

TABLE OF CONTENTS (continued)

	Page
4.3.1 Qualitative Results	25
4.3.2 Quantitative Results	26
5. PETROGRAPHIC EXAMINATION	31
5.1 Linear-Traversal Method	31
5.2 Test Results, Analysis and Discussion	32
6. TESTING PROCEDURE AND RESULTS	38
6.1 Sample Preparation	38
6.2 WHFT Formulas	40
6.3 Results and Discussion	41
6.4 Correlation Analysis	48
6.5 Repeatability of Test Results	49
6.6 Recommended Test Procedure	49
7. CONCLUSIONS AND RECOMMENDATIONS	84
7.1 Conclusions	84
7.2 Recommendations	86
REFERENCES	88
APPENDICES	
Appendix A - Petrographic Analysis	91
Results	91
CAS2000 Output	101

TABLE OF CONTENTS (continued)

	Page
Appendix B - WHFT	105
WHFT 1994	105
General Description	105
Procedure	105
Sample Preparation	105
Chamber Assembly	107
Chamber Pressurization	108
Chamber Opening	109
WHFT 1997	110
General Description	110
Data Acquisition System	110
Procedure	115
Sample Preparation	115
Chamber Assembly	115
Chamber Pressurization	116
Chamber Opening	118
Appendix C - Results	119

LIST OF TABLES

Table	Page
4.1 Pressure Increment Run by AutoPore II 9220	24
4.2 Expected Durability Factor (EDF)	27
4.3 Comparison of Dry Specific Gravities	28
4.4 Comparison of Durability Factors Obtained by Freeze and Thaw, and Mercury Intrusion Porosimeter Test	30
5.1 Percentage of Voids from Linear Traverse Method	34
5.2 Comparison of Percentage of Voids and Percent Expansion	35
6.1 Sample X-KSU ML, PF and HFI	50
6.2 X-12 Daily Data Sheet	51
6.3 WHFT 94 Mass Loss and Percent Fracture	52
6.4 WHFT 94 Individual HFI Results	54
6.5 WHFT 97 Mass Loss and Percent Fracture	56
6.6 WHFT 97 Individual HFI Results	58
6.7 WHFT 94 Average HFI Results	60
6.8 WHFT 97 Average HFI Results	62
6.9 Comparison of Durability Factors Obtained by Freeze/Thaw, WHFT 94, and WHFT 97	76
6.10 WHFT 94 Correlation Coefficients	77
6.11 WHFT 97 Correlation Coefficients	77
6.12 Relationship Between the Test Variables for WHFT 94	78
6.13 Relationship Between the Test Variables for WHFT 97	80
6.14 Expansion and Mass Loss Repeatability Test Results	82
6.15 Expansion and Percent Fracture Repeatability Test Results	83

LIST OF FIGURES

Figure	Page
3.1 Cylinder Model	16
3.2 Section Through Holes	16
3.3 Von Mises Stresses	17
3.4 Deflected Cylinder (100-1 scale)	17
3.5 Chamber Test Setup	18
3.6 Closeup of Tested Chamber	18
3.7 Comparison of Release Rates Between WHFT 94 and WHFT 97	19
3.8 Comparison of WHFT Calibration Curves	20
4.1 AutoPore II 9220	24
4.2 Pore Size Distributions of Aggregates with Different Total Intruded Pore Volume	25
4.3 Comparison of Specific Gravities	29
5.1 Number of Voids vs Void Size	36
5.2 Percentage of Voids vs Void Size	37
6.1 Comparison of Mass Loss (ML)	64
6.2 Comparison of Percent Fracture (PF)	64
6.3 WHFT 94 Mass Loss versus ASTM C666 (ILDOT Modified) Percent Expansion	65
6.4 WHFT 97 Mass Loss versus ASTM C666 (ILDOT Modified) Percent Expansion	65
6.5 WHFT 94 Percent Fracture versus ASTM C666 (ILDOT Modified) Percent Expansion	66
6.6 WHFT 97 Percent Fracture versus ASTM C666 (ILDOT Modified) Percent Expansion	66
6.7 WHFT 94 Mass Loss versus AASHTO T-104m Sodium Sulfate Soundness .	67
6.8 WHFT 97 Mass Loss versus AASHTO T-104m Sodium Sulfate Soundness .	67
6.9 WHFT 94 Percent Fracture versus AASHTO T-104m Sodium Sulfate Soundness	68
6.10 WHFT 97 Percent Fracture versus AASHTO T-104m Sodium Sulfate Soundness	68
6.11 WHFT 94 Mass Lose versus AASHTO T-96 L.A. Abrasion	69

LIST OF FIGURES

Figure		Page
6.12	WHFT 97 Mass Loss versus AASHTO T-96 L.A. Abrasion	69
6.13	WHFT 94 Percent Fracture versus AASHTO T-96 L.A. Abrasion	70
6.14	WHFT 97 Percent Fracture versus AASHTO T-96 L.A. Abrasion	70
6.15	WHFT 94 Mass Loss versus Percent Absorption	71
6.16	WHFT 97 Mass Loss versus Percent Absorption	71
6.17	WHFT 94 Percent Fracture versus Percent Absorption	72
6.18	WHFT 97 Percent Fracture versus Percent Absorption	72
6.19	WHFT 94 Mass Loss versus ASTM C457 Air Voids	73
6.20	WHFT 97 Mass Loss versus ASTM C457 Air Voids	73
6.21	WHFT 94 Percent Fracture versus ASTM C457 Air Voids	74
6.22	WHFT 97 Percent Fracture versus ASTM C457 Air Voids	74
6.23	Recommended WHFT 97 Procedure	75
B.1	WHFT 1994 Apparatus	106
B.2	WHFT 1997 Apparatus	112
B.3	Data Acquisition System	113
B.4	WHFT 1997 Setup	113
B.5	Data Acquisition Main Menu	114



1. INTRODUCTION

1.1 General

The importance of identifying D-cracking susceptible aggregates has led to a considerable number of aggregate identification test procedures. Unfortunately, the more reliable of the procedures may require 8 to 9 weeks or longer, expensive equipment, and highly skilled operators. Responding to these problems, the Strategic Highway Research Program (SHRP) developed a rapid test method for identifying aggregates susceptible to D-cracking. However, it is still necessary to identify the reliability and validity of this method.

The most commonly used method for identifying D-cracking susceptible aggregates is rapid freezing and thawing (AASHTO T-161, ASTM C 666). The method accurately identifies D-cracking susceptible aggregates. In this method, concrete prisms, or cylinders, are prepared from the coarse aggregates in question which are then cured for 14 days or longer and subjected to repeated cycles of freezing and thawing. Periodic measurements of relative dynamic modulus or length change, or both, are then made. In the State of Illinois, the test is concluded when either the specified number of cycles has been achieved (generally 300 or 350) or failure criteria has been reached, i.e., a relative dynamic modulus of 50 percent or an expansion of 0.060 percent.

The Washington Hydraulic Fracture Test reportedly enables simulation of the internal pressures that are believed to cause D-cracking susceptible aggregates. The escape path necessary for pressure dissipation could make this procedure sensitive to aggregate size, which is in agreement with field experience. The cost for special equipment is relatively low, and compared to most tests, this test is relatively fast and economical (approximately 6 to 8 days). The uniform pressure applied to individual aggregate particles within the chamber, along with standardization of the pressure and holding time, should make this test highly reproducible.

The mechanisms of D-cracking have not yet been completely clarified and they continue to be intensively studied. D-cracking can occur only when: (1) the concrete contains aggregates susceptible to D-cracking in sufficient quantity and size; (2) the concrete is exposed to sufficient moisture; and (3) the concrete is exposed to repeated cycles of freezing and thawing. To avoid D-cracking, the environment must be altered to prevent the coarse aggregates from becoming critically saturated, eliminate or reduce the number of freeze-thaw cycles, or the aggregates used in the concrete must be inherently durable [1]. The former alternative has been demonstrated not to be feasible with existing pavement designs, and no method has been found to reduce or eliminate freeze-thaw cycles, thus the use of inherently durable aggregates appears to be the only approach.

In Illinois, D-cracking is a major problem. At present, the Illinois Department of Transportation (ILDOT) tests aggregate using the procedures presented in AASHTO T-161, Method B, as modified by the department. This test determines the durability of aggregate subjected to 350 cycles of freezing and thawing, takes nine weeks to complete, and requires expensive equipment and skilled technicians. Recent attempts by eight states, including Illinois, to correlate data from the Washington Hydraulic Fracture Test with those obtained by AASHTO T-161, Method B, gave variable results. As a result, there was a need to conduct independent verification testing of the new test method to confirm its correlation with the currently specified freeze-thaw test method.

1.2 Objectives of Study

Except in extreme cases, very rapid tests frequently do not provide a sound basis for accepting or rejecting aggregates with respect to their freeze-thaw susceptibility. The question of whether an aggregate will perform satisfactorily under specific conditions in the field must be answered by field experience or by a laboratory test that closely simulates the anticipated conditions of field exposure.

The main objective of the study was to develop a new Washington Hydraulic Fracture Test apparatus that incorporates better features including an automated controller for the machine in order to make the results more reliable. The objectives included:

1. Determine if the test results from the Washington Hydraulic Fracture Tests (SHRP) can be correlated with the Illinois Department of Transportation (ILDOT) modified version of AASHTO T-161, Method B, to identify aggregates that are susceptible to D-cracking.
2. Recommend whether and how the Washington Hydraulic Fracture Test (SHRP) can be incorporated in ILDOT's testing procedure for concrete aggregates.

These objectives were carried out by the following methodology:

1. Conducting a literature review with respect to the various factors affecting D-cracking.
2. Design and construct the new chamber.
3. Conduct the mercury porosity intrusion test as well as the petrographic analysis.
4. Test the aggregate samples provided by ILDOT using both the 1994 and 1997 WHFT machines.
5. Analyzing the results in terms of all the factors affecting the identification of D-cracking susceptible aggregates.

2. LITERATURE REVIEW

A comprehensive literature review was conducted with respect to D-cracking. The collection process included the review of published and unpublished papers as well as reports related to relevant studies conducted through various agencies such as the U.S. Departments of Transportation, Federal Highway Administration, National Cooperative Highway Research Program, Transportation Research Board, and Strategic Highway Research Program. The focus of the research was to investigate the different methods used in determining the susceptibility of aggregates to D-cracking. Although D-cracking is influenced by many factors, the main cause of the distress is the coarse aggregates. The properties of interest in investigating the aggregates were linear expansion, volumetric expansion, permeability, pore size, pore size distribution, porosity, absorption, adsorption, critical saturation, capillarity, specific gravity, critical size, tensile strength, stress-strain-time characteristics, and thermal characteristics.

D-cracking is one of the most serious durability problems of concrete pavements in freeze/thaw climates. Previous research has indicated that the cause of D-cracking is not based on a single aggregate property but rather on a combination of properties. Coarse aggregates have long been recognized as a potential source of deterioration for concrete exposed to freezing and thawing. In general, carbonate aggregates are the most susceptible, with calcitic limestone being far more susceptible than dolomites. Furthermore, the larger the maximum aggregate size, the greater the susceptibility to D-cracking. Moisture and drainage are also important factors, where deterioration of pavements is more pronounced in poorly drained areas such as the inside of superelevated curves, wide flat airplane parking aprons, etc. Climate is also a factor, where the greater the number of freeze-thaw cycles, the greater the rate of deterioration. Other factors which may contribute to D-cracking include type of subgrade soil, type of fine aggregates, type of cement, concrete component properties, quality of concrete, pavement thickness, method of curing, weather conditions during construction, and traffic and loading conditions. These additional factors have been reported to be

insignificant with respect to D-cracking [2].

In order to minimize damage of concrete due to freeze-thaw susceptible aggregates, extensive research has been conducted in the past to identify those aggregates potentially deleterious by studying their chemical and physical properties. Primary considerations in the selection of materials for coarse aggregates are those pertaining to freeze-thaw durability and the development of D-cracking in highway and airfield pavements. Two aspects of the problem are of particular importance: moisture movements and critical saturation of the aggregates, and the response of the aggregates to cyclic freezing and thawing in concrete.

D-cracking is the term used to describe the distress in concrete that results from the disintegration of saturated coarse aggregates after being subjected to repeated cycles of freezing and thawing. Internal stresses are developed because freezing free water expands in volume by approximately 9 percent. Expanding ice, however, is not the major agent of disintegration. The major agent of disintegration is hydraulic pressure produced by water attempting to leave the frozen zone. It is difficult to control this type of damage for 2 reasons: first, the concrete does not dry because it is often covered with snow or ice, and secondly, the freeze-thaw cycle is repeated throughout the winter. Deicing salts are very helpful in maintaining traffic and improving safety under winter driving conditions, however, salt probably changes the freezing point of the water in the aggregate pore system and this has greater effect on D-cracking.

The complete interrelationship of the variables affecting the performance of aggregates in concrete has resulted in a variety of national tests that tend to provide a somewhat reliable means of separating durable and non-durable paving aggregates. The applicable test method developed to date can be divided into two primary groups. The first group consists of tests that attempt to simulate the environmental conditions to which the concrete aggregate is exposed. The most common environmental simulation test are the Sodium Sulfate Soundness, Rapid Freezing and Thawing, Powers Slow Cool, and Unconfined Aggregate Freezing and Thawing. The other group

consists of tests that correlate aggregate properties with known field performance and/or results from environmental tests. The most common of these tests are the Mercury Intrusion, Iowa Pore Index, Absorption-Adsorption, Freeze Thaw Soundness Test, and Petrographic Analysis. The difficulty lies in the fact that only the ASTM C666 method might give a universal durability factor for each concrete composition, since the way of concreting and different environmental conditions vary in practice.

The choice of the best method depends on the type of structure or structural elements and exposure conditions. The degree of damage due to freeze-thaw can mainly be measured by changes in strength, residual stresses, changes in weight or appearance, modulus of elasticity, etc. If the mechanical properties are not degraded over 25% according to the standard, the concrete is considered to be resistant to freeze/thaw. If good concrete freezes in the air and thaws under the water, several hundred cycles are necessary for the first signs of damage to appear.

Aggregate occupies about 70 percent of the concrete's volume. Consequently, the concrete's properties are significantly influenced by the aggregate's characteristics. Pore characteristics of aggregates have a profound effect on the performance of concrete exposed to freezing and thawing. The characteristics of the pores not only determines how much water the aggregates within the concrete will contain, but perhaps of more importance, it determines how that water is distributed within the aggregates. The size of the pores also determines how easily the aggregates will be filled with water and if such pores become filled with water, how easily a particular degree of saturation can be maintained. Hence, pore characteristics determine the flow of moisture into and out of an aggregate, its water retentivity, and the development of pressure during a freezing and thawing cycle.

Rhoades and Mielenz [3] asserted that aggregates' pore characteristics are important in controlling chemical and physical stability, and they strongly influence the bond with concrete. They significantly affect the strength of the material and determine absorption and permeability. Thus, pore characteristics control durability under freezing and thawing conditions and the rate of

chemical alteration.

A study by Sweet [4] indicated that critical pore size for freezing and thawing durability for limestone aggregates may be about 5 micron. Later research by Schuster and McLaughlin [5] showed that the significance of 5 micron pores is questionable: the freeze-thaw durability of concrete containing chert is apparently not as dependent on pores in chert less than 5 micron in diameter as has been postulated by Sweet. Due to these conflicting conclusions, it seemed desirable to make a more thorough research of the relationships of pore characteristics as determined from total porosity and pore size distribution measurements, with concrete durability when exposed to freezing and thawing.

Kaneuji et al. [6] investigated the relationship between the freeze/thaw durability of coarse aggregates and their pore structures. The pore size distributions of 14 different types of aggregates were determined by mercury intrusion and they were then compared to the durability factor derived from standard laboratory freeze/thaw test. They concluded that at constant total pore volume, smaller pore size yields lower durability. The reason is that the aggregates with smaller pores acquires water slower but retains it longer and hence will be likely to fail when frozen. Total pore volume is also important to the durability of an aggregate. They found that a greater pore volume of the same pore size results in less durable concrete. Lewis and Dolch [7] concluded from their experimental study that a harmful pore size is that which is sufficiently large to permit water to readily enter much of the pore space, but not large enough to permit easy drainage. Hiltrop and Lemish [8] concluded that shape of the pore size distribution curve alone does not indicate whether or not a specimen will pass freezing and thawing tests.

Gonnerman and Ward [9] reported that the disruptive action of the sulfate soundness tests on unconfined aggregates may not be representative of aggregates that are confined. The confining nature of the mortar in concrete, for example, is important in determining the rate and amount of moisture movement into and out of the aggregates. Therefore, the durability of concrete aggregates

cannot always be correlated with the durability of the concrete in which these aggregates are embedded. ILDOT evaluation indicates that aggregates that fail the soundness test fail the freeze-thaw tests. However, that fact is not accountable with respect to aggregates passing the sulfate soundness test.

Some states frequently use the petrographic analysis in special investigations for studying aggregates. Petrographic examination is the visual examination and analysis of aggregates in terms of both lithology and individual particle properties. This analysis requires the skills of a well-trained and experienced petrographer. The examination uses small sample sizes, thereby requiring a large amount of work to provide accurate results. Also, the analysis procedure does not provide definite specification limits because information obtained is the result of subjective appraisal by the petrographer and can be reduced to a numerical quantity only through personal interpretation.

Domaschuk et al. [2] conducted a study on D-cracking of concrete pavements in Manitoba, Canada. They noticed the severity of aggregates of size 40 mm on D-cracking. They concluded that according to the freeze and thaw test (ASTM 666B), reducing the top size of the aggregate from 40 to 20 mm rendered the aggregate non-susceptible to D-cracking.

Stark and Klieger [10] carried out a survey and experiments on aggregates obtained from 15 sources. The survey results indicated that D-cracking was apparent at the joint intersections where the large aggregates were used, whereas, in the section with the small size, D-cracking was not visible at the wearing surface. The principal finding of their research was that decreasing the maximum particle size from 38 to 25 and 13 mm (1.5 to 1 and 0.5 in.) progressively reduced expansion as much as two to four times.

D-cracking has been observed for years in Illinois but had not been considered a serious problem until 1978 [11]. In that year, two sections of D-cracked interstate pavement had deteriorated seriously and required immediate rehabilitation. As a result of these failures, the Illinois

Department of Transportation (ILDOT) initiated a program to identify the degree in which the various aggregate sources in Illinois were vulnerable to the distress, and eliminate the use of D-cracking susceptible aggregate. A statewide survey was scheduled to determine the extent and severity of D-cracking. A simple rating scale of zero (no D-cracking) to three (severe D-cracking) was used. Photographs depicting the distress at various stages of development were used to standardize the rating. The survey covered more than 3000 miles of pavement and showed that D-cracking was present in all areas of the state. Only 42 % of the mileage surveyed were free of D-cracking, while 40% had low-level D-cracking, 12% had intermediate-level D-cracking, and 6% was severely D-cracked.

Illinois has aggregate sources of which 137 are classified crushed-stone and 94 as gravel sources. The other sources have been rejected on the basis of Los Angeles abrasion test, NaSO_4 soundness, or deleterious count. In 1979, both the freeze-thaw and Iowa pore index tests were selected for use in the evaluation, and the necessary equipment was obtained. The Iowa pore index test (IPIT) measures certain characteristics of an aggregate pore structure. Nine kg (22 lb) of washed, oven dried aggregate was placed in the bottom of an air-entrainment pot. The bottom of the tube was open to the inside of the pot, and the top was connected to an air pressure source. After the top assembly had been securely fastened in place, water was introduced onto the bottom of the pot. The water first filled the spaces among the aggregates and then rose to an established mark on the tube. The system was then sealed and 241 kPa (35 psi) of air was applied. This increase in pressure forced the water into the pores of the aggregate, causing the column of water to fall, rapidly at first, and then slowly stabilized. The height of water in the tube was observed, and readings were taken after 30 seconds, 1, 2, 5, 10, and 15 minutes. The pore index is the volume of water that is forced into the aggregate during the time interval from 1 to 15 minutes after the air pressure is activated. A high pore index indicates a non-durable aggregate.

There were some obvious problems with using the Iowa pore index test for predicting performance. This test did not appear useful for gravel, and could not indicate to what extent a

reduction in top size would improve performance. Therefore, ILDOT concentrated on testing all their aggregates by using the freeze-thaw cabinets meeting ASTM C666 requirements. In this Illinois modified test method, concrete prisms or cylinders were prepared from the coarse aggregates in question. They were then cured for 14 days or longer and subjected to repeated cycles of freezing and thawing (Method B). Periodic measurements of the length change were then made. The test was concluded when either the specified number of cycles was achieved (generally 300 or 350 cycles). The failure criteria used is an expansion of 0.060 percent. Freezing and thawing tests of concrete (AASHTO T-161, ASTM C 666) currently comprise an excellent and accurate laboratory mean of evaluating the frost resistance of aggregates. Unfortunately, this most reliable procedure may require 8 to 9 weeks or longer, expensive equipment, and highly skilled operators.

In response to this problem, the Strategic Highway Research Program (SHRP) developed a rapid test method, "The Washington Hydraulic Fracture Test (WHFT)," for identifying aggregates susceptible to D-cracking. The WHFT's basic assumption is that the hydraulic pressure expected in concrete aggregates during freezing and thawing can be simulated by subjecting sample aggregates, submersed in water, to high negative pressures. As the external chamber pressure increases, the water penetrates into smaller and smaller pores. If the pressure is suddenly released, the air compressed within any pores will push the water back out, thereby simulating the hydraulic pressures generated during freezing. Fracturing of the aggregates should occur if the pressure in the pores cannot be dissipated quickly and the aggregates are unable to elastically accommodate the high internal pressure [12]. It requires only 8 working days (2 days for sample preparation, 5 days for testing, 1 day for final drying and aggregate piece counting) to complete the entire test. The cost for special equipment is relatively low. A number of states have conducted tests using this apparatus on the same aggregate source, and have found a scatter in the results [13]. These reports have prompted research on a newer modified apparatus that accounts for this variability by allowing for a larger specimen size and also introducing a computer interface to control every phase of the machine and data recording.

However, it is still necessary to identify the reliability of this method for future implications and to confirm its correlation with the currently specified freeze thaw test method. Research is needed to validate the procedure for a larger number of aggregates to determine pass or fail criteria (such as the number of cycles required to produce fracturing of 10 percent, or the total amount of fracturing produced at the end of 50 cycles), and to develop precision statements. It is also necessary to check whether the criteria defined as the aggregates with a Hydraulic Fracture Index (HFI) of more than 200 indicates a non susceptible to D-cracking aggregate is valid.

Alford and Janssen [14] carried out an experimental study to investigate the parameters affecting the WHFT mechanism. They concluded that the amount of fracturing produced was sensitive to both pressure release rate at short time duration (typically less than 0.02 seconds) and initial chamber pressure. Pressure release rates were determined from pressure-time histories and the amount of fracturing produced was compared. The researchers encountered a problem with the maintenance of the pressure-release valve. In order to overcome this problem, they added an electro-pneumatic actuator to the pressure release valve of the upgraded original apparatus. This addition dramatically increased the release rate due to the actuated valve being able to open much faster than a hand manual valve. Though there is no clear relation between release rate and percent fracture, release rates of 224,000 kPa/sec (32,510 psi/sec) and above produce a quite consistent percentage of fractures. A maximum rate and associated time duration to avoid excessive fracturing have yet to be determined.

Since the WHFT procedure is very sensitive to pressure release rates at short duration, a minimum rate of 300,000 kPa/sec (43,540 psi/sec) at a duration of 0.01 seconds has been proposed as an initial calibration standard. It is suggested that the following 3 important parameters be used to best describe the aggregate quality:

1. Percent Fracture (PF)
2. Percent Mass Loss (PML)
3. Hydraulic Fracture Index (HFI)

Janssen and Almond [15, 16] found in their experimental research that as the size of the material tested decreased, the percentage of fractures decreased. This is expected, since the length of the pores in the smaller material should have been much shorter than that in the larger material, providing a shorter path for the release of hydraulic pressure. They compared 4 aggregates using the Washington Hydraulic Fracture Test (WHFT). They found that the WHFT produces fracturing in aggregates and produces substantially more fracturing in aggregates susceptible to D-cracking than in aggregates not susceptible to D-cracking. They also found that the procedure is not limited to relatively uniform aggregates, such as crushed limestone, but is also applicable to materials such as gravel from glaciated regions. The promising results from the tests of diverse aggregates supported the validity of the mechanism used in the test procedure. They noticed that the major shortcoming of the test procedure is its inability to deal with rapidly absorbing aggregates. In order to overcome this problem, they suggested using a water-soluble, silane based sealer. A solution of alkylalloxysilane in water (referred to as silane solution) treatment makes the aggregates hydrophobic. The assumed effect of the sealer treatment in reducing the surface tension absorption of water into the aggregate pores appears to allow the pressurization mechanism to function properly.

Janssen and Snyder [17] also found that some aggregates absorb water at a very rapid rate, which prevents them from fracturing and affects the test output. Hence, the aggregates must be treated with silane solution to make them hydrophobic, thereby reducing the effect of absorption rate on the WHFT test results. This treatment has been demonstrated to have no effect on the hydraulic fracture performance of aggregates with slower absorption rates.

Winslow [18] carried out tests on six Indiana aggregates in order to investigate the effect of the rate of absorption of aggregates. It was found that the rate of absorption varied greatly from rock to rock, and aggregates with larger pore diameters absorbed more rapidly. He concluded that there is absolutely no correlation between initial rate of water uptake and resistance to D-cracking, although durable aggregates take in water slowly and non-durable ones take it rapidly. His finding contradicts that of Janssen and Snyder.

Hossain and Zubery [19] carried out the WHFT test using the following test parameters:

- Aggregate size range: 19 to 13 mm, 13 to 9.5 mm
- Aggregate pretreatment: Silane
- Chamber pressure: 7240 kPa (1050 psi)
- Air pressure: 483 kPa (70 psi)
- Pressure duration: 23 min. (1 cycle, 5 min. + 9 cycles, 2 min. each)
- Number of cycles: 50 (maximum)

They found that if 5% or more fracture was used as the failure criteria, then 14 out of 32 aggregates (only 44%) were identified correctly with respect to the Kansas Department of Transportation (KDOT) criteria. On the other hand, if 3% or more fracture is used as the failure criteria, then 18 out of 32 aggregates (56%) were identified correctly with respect to the KDOT criteria. They calculated HFI values based on 5% fracture, although the proposed procedure by Janssen used 10% fracture as the basis for computation of the HFI parameter. Since the percent of fracture in their test rarely exceeded 5%, they used 5% as the threshold percentage for the fracture based on Janssen's later recommendation. The pressure they used was also lower. The main drawback of their test was that since the apparatus used was not accompanied by any device to measure the pressure release rate, the effect of pressure release rate could not be evaluated. In their test, they used air pressure to control the chamber pressure release rate. They reported that slower release lowers the pressure release rate, which in turn reduces the percent fracture. Their results indicated that increasing the number of cycles did not make much of a difference in the percent fracture produced, but increasing the pressure duration and chamber pressure produced a higher fracture percent. They encountered frequent problems during testing with the release of pressure from the chamber after the pressurization cycles. They also could not ensure complete removal of the air bubbles trapped in the chamber during the water filling process.

3. DESIGN AND FABRICATION OF CHAMBER

The Washington Hydraulic Fracture Test (WHFT 97) is a modified version of the 1994 apparatus (Fig. C.2). It contains the following changes to facilitate the operation of this test: (1) WHFT 97 has a larger chamber with a 254 mm (10 in.) inside diameter and a 28.6 cm (11¼ in.) height. (2) Operator and handling time is reduced by using pressure to hold the chamber lid down instead of 16 high strength bolts. (3) Air driven water is used instead of the Nitrogen gas to pressurize the chamber. (4) The machine is fully automated in terms of controlling the entire testing procedure for each respective 10 cycles of operation. (5) It has a more accurate controlled release rate. (6) A controlled interface is connected to the machine that reads pressure and temperature, hence good quality control of the system and much better results are expected. (7) The controller interface provides a plot of the release for each cycle.

Prior to fabricating the chamber, stress analysis was performed to determine the adequacy of the design. This was performed through the finite element method presented below. Details of the testing apparatus are presented in the appendices.

3.1 Finite Element Analysis

The purpose of this analysis was to determine the level of stress experienced in the vicinity or at the hole by applying a 15160 kPa (2200 psi) hydrostatic pressure on the internal surfaces of the cylinder, as well as on the internal surfaces of the openings. The stress analysis consisted of modeling the aluminum cylinder by using the finite element package "ALGOR." In order to predict the stress level and stress distribution across the thickness of the cylinder wall, three dimensional eight noded brick elements were used.

Model Geometry

Height	=	28.6 cm (11¼ in.)
Inside Diameter	=	25.4 cm (10 in.)
Outside Diameter	=	30.5 cm (12 in.)
Wall Thickness	=	2.54 cm (1 in.)
One Hole, Diameter	=	1.5 cm (0.60 in.)
Two Holes, Diameter	=	1.3 cm (0.50 in.)

Material Properties

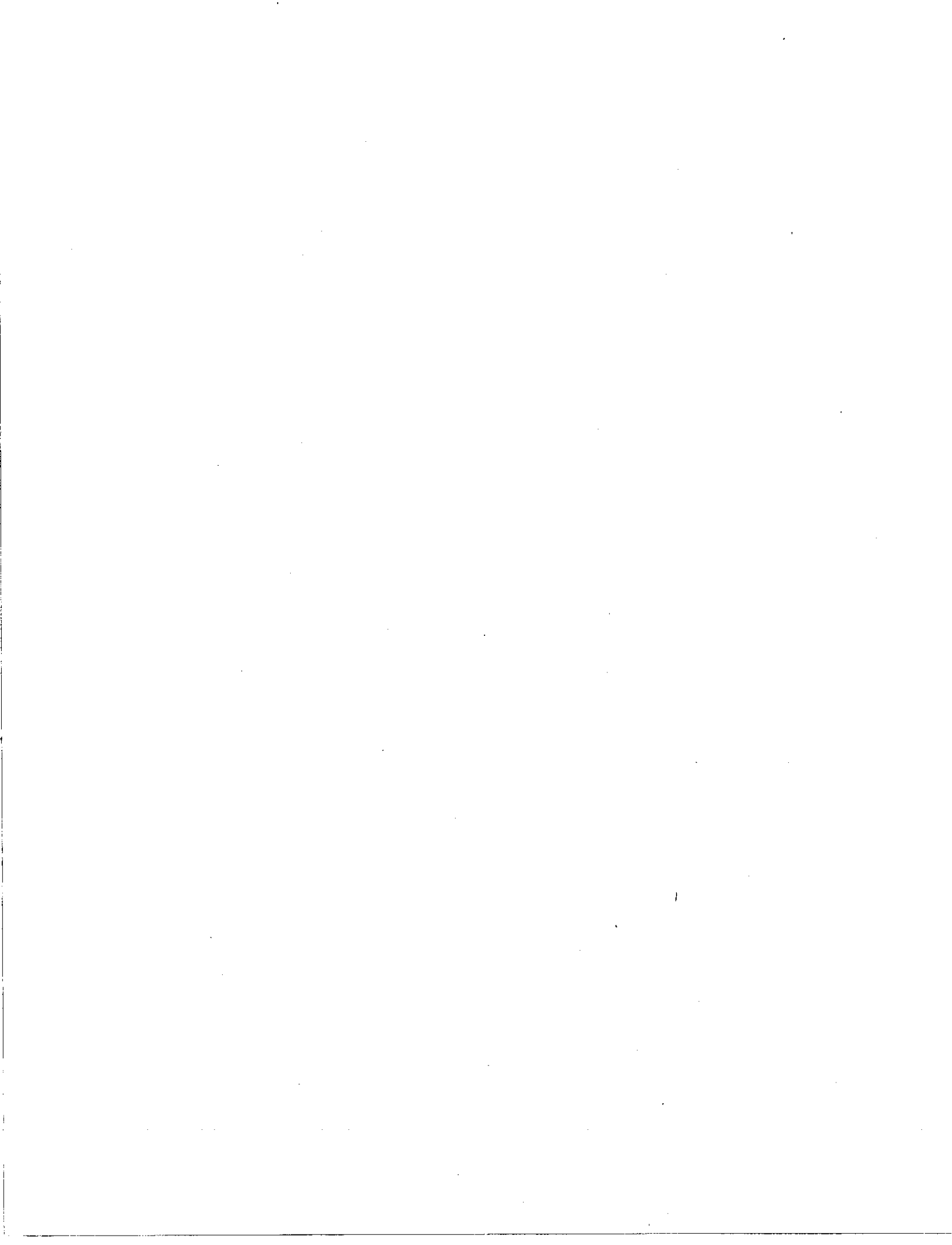
Material	=	6061-T6 Aluminum Alloy
Modulus of Elasticity	=	68900 MPa (10,000 ksi)
Density	=	0.026 N/cm ³ (0.096 lb/in ³)
Poisson's Ratio	=	0.33
Yield Stress	=	276 MPa (40.0 ksi)
Ultimate Stress	=	303 MPa (44.0 ksi)

3.2 Results

The most widely used failure criteria for ductile materials is Von Mises. Therefore, the results of Von Mises stresses for the modeled aluminum cylinder were studied carefully and compared with the allowable stresses to serve as a useful guide in the evaluation to assure safety. The resulting maximum value of Von Mises stress was 200 MPa (29 ksi), which was found in the vicinity of the holes (see Figs. 3.1 through 3.4).

3.3 Chamber Testing

After the chamber was fabricated, an actual compression test was conducted on it using a 1792 kN (400,000 lb) capacity Tinius Olsen Machine. The chamber was internally pressurized with Nitrogen gas up to 15160 kPa (2200 psi), and externally loaded to keep the lid on top of the chamber. This experimental test showed that the chamber was able to resist these loads with no visible deflection or damage. Figs. 3.5 and 3.6 depict the actual testing.



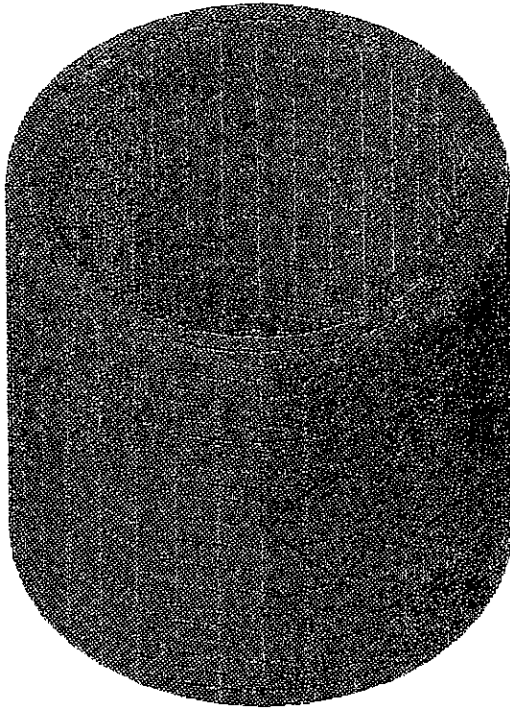


Fig. 3.1 Cylinder Model

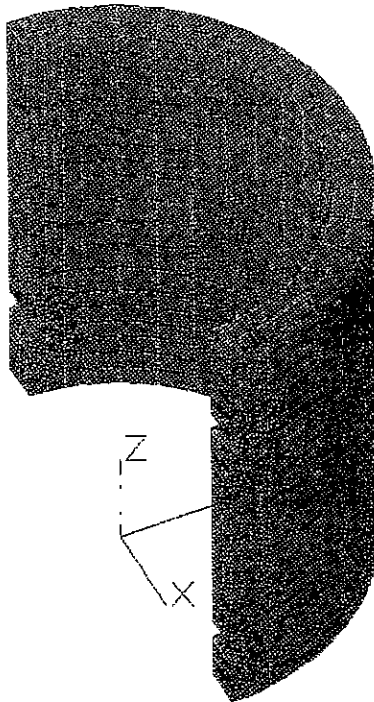


Fig. 3.2 Section Through Holes



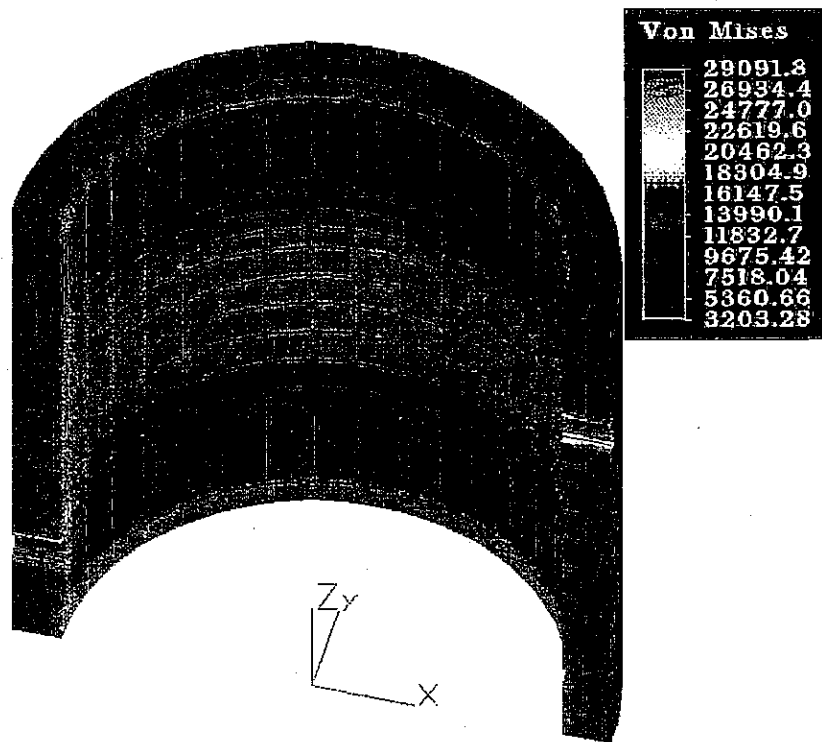


Fig. 3.3 Von Mises Stresses

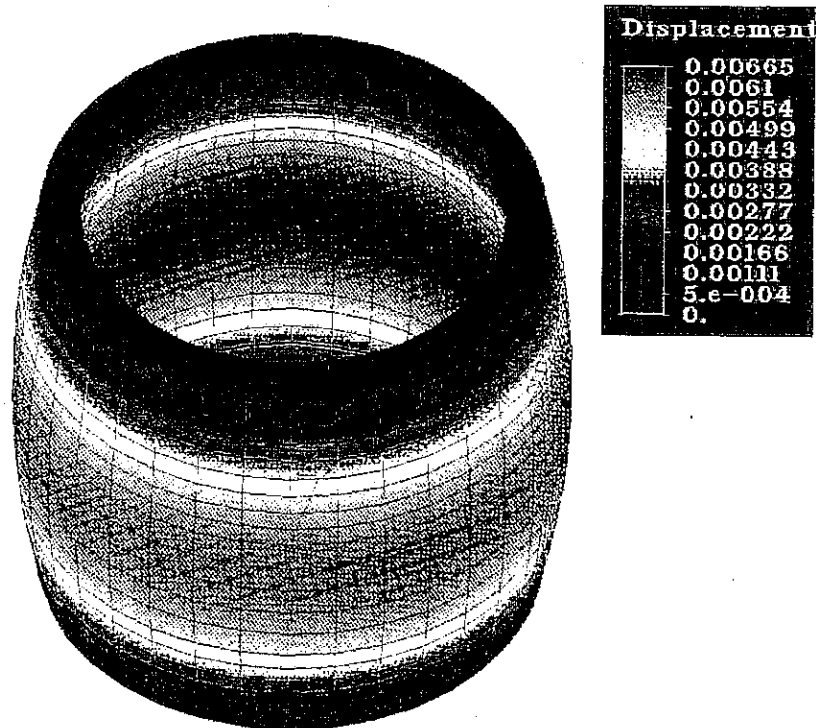


Fig. 3.4 Deflected Cylinder (100-1 scale)

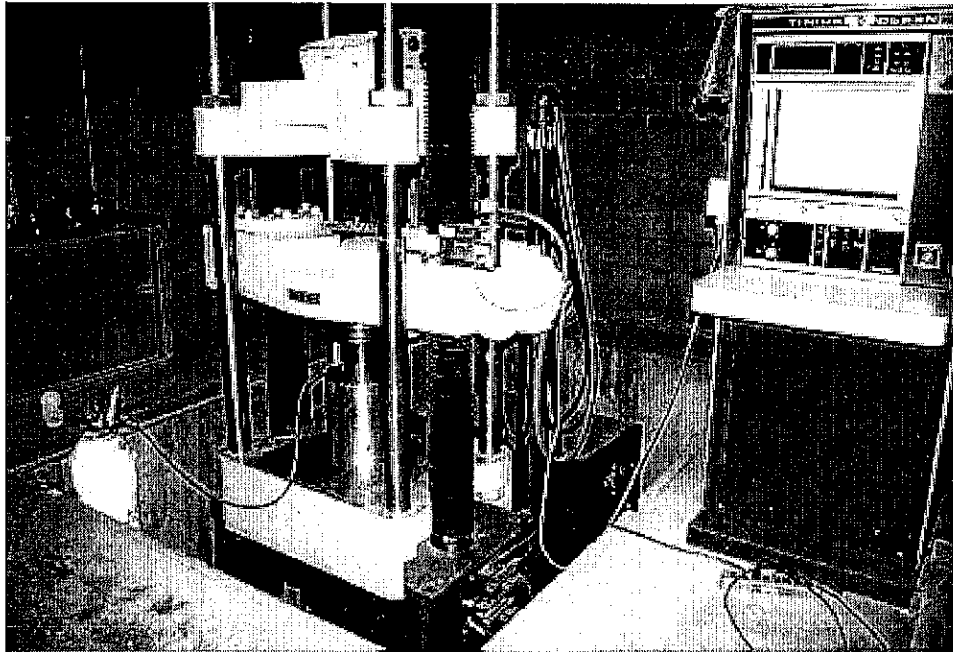


Fig. 3.5 Chamber Test Setup

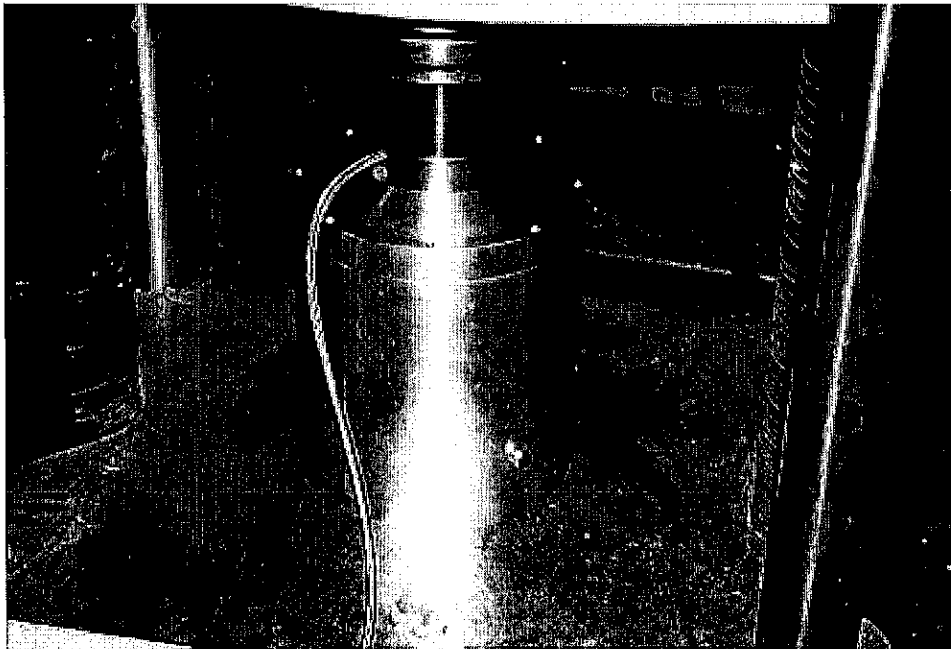


Fig. 3.6 Closeup of Tested Chamber

3.4 Release Valve

As mentioned in the literature review, the WHFT is very sensitive to pressure release rate. As a result, a solenoid valve was added that automatically opened when the pressure was released. For calibration purposes, Fig. 3.7 presents a comparison of pressure versus time at release between the WHFT 94 and WHFT 97 machines. Clearly, the required release rate was successfully achieved on the WHFT 97 apparatus. Fig. 3.8 is a plot of the pressure release rate versus time duration for both machines. They are also compared to the WHFT calibration provided with the WHFT 94 apparatus when it was received. It is evident that both machines are well calibrated.

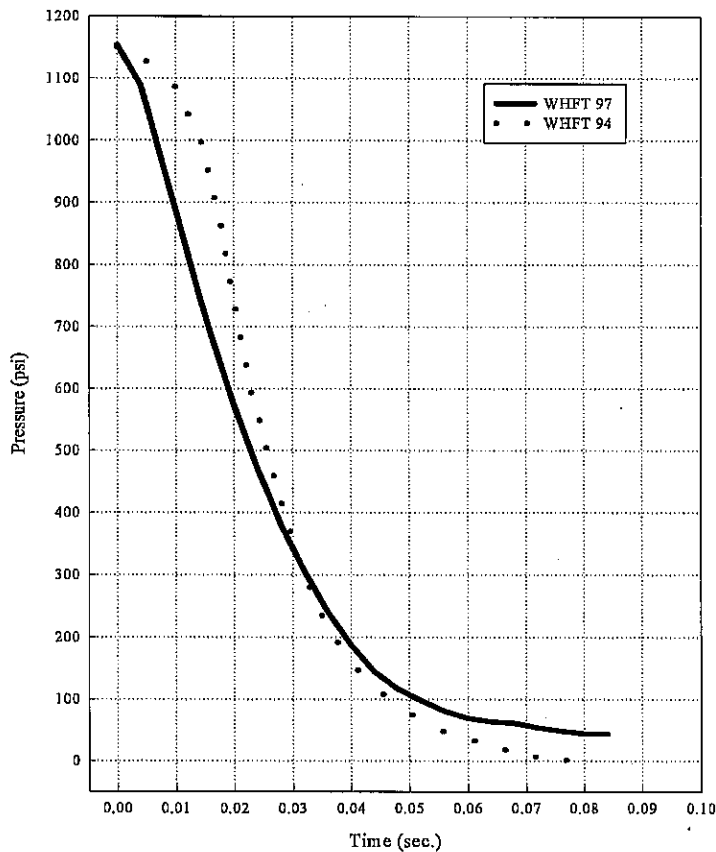


Fig. 3.7 Comparison of Release Rates Between WHFT 94 and WHFT 97

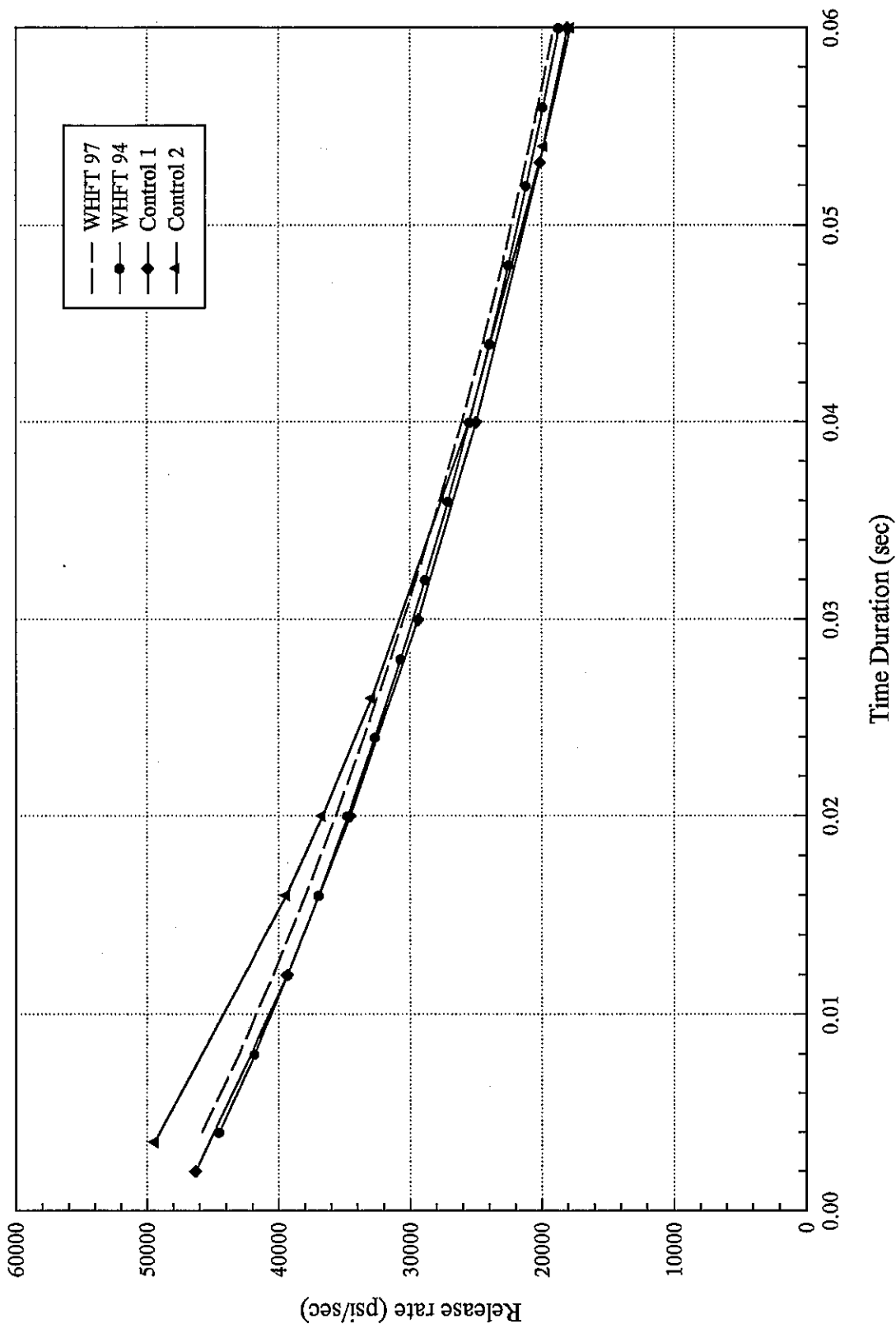


Fig. 3.8 Comparison of WHFT Calibration Curves

4. MERCURY INTRUSION POROSIMETRY

The objective of the Mercury Intrusion Porosimeter (MIP) test was to determine the total volume and volume distribution of pores in the aggregate samples with respect to the apparent diameter of the entrances of the pores. This test was conducted at Purdue University, Indiana.

4.1 Introduction

The properties of man-made and natural materials are dependent on total pore volume and the distribution of pore sizes within their structure. Mercury intrusion porosimetry (MIP) is a tool for assessing the behavior of these materials. Measurements of pore size, volume, and distribution define more precisely the material surface available for chemical and physical reactions.

No other technique yields as much information as rapidly with so little sample preparation as MIP. This tool has become increasingly important because of two factors: it can be applied to an immense variety of materials, and accurate data can be obtained with great speed. The many applications for MIP include rocks and ores, minerals, cement, bricks, construction and building materials. However, the relatively small amount of material used in this test is questionable in terms of accurately predicting the durability of aggregates.

In addition to pore size, volume, and distribution, such properties as bulk and apparent densities, pore surface area, and particle size can also be determined by porosimetry. These data correlate well with data obtained using other techniques.

The surface tension of a non-wetting liquid (a liquid that forms a contact angle of at least 90 degrees with a solid) prevents it from entering a pore. This phenomenon is called capillary depression. By applying pressure to the liquid, this opposition can be overcome, and the liquid will enter the pore. The pressure required to force a non-wetting liquid into a pore is a function of the

surface properties of the liquid and solid involved, and of the pore geometry. The size of the pore intruded is inversely proportional to the pressure.

Mercury is an ideal liquid because it has a low vapor pressure, and it neither wets nor reacts with most materials. Where mercury does wet or react with a material's surface (i.e., amalgamates with a clean metallic surface of gold, silver, or copper) this method is not applicable [20]. Pore diameter and volume data are obtained from the equilibrium pressures and volume of mercury intruded into given size pores. This relationship between pore diameter and pressure is called the Young-Laplace or Washburn equation:

$$D = \frac{-4\gamma\cos\theta}{P}$$

where: D = diameter of the pore
 P = external pressure
 γ = surface energy of the liquid
 θ = contact angle between the liquid and solid

The surface tension, γ , and the interfacial contact angle, θ , of mercury are assumed to remain unchanged during an analysis, and therefore make the numerator of the Washburn equation a constant. Therefore the relationship between the pressure and the pore diameter becomes a linear inverse. Although the mercury contact angle can vary between 110° and 160° for a variety of materials, a fixed value of 130° or 140° is typically used.

The total volume of mercury intruded at a given pressure, P , corresponds to the total volume of pores of the specific radius, r . Thus, by successively applying a series of increasing pressures and measuring the volumes of intruded mercury over the range of pressure applied, a pore-size distribution in the material can be obtained.

4.2 Apparatus

The AutoPore II 9220 machine (Fig. 4.1) measures the volume distribution of pores in materials by mercury intrusion and extrusion. As mentioned earlier, mercury has a high surface tension and is non-wetting to all materials with the exception of a few noble metals. These properties cause a mercury surface in contact with a solid to assume the minimum surface area and largest radius of curvature possible at a given pressure. An increase in the pressure on the mercury shifts the balance between surface tension and surface area, causing the radius of curvature of the mercury drop containing the surface of the solid to become smaller. When the radius of curvature is equal to that of a pore entrance, mercury fills the volume within the pore.

The AutoPore II 9220 features automatic, microprocessor-controlled operation to 414 MPa (60,000 psi) with automatic data acquisition, reduction, and printout. It produces pore volume and pore size distribution measurements of porous materials for pore sizes nominally from 360 to 0.003 μm diameter, with intrusion volume up to 1.8 cc (0.11 in³) It accommodates any size sample up to a volume of 15 cc (0.92 in³) in a solid penetrometer, e.g., a 25.4 mm (1 in.) diameter x 25.4 mm (1 in.) long cylinder.

Table 4.1 Pressure Increment Run by AutoPore II 9220

Increment	Pressure (psia)	Increment	Pressure (psia)	Increment	Pressure (psia)
1	0.8	8	90	15	4000
2	1.6	9	150	16	7000
3	3	10	250	17	12000
4	6	11	450	18	20000
5	12	12	800	19	30000
6	25	13	1300	20	60000
7	50	14	2300		

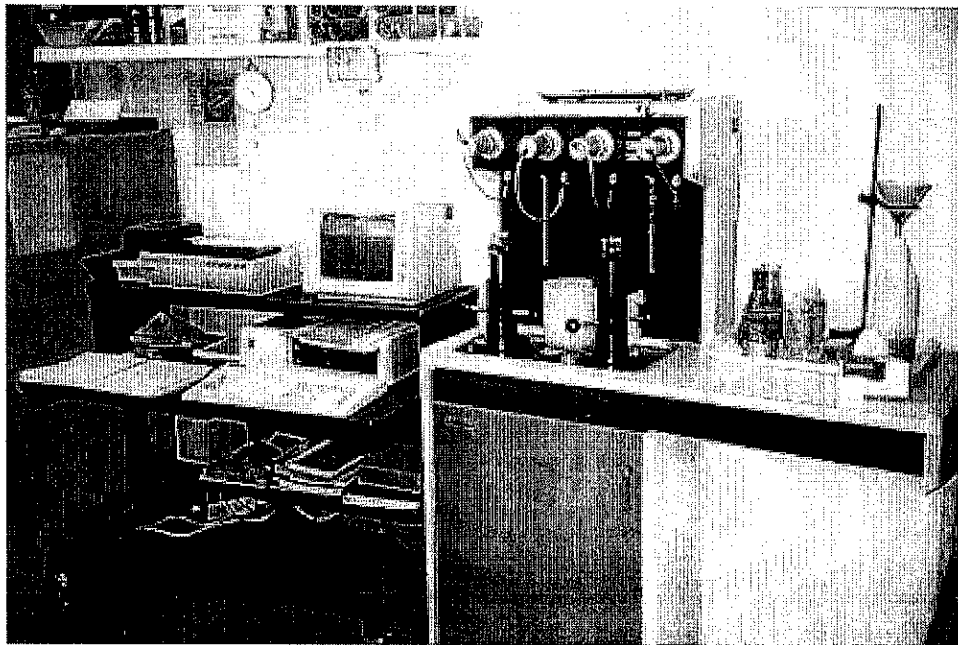


Fig. 4.1 AutoPore II 9220

4.3 RESULTS

4.3.1 Qualitative Results

The pore size distribution of the tested aggregates show some obvious qualitative correlations. For example, Fig. 4.2 shows the pore size distributions of three aggregates with similar predominating pore sizes but with different total pore volume. Clearly, a greater pore volume of the same size results in a less durable aggregate.

Among all the samples tested, none of them showed approximately the same total pore volume. They all possessed different predominant pore sizes. However, previous experiments indicate that at constant total pore volume, a smaller pore size results in a lower durability [6].

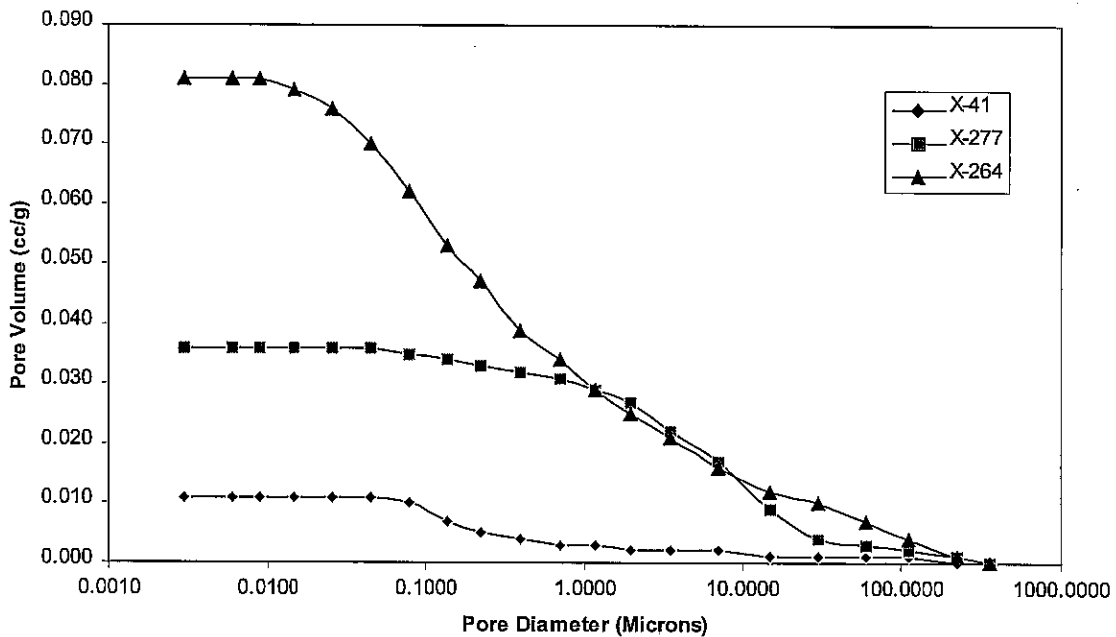


Fig. 4.2 Pore Size Distributions of Aggregates with Different Total Intruded Pore Volume

4.3.2 Quantitative Results

The qualitative influences of pore structure upon durability that have been presented were also developed into a quantitative correlation by multiple regression analysis. The two numerical parameters that are extracted from each distribution are the median pore diameter and the total intruded pore volume. Kaneuji [21] examined several different functional relationships, and the best correlation between these two parameters and the durability factor was found to have the form:

$$EDF = \frac{0.579}{PV} + 6.12(MD) + 3.04$$

where,

EDF = expected durability factor

PV = intruded volume of pores larger than 45Å in diameter, cc/g

MD = median diameter of pores > 45Å in diameter as measured by mercury porosimeter

Based on the field performance of aggregate from pavement showing varying degrees of D-cracking, Kaneuji concluded that non-durable aggregates have EDF values of less than 40, marginal, 40 to 50, and durable, over 50. Table 4.2 summarizes the EDF results of the 21 different Illinois aggregates tested. This table shows that 10 aggregates are durable, 5 are non-durable, and 5 are marginal. One of the tested aggregates (X-285) gave some problem during the mercury intrusion test. For some reason, the AutoPore II 9220 was unable to evacuate all the air in the sample in order to start the mercury intrusion. The sample was then oven dried for 24 hours, but still the same problem existed. Therefore, no results were obtained for this sample.

Table 4.3 is a list of the dry specific gravities obtained from both the Mercury Intrusion Test results and the ones provided by ILDOT. Fig. 4.3 shows graphically that the differences between the two are minor. This difference could be due to the fact that only a small sample is used in the Mercury Intrusion Test, which is not a perfect representation of the entire aggregate type.

Table 4.4 is a comparison of durability factors obtained by Freeze and Thaw and Mercury Intrusion Porosimeter Test. This table shows that 11 out of 20 (55%) aggregate samples are identified correctly between the two tests.

Table 4.2 Expected Durability Factor (EDF)

Sample ID	Type Rock	Median Diameter (MD)	Intruded Volume (PV)	EDF	Predicted Durability
X-1	Dolo	0.716	0.008	79.8	Durable
X-5	Grav	0.716	0.004	152.2	Durable
X-7	LS	0.716	0.003	200.4	Durable
X-12	LS	0.716	0.017	41.5	Marginal
X-31	Dolo	0.716	0.060	17.1	Non-durable
X-32	Dolo	0.716	0.014	48.8	Marginal
X-41	LS	0.716	0.011	60.1	Durable
X-42	Dolo	0.716	0.024	31.6	Non-durable
X-98	LS	0.716	0.016	43.6	Marginal
X-167	LS	0.716	0.013	52.0	Durable
X-262	LS	0.716	0.016	43.6	Marginal
X-263	Grav	0.716	0.002	296.9	Durable
X-264	ACBF	0.716	0.081	14.6	Non-durable
X-275	Grav	0.716	0.001	586.4	Durable
X-277	Dolo	0.716	0.036	23.5	Non-durable
X-281	LS	0.716	0.099	13.3	Non-durable
X-282	Dolo	0.716	0.010	65.3	Durable
X-285	Grav	-	-	-	-
X-290	Dolo	0.716	0.004	152.2	Durable
X-305	LS	0.716	0.015	46.0	Marginal
X-309	LS	0.716	0.007	90.1	Durable

Note: Aggregates are considered durable when the EDF value is above 50, marginal, between 40 and 50, non-durable, less than 40.

Table 4.3 Comparison of Dry Specific Gravities

Sample ID	Type Rock	MIP Specific Gravity	ILDOT Specific Gravity
X-1	Dolo	2.774	2.747
X-5	Grav	2.754	2.566
X-7	LS	2.633	2.845
X-12	LS	2.521	2.627
X-31	Dolo	2.373	2.470
X-32	Dolo	2.662	2.676
X-41	LS	2.597	2.665
X-42	Dolo	2.578	2.627
X-98	LS	2.576	2.634
X-167	LS	2.624	2.649
X-262	LS	2.567	2.634
X-263	Grav	2.764	2.593
X-264	ACBF	2.220	2.310
X-275	Grav	3.038	2.669
X-277	Dolo	2.185	2.638
X-281	LS	2.466	2.641
X-282	Dolo	2.671	2.713
X-285	Grav	-	2.645
X-290	Dolo	2.828	2.688
X-305	LS	2.549	2.618
X-309	LS	2.568	2.664

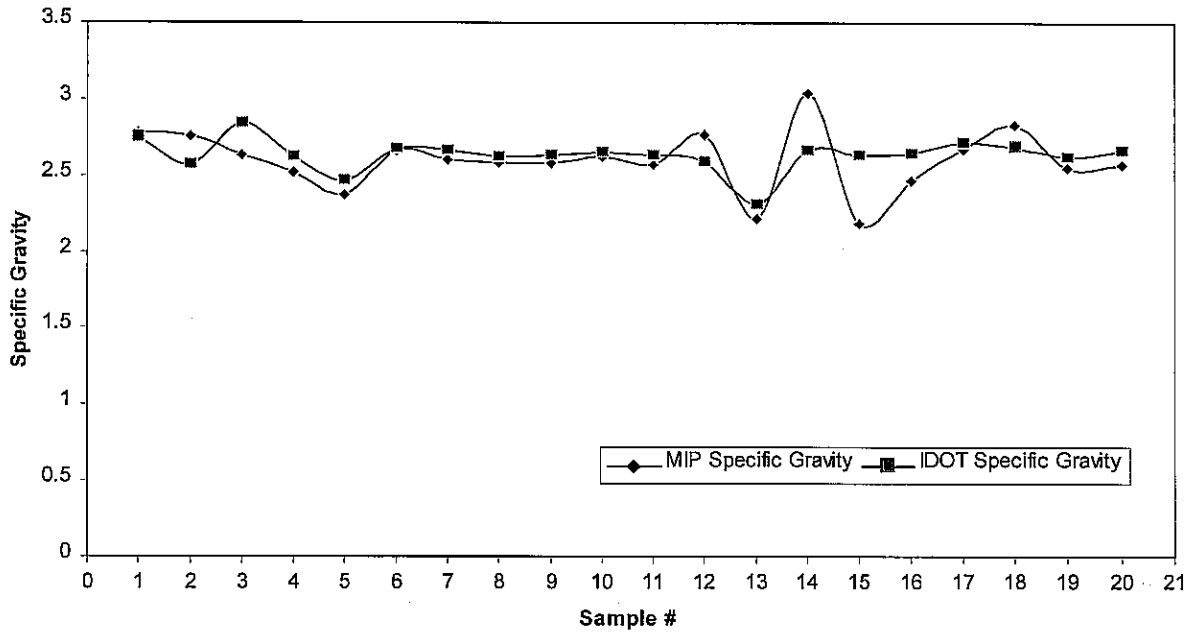


Fig. 4.3 Comparison of Specific Gravities

Table 4.4 Comparison of Durability Factors Obtained by Freeze and Thaw, and Mercury Intrusion Porosimeter Test

Sample ID	Type Rock	Mercury Intrusion		Freeze and Thaw	
		EDF	Predicted Durability	Expansion (%)	Predicted Durability
X-1	Dolo	79.8	Durable	0.006	Pass
X-5	Grav	152.2	Durable	0.057	Pass
X-7	LS	200.4	Durable	0.055	Pass
X-12	LS	41.5	Marginal	0.117	Fail
X-31	Dolo	17.1	Non-durable	0.010	Pass
X-32	Dolo	48.8	Marginal	0.038	Pass
X-41	LS	60.1	Durable	0.021	Pass
X-42	Dolo	31.6	Non-durable	0.006	Pass
X-98	LS	43.6	Marginal	0.074	Fail
X-167	LS	52.0	Durable	0.020	Pass
X-262	LS	43.6	Marginal	0.033	Pass
X-263	Grav	296.9	Durable	0.073	Fail
X-264	ACBF	14.6	Non-durable	0.008	Pass
X-275	Grav	586.4	Durable	0.029	Pass
X-277	Dolo	23.5	Non-durable	0.006	Pass
X-281	LS	13.3	Non-durable	0.066	Fail
X-282	Dolo	65.3	Durable	0.007	Pass
X-285	Grav	-	-	0.010	Pass
X-290	Dolo	152.2	Durable	0.004	Pass
X-305	LS	46.0	Marginal	0.022	Pass
X-309	LS	90.1	Durable	0.085	Fail

5. PETROGRAPHIC EXAMINATION

A quantitative determination of the constituents of aggregates was carried out via an automated concrete analysis system (CAS 2000). ASTM C457 describes two procedures for the microscopical quantification, namely, the linear-traverse method and the modified point-count method. However, only the linear-traverse method was used in this investigation. Both methods are incorporated into the CAS 2000.

The samples had to be prepared in accordance with ASTM standards before the test procedures were applied. From the aggregates that were retained on the 19 mm ($\frac{3}{4}$ ") sieve, three different aggregates were chosen per sample in order to perform the petrographic analysis. A wooden mold was fabricated with dimensions of 32 mm x 32 mm x 25 mm (1.25" x 1.25" x 1.0"). Each aggregate sample was placed in an individual compartment and a mortar mix was poured into the mold. A total of 63 specimens were cast, i.e., 3 per aggregate sample. After the mix hardened, the specimens were de-molded and marked at a certain distance for slicing. This distance was predetermined before casting which yielded a maximum surface area of 0.5" x 0.5" for each aggregate chosen. A diamond saw was used to slice the specimens, and a polishing machine with various silicon carbide grits was used to polish the sliced surface. After sawing the samples (using a diamond saw), all scratches and unwanted debris had to be polished off by the use of a lapping machine. Each sample was lapped and washed according to ASTM standards. A magnification of 50x was used to perform the linear-traverse method. This test method can be summarized as follows:

5.1 Linear-Traverse Method

This procedure consisted of the determination of the volumetric composition of aggregates by summing the distances traversed across a given component along a series of regularly spaced lines in one or more planes intersecting the sample. When traversing through a specific sample great

care was taken in all of the following:(1) the operator was very careful in adjusting the speed so as to not pass through a given void too quickly; consequences of this error could have lead to uncounted, or semi-counted voids. (2) The lighting, which enhanced the perception of the voids, had to be directed at a small angle towards the sample to allow the appearance of a dark shadow on each void, and (3) the sample had to be leveled perfectly under the stereomicroscope in order to reduce adjustment in focusing.

Before initiating the procedure for the linear traverse method, an identification of the sample was made. This identification involved, the names of the originator and the operator, the date, project number, sample name, the distance traversed in the x and y directions, and the maximum aggregate size.

At the end of the linear traverse procedure, results were recorded on a separate file. This file consisted of data depicting the distance traversed, the area covered, the range and size of all the voids, the air content, and total number of voids. A 3-D representation of all the voids on different parts of the sample was also obtained. To check the reproducibility of the test, three trials for each sample were made. The files were merged in order to find the average air content of the specific sample.

5.2 Test Results, Analysis and Discussion

A petrographic analysis was performed on 21 different samples with a total of 63 aggregates, i.e., three aggregate pieces per sample. Each sample was examined three times using the linear transverse method. The method utilized is based on the percentage of air voids intercepted by the linear transverse. Several of the samples, whose percentage was zero to one percent, were examined with only two runs, where a third run was not necessary.

The air-void system parameters used as measures of freeze-thaw resistance are: (1) void frequency - number of voids per linear inch of traverse and (2) Air content - the proportion of the

total volume of the aggregate that is air voids. The results of the air-content obtained by the linear-traverse method are summarized in Table 5.1. These values are the averages and standard deviations of three trials on each sample. Figs. 5.1 and 5.2 present typical histograms with respect to the number of voids versus void size and percentage of voids versus void size, respectively. These figures represent the results obtained for the sample with the largest number of voids. The average air-void content from all runs corresponding to each sample was 10.862 percent. The remaining histograms for each sample are presented in Appendix A. Typical output from the CAS2000 is shown in the Appendix A.

Frequently differences were found between samples of the same rock types. This was expected since these types of tests are dependent on the location where the rocks were collected and mineralogic formation. However, the concepts utilized were sufficient to minimize this discrepancy.

Comparison with other methods is not possible since a limiting guideline is not available to provide a criteria for aggregates that are non-susceptible to D-cracking. However, using the means available for the air void system in concrete, we can clearly indicate that the X-264 and X-42 have a high level of air voids (7-10% of air voids), the X-31, X-277 and X-282 can be classified to be in the intermediate range (3-7% of air voids), and the remaining samples are considered excellent rocks.

In order to check Kaneuji et al. [6] investigating as mentioned in the literature review regarding the relationship between total pore volume and freeze/thaw expansion results, three different aggregate samples from Table 5.1 with approximately the same total pore volume were chosen. Then the percent of voids less than 50 μm was found from the petrographic analysis results and compared to the percent expansion of ASTM C666 (ILDOT modified). Indeed, it could be concluded, as Kaneuji concluded that at constant total pore volume, smaller pore size yields lower durability. The results of this investigation are tabulated in Table 5.2.

Table 5.1 - Percentage of Voids from Linear Transverse Method

Sample ID	Sample A				Sample B				Sample C				Final Avg.
	Run #1	Run #2	Run #3	Avg.	Run #1	Run #2	Run #3	Avg.	Run #1	Run #2	Run #3	Avg.	
X-1	0.33	0.50	-----	0.415	0.47	0.53	-----	0.500	2.42	4.41	3.40	3.410	1.442
X-5	1.45	0.93	1.16	1.180	0.47	0.27	-----	0.370	0.46	0.64	-----	0.550	0.700
X-7	0	0.23	-----	0.115	0.08	0	-----	0.040	0	0	-----	0.000	0.052
X-12	2.00	1.77	2.07	1.947	0.49	0.31	-----	0.400	0.08	0.07	-----	0.075	0.807
X-31	1.78	2.18	2.33	2.097	10.05	10.11	11.08	10.413	0.46	0.37	-----	0.415	4.308
X-32	0.25	0.25	-----	0.250	1.32	1.51	1.43	1.420	0	0	-----	0.000	0.557
X-41	0	0	-----	0.000	0	0	-----	0.000	0.05	0.07	-----	0.060	0.020
X-42	3.10	2.82	3.85	3.257	4.28	5.18	4.38	4.613	13.58	14.36	15.88	14.607	7.492
X-98	0.77	0.74	-----	0.755	0.13	0.25	-----	0.190	0.37	0.29	-----	0.330	0.425
X-167	0	0	-----	0.000	0	0	-----	0.000	0	0	-----	0.000	0.000
X-262	0	0	-----	0.000	0	0	-----	0.000	0.24	0.11	-----	0.175	0.058
X-263	0.35	0.49	-----	0.420	2.06	1.42	1.25	1.577	0	0	-----	0.000	0.666
X-264	1.28	1.33	1.61	1.407	16.89	16.85	15.85	16.530	11.60	15.77	16.58	14.650	10.862
X-275	0	0.06	-----	0.030	0.88	1.00	-----	0.940	0.87	1.14	0.97	0.993	0.654
X-277	5.60	5.76	6.46	5.940	5.71	5.41	4.37	5.163	1.89	1.63	1.51	1.677	4.260
X-281	0.73	1.12	1.17	1.007	0.22	0.17	-----	0.195	0	0	-----	0.000	0.401
X-282	4.68	4.18	4.98	4.613	4.83	3.89	3.59	4.103	1.38	1.69	1.88	1.650	3.456
X-285	0	0.13	-----	0.065	0.47	0.52	-----	0.495	0.15	0	-----	0.075	0.212
X-290	0.40	0.49	-----	0.445	1.40	1.20	1.26	1.287	0.21	0.37	-----	0.290	0.674
X-305	0.27	0	-----	0.135	0	0	-----	0.000	0.45	0.32	-----	0.385	0.173
X-309	0	0.34	-----	0.170	0.17	0.18	-----	0.175	0	0	-----	0.000	0.115

Table 5.2 - Comparison of Percentage of Voids and Percent Expansion

Sample ID	Type Rock	Pore Volume (%)	Voids < 50 μm (%)	Expansion (%)
X-263	Grav	0.666	57	0.073
X-5	Grav	0.700	35	0.057
X-275	Grav	0.654	27	0.029

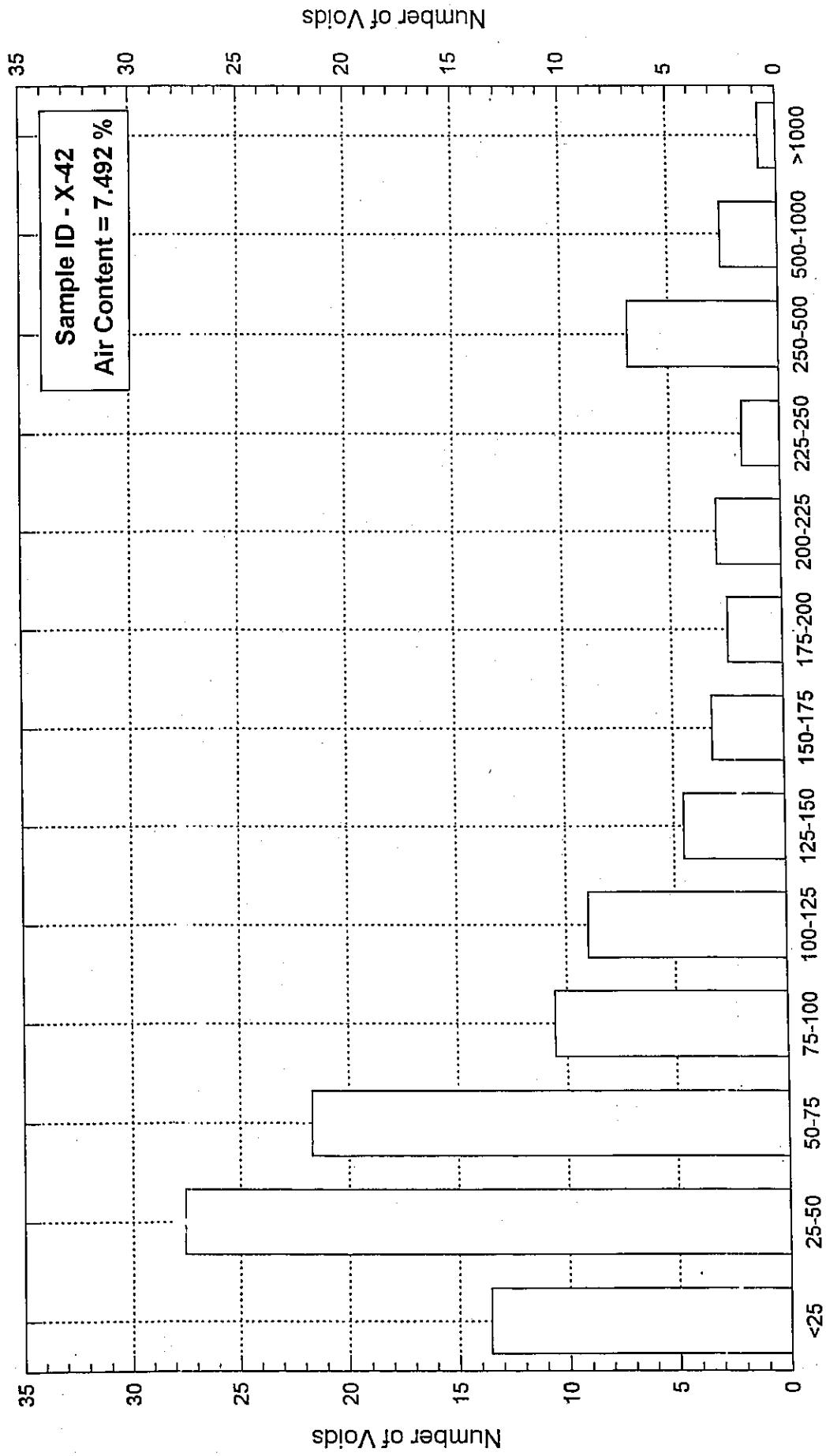
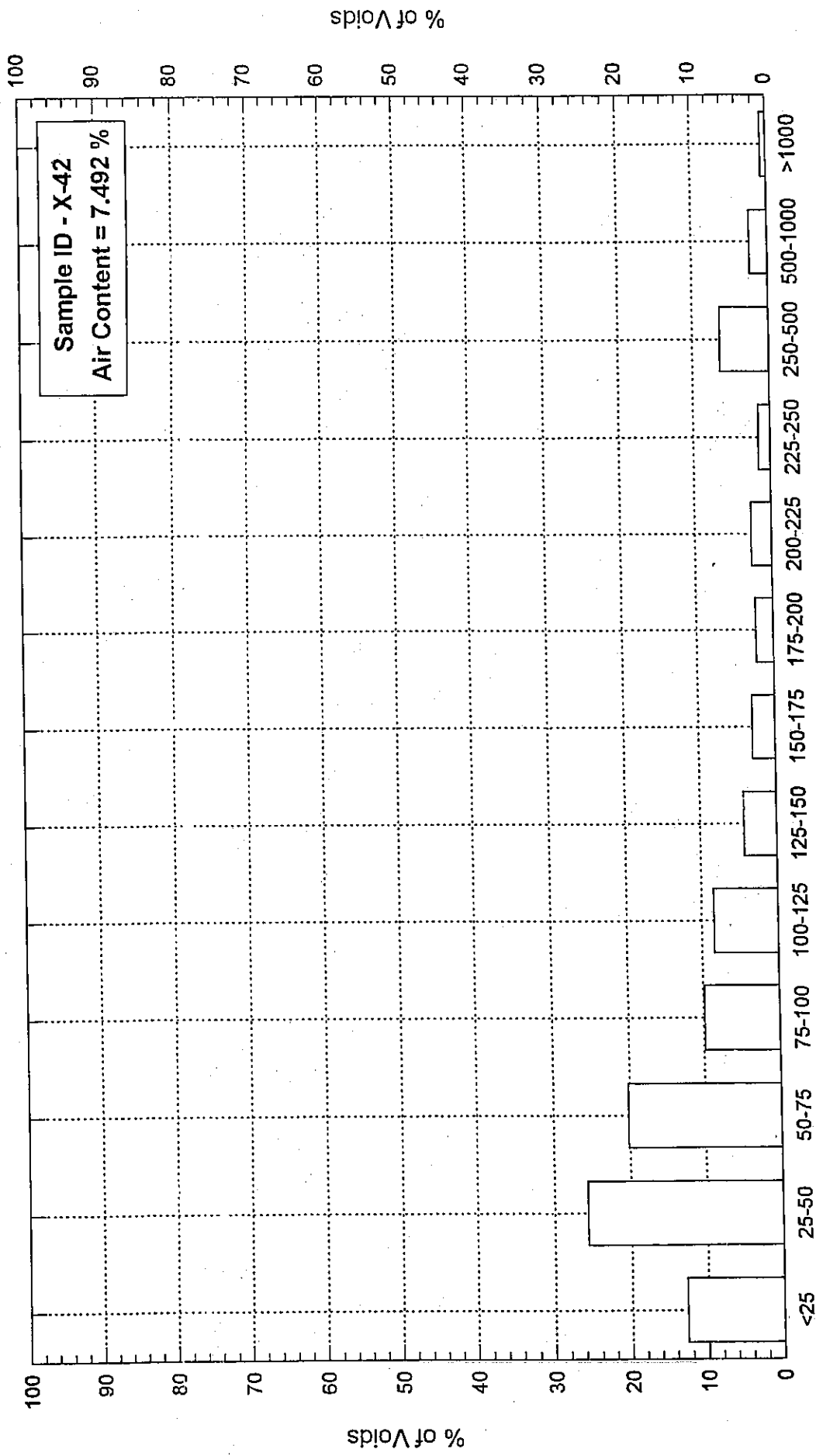


Fig. 5.1 Number of Voids vs Void Size

Size Range of Air Voids (microns)



Size Range of Air Voids (microns)

Fig. 5.2 Percentage of Voids vs Void Size

6. TESTING PROCEDURE AND RESULTS

The 1994 WHFT relies on the pressure differential between the inside and outside of the aggregate pieces to cause D-cracking susceptible pieces to fracture. Aggregates that exhibit a high percentage of fracturing under repeated pressurization cycles are considered to be more likely to cause D-cracking in field applications. The relatively short time (approximately 8 working days) required for completion of this procedure makes it appropriate for use as a screening test to identify questionable aggregates requiring additional (more time consuming) testing, such as the AASHTO T161 test prior to final approval. It is recommended that aggregates with HFI of greater than 75 are not susceptible to D-cracking. If for any aggregate this value of HFI falls below 75, then before rejecting the aggregates, it is suggested to perform the freezing and thawing test.

The 1997 Washington Hydraulic Fracture Test (WHFT 97) is a modified version of the 1994 apparatus. It contains the following changes to facilitate the operation of this test: (1) WHFT 97 has a larger chamber with a 254 mm (10 in.) inside diameter and a 30.5 cm (12 in.) height. (2) Operator and handling time is reduced by using pressure to hold the chamber lid down instead of 16 high strength bolts. (3) Air driven water is used instead of the Nitrogen gas to pressurize the chamber. (4) The machine is fully automated in terms of controlling the entire testing procedure for each respective 10 cycles of operation. (5) It has a more accurate controlled release rate. (6) A controlled interface is connected to the machine that reads pressure, hence good quality control of the system and much better results are expected. (7) The computer interface provides a plot of the release for each cycle.

6.1 Sample Preparation

Sample preparation for the 1994 WHFT apparatus and 1997 WHFT machine was identical with exception of sample size. Sample preparation is as follows:

1. Separate the sample into the appropriate size, i.e., passing the 31.5 mm (1¼ in.) but retained on the 19 mm (¾ in.) sieves and passing the 19 mm (¾ in.) but retained on the 13 mm (½ in.) sieves. A sample size of approximately 3.2 kg (7.0 lb) was needed for the WHFT 94 machine, while a sample size of approximately 16 kg (35 lbs) was used for the WHFT 97 machine.
2. The aggregates are thoroughly washed and dried to a constant mass at a temperature of $120^{\circ}\text{C} \pm 5^{\circ}\text{C}$ ($250^{\circ}\text{F} \pm 9^{\circ}\text{F}$) for at least 12 hours and allowed to cool to room temperature.
3. The aggregate specimen is then placed in silane solution for 30 seconds \pm 5 seconds making sure that all aggregate pieces are covered.
4. The specimen is then removed from the silane solution and the excess solution is allowed to drain for 5 minutes.
5. The specimen is dried to a constant mass at a temperature of $120^{\circ}\text{C} \pm 5^{\circ}\text{C}$ ($250^{\circ}\text{F} \pm 9^{\circ}\text{F}$) overnight and allowed to cool to room temperature.
6. Enough of the specimen is placed into the tumbler to fill it approximately half way and tumbled for 1 minute. Any pieces passing the 9.5 mm (¾ in.) sieve are then separated. This process is repeated for the remainder of the specimen. As a result, the mass (m_o) is determined to the nearest gram and the number of pieces (n_o) retained on the 9.5 mm (¾ in.) sieve is carefully counted. Details on the two WHFT machines as part description and test procedure are presented in Appendix B.

6.2 WHFT Formulas

1. Percent Fracture (PF) - Calculate the percent fracture after each 10 pressurization cycles as follows:

$$PF_i = 100(n_{4_i}/2 + n_i - n_o)/n_o$$

where:

PF_i = percent fracture after "i" pressurization cycles

n_{4_i} = cumulative number of pieces passing the 9.5 mm ($\frac{3}{8}$ in.) sieve but retained on the No. 4 sieve after "i" pressurization cycles

n_i = number of pieces retained on the 9.5 mm ($\frac{3}{8}$ in.) sieve after "i" pressurization cycles

n_o = initial number of pieces tested

2. Percent Mass Loss (ML) - Determine the percent mass loss as follows:

$$ML_i = (100/m_o)[m_o - (m_{4_i} + m_i)]$$

where:

ML_i = percent of mass loss after "i" cycles of pressurization

m_{4_i} = cumulative mass of the material passing the 9.5 mm ($\frac{3}{8}$ in.) sieve but retained on the No. 4 sieve after "i" pressurization cycles

m_i = mass of the pieces retained on the 9.5 mm ($\frac{3}{8}$ in.) sieve after "i" pressurization cycles

m_o = initial mass of the specimen tested

3. Hydraulic Fracture Index (HFI) - Calculate the hydraulic fracture index as the number of cycles necessary to produce 2 percent fracturing by the following methods:

If 2 percent fracturing is achieved in 50 or fewer cycles, calculate the HFI as linear interpolation of the number of cycles that produced 2 percent fractures:

$$\text{HFI} = A + 10[(2 - \text{PF}_A)/(\text{PF}_B - \text{PF}_A)]$$

where:

- A = number of cycles just prior to achieving 2 percent fracturing
- PF_A = percent of fracturing just prior to achieving 2 percent fracturing
- PF_B = percent of fracturing just after achieving 2 percent fracturing

If 2 percent fracturing is not achieved in 50 pressurization cycles, calculate HFI as an extrapolation from no fracturing at 0 cycles, through the amount of fracturing at 50 cycles:

$$\text{HFI} = 50(2/\text{PF}_{50})$$

where:

- PF_{50} = percent of fracturing after 50 pressurization cycles.

6.3 Results and Discussion

All twenty-one different aggregate samples provided by ILDOT were tested using both the WHFT 94 and WHFT 97 machines. All sample tests were performed three times on the WHFT 94 apparatus in order to get more accurate and reliable results. However, due to the limited amount of aggregates provided, not all samples were tested three times on the WHFT 97. In some cases only one or two tests were conducted. A new sample was prepared for each run. Before testing using the WHFT 97 machine, calibration was successfully performed to obtain the same actual release rate as that from the WHFT 94 (Fig. 3.8).

Once the testing chamber was pressurized, it was not apparent as to when equilibrium occurred, hence, maximum compression of the pore air bubble was reached. For this reason, Almond [22] conducted a simple test on his apparatus, which is the same as the WHFT 94 apparatus, to determine at what time equilibrium was reached after initial pressurization. To accomplish this,

Almond filled and secured the chamber with a sample of aggregates and applied the external pressure. After reaching the desired test pressure, the nitrogen tank was secured for 30 seconds. The tank was then reopened and the system was allowed to return to the desired test pressure. This process was repeated for 10 minutes on a few different samples. If equilibrium had not been reached, the pressure gauge indicated a drop in pressure while the compression nitrogen tank was secured. It was noted that after 4 to 5 minutes there was very little if any change in the chamber pressure while the tank was secure. This was believed to indicate that the internal pressure of the aggregate had reached equilibrium with the chamber pressure. Based on this test, Almond determined that the sequence of an initial 5 minutes of pressurization, followed by 1 minute of depressurization, and then 9 repeated cycles of 2 minutes pressurization and 1 minute depressurization was the most feasible procedure to use.

The experimental results indicate an obvious difference between the various aggregates tested. Some samples show a high percentage of aggregate fracture while others show a limited amount of fracture after the fifty pressurization cycles. Some of these aggregates, even though did not change significantly in count number, had a noticeable mass loss. This indicates that both percent fracture and mass loss are important in determining aggregate susceptibility to D-cracking.

The percent fracture, percent mass loss, and hydraulic fracture index (HFI) were calculated based on the formulas in the previous section. Computation of the HFI parameters was based on 10%, 5%, 2% as well as 1.5%. The 10% fracture was developed as a result of the testing conducted by Janssen [17] on the 1994 WHFT due to the fact that the aggregates used yielded approximately 10% fracture. Hossain and Zubery [19] reported only a 5% fracture as a result of their testing and recommended that percent for the 1994 WHFT. In the study conducted here at the University of Illinois at Chicago, the percent fracture was mostly below 2%. The results are presented in all four percentages for comparison purposes only. However, the recommended failure criteria is based on 2% fracture.

To verify quantitatively that the WHFT 94 apparatus is properly calibrated, a previously tested aggregate (X-KSU), which was provided by the Department of Civil Engineering at Kansas State University (KSU), was tested. Table 6.1 summarizes the Mass Loss (ML), Percent Fracture (PF), and Hydraulic Fracture Index (HFI) obtained. Clearly, this unknown source of aggregate is non-durable and well below the 200 HFI value. After completion of the test, KSU was contacted for comparison of results. KSU reported a value of 1.4 as the HFI which is very close to the value of 1.7 obtained at UIC. This good correlation indicates that the test results are consistent and reliable.

Table 6.2 is a typical Daily Data Sheet for aggregate ID X-12. As suggested by Janssen [17], when data from more than one specimen were combined for determining final results, the raw data, m_0 , n_0 , m_{4_i} , n_{4_i} , m_i , and n_i were combined prior to calculation of ML_i , PF_i , and HFI. This is shown in the column labeled "Total" of Table 6.2. All other data sheets are presented in Appendix C. Table 6.3 provides a summary of individual as well as average mass loss (ML_{50}) and percent fracture (PF_{50}) for all samples tested on the WHFT 94. Table 6.4 presents a summary of the individual PF_{50} and individual HFI based on 10%, 5%, 2%, and 1.5% fracture as mentioned above for the WHFT 94 machine. Only some aggregate types fall below the recommended HFI value of 200 based on the 2% fracture presented in Table 6.4. Whenever more than one test was performed on the same aggregate type, the average ML_{50} and PF_{50} were calculated. This average value was very close to the total value obtained from treating all three sample tests of the same aggregate as one test.

Table 6.5 provides a summary of individual as well as average mass loss (ML_{50}) and percent fracture (PF_{50}) for all samples tested on the WHFT 97 machine. Table 6.6 presents a summary of the individual PF_{50} and individual HFI based on 10%, 5%, and 2%, and 1.5% fracture as mentioned above for the WHFT 97 machine.

In comparing the actual testing on both machines, the WHFT 94 could only accommodate approximately 3.2 kg (7 lbs.), which is about 700 aggregate pieces for the aggregate size used. The

WHFT 97, on the other hand, has a bigger chamber which can accommodate about 16 kg (35 lbs.), i.e., about 3000 aggregate pieces. This increase provides a more reliable representation of the sample tested, hence giving better results. In comparing Tables 6.3 and 6.5, the mass loss (ML_{50}) and percent fracture (PF_{50}) for the three tests on the same aggregate sample show a wider variation using the WHFT 94 than the same sample tested on the WHFT 97. For example, when aggregate sample X-275 was tested on each machine, the mass losses on the WHFT 94 were 0.387%, 0.060%, and 0.140%. However, these same values were 0.229%, 0.219%, and 0.156% on the WHFT 97. This clearly indicates that the larger sample tested provided more reliable results.

The WHFT 94 is very difficult to operate since it requires a significant amount of manual labor and exact timing for opening and closing the various valves including the 16 high strength bolts that need to be tightened and removed after each 10 pressurization cycles. However, the WHFT 97 is completely automated and requires minimal manual labor.

In Tables 6.7 and 6.8, the average PF_{50} and HFI are calculated and summarized for the WHFT 94 and WHFT 97, respectively. As recommended by Janssen [17], all tests conducted pertaining to the same aggregate type were combined based on the total mass loss and percent fracture for all the tests. When comparing Tables 6.4 with 6.7 and 6.6 with 6.8, the average of the individual percent fracture obtained after 50 pressurization cycles was equal to the percent fracture obtained from treating the three individual samples tested as one test. For example, sample X-1 of Table 6.4 has an average percent fracture of 0.219, and the corresponding percent fracture in Table 6.7 is also 0.219. Similarly, sample X-1 has an average percent fracture of 0.165 in Table 6.6 and a total percent fracture of 0.165 in Table 6.8

Figure 6.1 shows a comparison of the mass loss (ML) results for both machines. Five samples have almost identical results, eight samples have a higher ML on the WHFT 94 apparatus, and five samples have higher ML on the WHFT 97 apparatus. Figure 6.2 shows a comparison of PF. In general, the WHFT 97 yields lower PF than WHFT 94. Six samples have almost similar PF,

twelve samples have a higher PF on the WHFT 94 apparatus, and only one sample has a higher PF on the WHFT 97 apparatus. The mass loss and percent fracture rarely exceeded 0.5% on both WHFT apparatus.

Most samples that show a huge difference in PF between the two machines were the samples that were tested only once or twice on the WHFT 97. For example, X-41 has a fracture of 1.513% on the WHFT 94 apparatus, and only 0.774% on the WHFT 97. Since some aggregate samples remained after conducting all the tests on the WHFT 97, more tests were repeated on the WHFT 94. This yielded more consistent results on samples that showed a big variation.

The test results for the percent fracture, Sodium Sulfate Soundness, L.A. Abrasion, absorption tests were provided by ILDOT. Figures 6.3 and 6.4 show the scatter plot of the WHFT mass loss versus (ILDOT modified) C666 percent expansion. For the WHFT 94 apparatus, twelve samples have an expansion less than 0.06% and a mass loss less than 0.5%, five samples show an expansion greater than 0.06% and mass loss below 0.5%, and four samples have an expansion less than 0.06% and mass loss greater than 0.5% (Fig. 6.3). For the WHFT 97 apparatus, fourteen samples have an expansion less than 0.06% and mass loss less than 0.5%, five samples exceed the expansion of 0.06% and the mass loss remain less than 0.5%, and two samples have an expansion less than 0.06% and mass loss higher than 0.5% (Fig. 6.4).

Figures 6.5 and 6.6 show the scatter plots of WHFT percent fracture versus ASTM C666 (ILDOT modified) percent expansion. For the WHFT 94 apparatus, fourteen samples have an expansion less than 0.060% and a percent fracture less than 0.5%, four samples have an expansion greater than 0.060% and percent fracture below 0.5%, two samples show a percent fracture higher than 0.5% with the expansion less than 0.060%, and only one sample has an expansion higher than 0.060% and a percent fracture higher than 0.5% (Fig. 6.5). For the WHFT 97 apparatus, fifteen samples have an expansion less than 0.060% and a percent fracture less than 0.5%, four samples show an expansion greater than 0.060% and percent fracture less than 0.5%, one sample has a

percent fracture greater than 0.5% and the expansion less than 0.060%, and only one sample has the expansion greater than 0.060% and percent fracture greater than 0.5% (Fig. 6.6).

Figures 6.7 through 6.10 are scatter plots of mass loss and percent fracture of both WHFT 94 and WHFT 97 versus Sodium Sulfate Soundness. Shakoor [23] suggests that when the soundness loss exceeds 10%, the aggregate should be looked upon with suspicion. With this in mind, the WHFT 94 apparatus indicates that twelve samples fall within the 10% soundness and the 0.5% mass loss, four samples have a soundness less than 10% and mass loss greater than 0.5%, and the other five samples exceed the 10% soundness and have a mass loss less than or equal to 0.5% (Fig. 6.7). For the WHFT 97 apparatus, fourteen samples have values below 10% soundness and 0.5% mass loss, two samples have less than 10% soundness and a mass loss greater than 0.5%, and five samples have a soundness greater than 10% and mass loss less than 0.5% (Fig. 6.8).

For the WHFT 94 apparatus, thirteen samples are below 10% soundness and 0.5% percent fracture, three samples have soundness less than 10% and percent fracture greater than 0.5%, four samples have soundness greater than 10% and percent fracture less than 0.5%, and only one sample has soundness greater than 10% and percent fracture greater than 0.5% (Fig. 6.9). For the WHFT 97 apparatus, fourteen samples show less than 10% soundness and 0.5% percent fracture, five samples have a soundness greater than 10% and percent fracture less than 0.5%, and two samples have a percent fracture greater than 0.5% and less than 10% soundness (Fig. 6.10).

Figures 6.11 through 6.14 are scatter plots of mass loss and percent fracture of both WHFT 94 and WHFT 97 versus L.A. Abrasion. It is evident that as the mass loss increases, the L.A. Abrasion percentage increases. If 30% is taken as the cutoff point for aggregates, then the WHFT 94 apparatus indicates that sixteen samples have an abrasion less than 30% and mass loss less than 0.5%, three samples have an abrasion less than 30% and mass loss between 0.5% and 1%, and only two samples have an abrasion greater than 30% and mass loss greater than 0.5% (Fig. 6.11). For the WHFT 97 apparatus, eighteen samples have an abrasion less than 30% and a mass loss less than

0.5%, and the other three samples fall outside this range (Fig 6.12).

The WHFT 94 apparatus shows that seventeen samples have an abrasion less than 30% and percent fracture less than 0.5%, three samples have percent fracture between 0.5% and 1.5% and an abrasion less than 30%, and only one sample has an abrasion greater than 30% and a percent fracture greater than 0.5% (Fig 6.13). For the WHFT 97 apparatus, seventeen samples fall below 30% abrasion and 0.5% percent fracture, two samples have an abrasion less than 30% and percent fracture between 0.5% and 0.8%, and the other two samples have an abrasion greater than 30% and a percent fracture less than 0.5% (Fig 6.14).

Figures 6.15 through 6.18 are scatter plots of mass loss and percent fracture of both WHFT 94 and WHFT 97 versus Absorption. These figures indicate that, in general, the lower the mass loss and percent fracture values are the lower the absorption rate. In general, 2% absorption is used as a cut off point in choosing coarse aggregates for concrete. For the WHFT 94 apparatus, seventeen samples have an absorption less than 2% and mass loss less than 0.5%, two samples have an absorption greater than 2% and mass loss greater than 0.5%, and only two samples have an absorption less than 2% and mass loss between 0.5% and 1% (Fig. 6.15). For the WHFT 97 apparatus, nineteen samples are below 2% absorption and 0.5% mass loss, one sample has absorption higher than 2% and mass loss above 0.5%, and only one sample has a mass loss less than 0.5% and an absorption greater than 2% (Fig 6.16).

The WHFT 94 apparatus has seventeen samples with absorption less than 2% and percent fracture less than 0.5%, three samples with percent fracture above 0.5% and the absorption below 2%, and only one sample with an absorption greater than 2% and a percent fracture greater than 0.5% (Fig. 6.17). For the WHFT 97 apparatus, seventeen samples have less than 2% absorption and 0.5% percent fracture, two samples with absorption higher than 2% and percent fracture less than 0.5%, one sample with a percent fracture above 0.5% and an absorption below 2%, and only one sample with a percent fracture above 0.5% and an absorption above 2% (Fig. 6.18).

Figures 6.19 through 6.22 are scatter plots of mass loss and percent fracture of both WHFT 94 and WHFT 97 versus air voids. The air void test results are presented in Chapter 5. Once again, the lower the mass loss and percent fracture, the lower the air voids. Most samples indicate that for a mass loss and percent fracture value of less than 0.5%, the percent air void is less than 1%.

A comparison of ILDOT criteria for expansion (0.060 % max) and fracture criteria obtained in the WHFT test are tabulated in Table 6.9. When the recommended 2% is used as the failure criteria, the 14 of 21 aggregates (67%) on the WHFT 94 and 16 of 21 aggregates (76%) on WHFT 97 are identified correctly with respect to the ILDOT criteria. This indicates that the WHFT 97 yields more consistent results than the WHFT 94 in comparing their results to the freeze-thaw test.

Since it required Almond [22] at least 5 minutes to achieve equilibrium between the external pressure and the aggregate pore pressure, the 2 minutes pressurization cycles as stated in the test procedure contradicts his findings. Therefore, it is suggested that all consecutive pressurization cycles be 5 minutes long. This increase in cycle duration could indeed increase the percent fracture and mass loss, and more accurately correlate with percent expansion as well as other related mentioned tests.

6.4 Correlation Analysis

In order to find the interrelationship among the various variables, a correlation study was performed for the following variables: (a) percent expansion, (b) sodium sulfate soundness, (c) L.A. abrasion, (d) absorption, (e) mass loss, and (f) percent fracture. Tables 6.10 and 6.11 show the correlation coefficients obtained from this analysis. Correlation coefficients of greater than zero indicate a positive linear relationship, and correlation coefficients of less than zero indicate a negative linear relationship between the variables.

Regression analyses were performed to find the relationship between each of the output parameters for the WHFT test (mass loss and percent fracture) and percent expansion (Exp %),

Sodium Sulfate Soundness (Snd), L.A. Abrasion (Abr %), and Absorption (Abs %). Four different types of relationships were investigated where each of the test output in the WHFT test was a dependent variable: linear, exponential, logarithmic, and power. The relationships derived between the test variables are shown in Tables 6.12 and 6.13 for the WHFT 94 and WHFT 97, respectively. In general linear and logarithmic relationships yielded the highest coefficients of determination. A linear relationship between mass loss and percent abrasion produced the highest coefficients of 0.51 and 0.57 on the WHFT 94 and WHFT 97, respectively. Another linear relationship between mass loss and absorption yielded the highest coefficients of 0.21 on the WHFT 94, and 0.33 on the WHFT 97. However, a logarithmic relationship between mass loss and Sodium Sulfate Soundness produced the highest coefficients of 0.20 and 0.21 on the respective machines.

6.5 Repeatability of Test Results

In order to assess the repeatability of the test method, all aggregates were tested three time as stated earlier. The results of these tests are tabulated in Tables 6.14 and 6.15. Table 6.14 shows the average, standard deviation, and coefficients of variation of the percent expansion, WHFT 94 mass loss, and WHFT 97 mass loss. Table 6.15 tabulates percent expansion, WHFT 94 percent fracture, and WHFT 97 percent fracture. Whenever only one test was performed on the WHFT 97, no standard deviation and coefficient of variation were tabulated. The average coefficient of variation (CV) for the percent expansion is about 24 %. The average CV for mass loss is 24% and 16% on the WHFT 94, and WHFT 97, respectively. With respect to percent fracture, the average CV values on the WHFT 94 and WHFT 97 were 21% and 16%, respectively. This clearly indicates that the larger sample tested provides more reliable results.

6.6 Recommended Test Procedure

Twenty-one different aggregate samples, with different degrees of freeze-thaw susceptibility, were tested according to the WHFT test procedure on both machines to establish a direct correlation, if possible, between the results of the proposed WHFT test and those reported for the ASTM C 666 Method B as modified by ILDOT. Unfortunately, a comparison of WHFT to ASTM C 666 Method

B (ILDOT modified) test results showed a lack of direct correlation across the vast majority of the 21 test samples. This lack of direct correlation precludes the use of the WHFT test as a direct replacement for the ASTM C 666 Method B test procedure. Since a direct correlation was not established, the test data was compared using the two test methods failure modes to establish the WHFT 97's potential as a screening test.

A draft screening procedure was developed based on aggregate type and petrographical analysis for use prior to the testing on the WHFT apparatus. The percentage of air voids in limestone is suggested as a way to identify limestones that must be tested in the WHFT 97 test. Based on the results obtained from the freeze-thaw test and petrographic analysis (Table 5.1), as the air void percentage exceeds 0.1, the limestone aggregate can be classified as non-durable and testing on the WHFT 97 machine is not necessary. If the air void percentage is less than 0.1, the aggregate should be tested to determine its susceptibility to D-cracking. A flow chart was developed based on the results provided through testing as shown in Fig. 6.23. However, this procedure for limestones was based on extremely limited samples and will require additional research on a wider range of durable and non-durable rock types to achieve validation. Overall, the WHFT test method needs further modification to yield better correlation for reliability and test applicability for durability assessment.

Table 6.1 Sample X-KSU ML, PF and HFI

Sample ID	X-KSU			
Provided by	Kansas State University (KSU)			
	Trial #1	Trial #2	Trial #3	Average
Mass Loss (ML ₅₀)	13.620	15.538	13.924	14.361
Percent Fracture	66.714	62.657	49.714	59.695
Hydraulic Fracture Index	1.5	1.6	2.0	1.7

Table 6.2 X-12 Daily Data Sheet

Trial #	WHFT 94				WHFT 97				
	1	2	3	Total	1	2	3	Total	
Date Treated	8/30/98	8/30/98	8/30/98	8/30/98	6/21/98	10/4/98	10/4/98	10/4/98	
initial m_0 , g	3227.5	3212.5	3253.0	9693.0	15890.5	15940.0	15859.0	47689.5	
initial n_0	558	575	622	1755	2908	2804	3024	8736	
Date Pressurized	8/31/98	8/31/98	8/31/98	8/31/98	6/22/98	10/5/98	10/5/98	10/5/98	
10 Cycles	m_{10} , g	3218.5	3205.5	3247.5	9671.5	15864.5	15915.5	15833.0	47613.0
	$m_{4_{10}}$, g	2.5	1.5	1.0	5.0	5.0	6.0	4.5	15.5
	PML_{10}	0.201	0.171	0.138	0.170	0.132	0.116	0.136	0.128
	n_{10}	556	576	621	1753	2902	2804	3020	8726
	$n_{4_{10}}$	12	8	5	25	12	13	8	33
	PF_{10}	0.717	0.870	0.241	0.598	0.000	0.232	0.000	0.074
Date Pressurized	9/1/98	9/1/98	9/1/98	9/1/98	6/23/98	10/6/98	10/6/98	10/6/98	
20 Cycles	m_{20} , g	3214.0	3198.0	3244.5	9656.5	15843.5	15900.0	15810.5	47554.0
	$m_{4_{20}}$, g	3.0	3.0	1.0	7.0	7.5	9.0	10.5	27.0
	PML_{20}	0.325	0.358	0.231	0.304	0.249	0.194	0.240	0.228
	n_{20}	557	572	623	1752	2902	2800	3022	8724
	$n_{4_{20}}$	14	14	5	33	19	22	19	60
	PF_{20}	1.075	0.696	0.563	0.769	0.120	0.250	0.248	0.206
Date Pressurized	9/2/98	9/2/98	9/2/98	9/2/98	6/24/98	10/7/98	10/7/98	10/7/98	
30 Cycles	m_{30} , g	3207.5	3194.0	3242.0	9643.5	15826.5	15886.5	15793.5	47506.5
	$m_{4_{30}}$, g	6.5	3.5	1.0	11.0	9.5	11.0	15.0	35.5
	PML_{30}	0.418	0.467	0.307	0.397	0.343	0.267	0.318	0.309
	n_{30}	556	574	623	1753	2901	2799	3016	8716
	$n_{4_{30}}$	18	16	5	39	22	25	30	77
	PF_{30}	1.254	1.217	0.563	0.997	0.138	0.267	0.231	0.212
Date Pressurized	9/3/98	9/3/98	9/3/98	9/3/98	6/25/98	10/8/98	10/8/98	10/8/98	
40 Cycles	m_{40} , g	3205.0	3190.5	3238.5	9634.0	15808.5	15878.5	15785.0	47472.0
	$m_{4_{40}}$, g	7.0	4.0	2.0	13.0	11.5	11.5	15.0	38.0
	PML_{40}	0.480	0.560	0.384	0.475	0.444	0.314	0.372	0.376
	n_{40}	555	574	622	1751	2898	2799	3016	8713
	$n_{4_{40}}$	19	17	8	44	26	26	30	82
	PF_{40}	1.165	1.304	0.643	1.026	0.103	0.285	0.231	0.206
Date Pressurized	9/4/98	9/4/98	9/4/98	9/4/98	6/26/98	10/9/98	10/9/98	10/9/98	
50 Cycles	m_{50} , g	3202.5	3188.5	3231.5	9622.5	15791.0	15869.5	15780.0	47440.5
	$m_{4_{50}}$, g	7.0	4.0	6.0	17.0	18.0	11.5	17.5	47.0
	PML_{50}	0.558	0.623	0.476	0.552	0.513	0.370	0.388	0.424
	n_{50}	555	574	622	1751	2898	2800	3016	8714
	$n_{4_{50}}$	19	17	14	50	36	26	36	98
	PF_{50}	1.165	1.304	1.125	1.197	0.275	0.321	0.331	0.309
HFI	429	383	444	418	1818	1558	1512	1618	

Source: ILDOT

Chamber psi: 1150

Size: 1/2"

Tested by: Mark Bendok

Table 6.3 WHFT 94 Mass Loss and Percent Fracture

Sample ID	Type of Rock	Freeze/Thaw		Mass Loss			Percent Fracture	
		Expansion (%)	Predicted Durability	Trial #	ML ₅₀	Average ML	PF ₅₀	Average
X-1	Dolo	0.006	Pass	1	0.201	0.207	0.243	0.219
				2	0.217		0.244	
				3	0.202		0.171	
X-5	Grav	0.057	Borderline	1	0.138	0.208	0.314	0.405
				2	0.223		0.455	
				3	0.264		0.445	
X-7	LS	0.055	Borderline	1	0.231	0.225	0.248	0.270
				2	0.215		0.319	
				3	0.230		0.244	
X-12	LS	0.117	Fail	1	0.558	0.552	1.165	1.198
				2	0.623		1.304	
				3	0.476		1.125	
X-31	Dolo	0.010	Pass	1	0.510	0.561	0.579	0.630
				2	0.617		0.659	
				3	0.555		0.651	
X-32	Dolo	0.038	Pass	1	0.795	0.681	0.085	0.086
				2	1.013		0.082	
				3	0.234		0.091	
X-41	LS	0.021	Pass	1	0.915	1.007	1.144	1.513
				2	1.151		1.803	
				3	0.954		1.592	
X-42	Dolo	0.006	Pass	1	0.492	0.482	0.559	0.464
				2	0.478		0.318	
				3	0.477		0.515	
X-98	LS	0.074	Fail	1	0.299	0.299	0.268	0.303
				2	0.298		0.462	
				3	0.299		0.178	
X-167	LS	0.020	Pass	1	0.638*	0.229	1.901*	0.389
				2	0.199		0.372	
				3	0.259		0.406	
X-262	LS	0.033	Pass	1	0.354	0.247	0.577	0.482
				2	0.215		0.454	
				3	0.173		0.416	
X-263	Grav	0.073	Fail	1	0.186	0.149	0.424	0.453
				2	0.152		0.488	
				3	0.109		0.446	

* Value not used in computing average due to wide variation

Freeze/Thaw Failure Criteria: Pass : < 0.060, Fail : > 0.060

Table 6.3 WHFT 94 Mass Loss and Percent Fracture (continued)

Sample ID	Type of Rock	Freeze/Thaw		Mass Loss			Percent Fracture	
		Expansion (%)	Predicted Durability	Trial #	ML ₅₀	Average ML	PF ₅₀	Average
X-264	ACBF	0.008	Pass	1	1.239	1.369	2.336	4.469
				2	1.590		6.857	
				3	1.277		4.214	
X-275	Grav	0.029	Pass	1	0.387	0.196	0.535	0.480
				2	0.062		0.489	
				3	0.140		0.416	
X-277	Dolo	0.006	Pass	1	0.339	0.330	1.458	0.614
				2	0.278		0.078	
				3	0.373		0.305	
X-281	LS	0.066	Fail	1	0.349	0.318	0.595	0.506
				2	0.372		0.489	
				3	0.234		0.433	
X-282	Dolo	0.007	Pass	1	0.335*	0.305	0.718*	0.434
				2	0.245		0.425	
				3	0.366		0.442	
X-285	Grav	0.010	Pass	1	0.232	0.331	0.072	0.079
				2	0.280		0.081	
				3	0.481		0.083	
X-290	Dolo	0.004	Pass	1	0.262	0.338	0.221	0.223
				2	0.299		0.214	
				3	0.453		0.234	
X-305	LS	0.022	Pass	1	0.188	0.277	0.244	0.223
				2	0.293		0.158	
				3	0.351		0.268	
X-309	LS	0.085	Fail	1	0.299	0.270	0.074	0.074
				2	0.307		0.073	
				3	0.203		0.076	

* Value not used in computing average due to wide variation

Freeze/Thaw Failure Criteria: Pass : < 0.060, Fail : > 0.060

Table 6.4 WHFT 94 Individual HFI Results

Sample ID	Type of Rock	Freeze/Thaw		Percent Fracture			Hydraulic Fracture Index			
		Expansion (%)	Predicted Durability	Trial #	PF ₅₀	Average	10%	5%	2%	1.5%
X-1	Dolo	0.006	Pass	1	0.243	0.219	2057	1028	411	309
				2	0.244		2047	1023	409	307
				3	0.171		2926	1463	585	439
X-5	Grav	0.057	Borderline	1	0.314	0.405	1592	796	318	239
				2	0.455		1099	549	220	165
				3	0.445		1124	562	225	169
X-7	LS	0.055	Borderline	1	0.248	0.270	2020	1010	404	303
				2	0.319		1567	784	313	235
				3	0.244		2053	1027	411	308
X-12	LS	0.117	Fail	1	1.165	1.198	429	215	86	64
				2	1.304		383	192	77	58
				3	1.125		444	222	89	67
X-31	Dolo	0.010	Pass	1	0.579	0.630	864	432	173	130
				2	0.659		759	379	152	114
				3	0.651		768	384	154	115
X-32	Dolo	0.038	Pass	1	0.085	0.086	5882	2941	1176	882
				2	0.082		6098	3049	1220	915
				3	0.091		5495	2747	1099	824
X-41	LS	0.021	Pass	1	1.144	1.513	437	219	87	66
				2	1.803		277	139	55	42
				3	1.592		314	157	63	47
X-42	Dolo	0.006	Pass	1	0.559	0.464	894	447	179	134
				2	0.318		1572	786	314	236
				3	0.515		971	485	194	146
X-98	LS	0.074	Fail	1	0.268	0.303	1864	932	373	280
				2	0.462		1082	541	216	162
				3	0.178		2815	1408	563	422
X-167	LS	0.020	Pass	1	1.901	0.893	263	131	53	39
				2	0.372		1344	672	269	202
				3	0.406		1232	616	246	185
X-262	LS	0.033	Pass	1	0.577	0.482	867	434	173	130
				2	0.454		1102	551	220	165
				3	0.416		1202	601	240	180
X-263	Grav	0.073	Fail	1	0.424	0.453	1180	590	236	177
				2	0.488		1025	512	205	154
				3	0.446		1121	561	224	168

Freeze/Thaw Failure Criteria:

Pass : < 0.060, Fail : > 0.060

HFI Failure Criteria:

Pass : > 200, Fail : < 200

Table 6.4 WHFT 94 Individual HFI Results (continued)

Sample ID	Type of Rock	Freeze/Thaw		Percent Fracture			Hydraulic Fracture Index			
		Expansion (%)	Predicted Durability	Trial #	PF ₅₀	Average	10%	5%	2%	1.5%
X-264	ACBF	0.008	Pass	1	2.336	4.469	214	107	46	40
				2	6.857		73	28	20	13
				3	4.214		119	59	17	15
X-275	Grav	0.029	Pass	1	0.535	0.480	935	467	187	140
				2	0.489		1022	511	204	153
				3	0.416		1202	601	240	180
X-277	Dolo	0.006	Pass	1	1.458	0.614	343	171	69	51
				2	0.078		6410	3205	1282	962
				3	0.305		1639	820	328	246
X-281	LS	0.066	Fail	1	0.595	0.506	840	420	168	126
				2	0.489		1022	511	204	153
				3	0.433		1155	577	231	173
X-282	Dolo	0.007	Pass	1	0.718	0.528	697	348	139	105
				2	0.425		1176	588	235	176
				3	0.442		1131	566	226	170
X-285	Grav	0.010	Pass	1	0.072	0.079	6944	3472	1389	1042
				2	0.081		6173	3086	1235	926
				3	0.083		6024	3012	1205	904
X-290	Dolo	0.004	Pass	1	0.221	0.223	2263	1132	453	340
				2	0.214		2333	1167	467	350
				3	0.234		2137	1068	427	321
X-305	LS	0.022	Pass	1	0.244	0.223	2047	1023	409	307
				2	0.158		3171	1585	634	476
				3	0.268		1866	933	373	280
X-309	LS	0.085	Fail	1	0.074	0.074	6757	3378	1351	1014
				2	0.073		6849	3425	1370	1027
				3	0.076		6579	3289	1316	987

Freeze/Thaw Failure Criteria:

Pass : < 0.060, Fail : > 0.060

HFI Failure Criteria:

Pass : > 200, Fail : < 200

Table 6.5 WHFT 97 Mass Loss and Percent Fracture

Sample ID	Type of Rock	Freeze/Thaw		Mass Loss			Percent Fracture	
		Expansion (%)	Predicted Durability	Trial #	ML ₅₀	Average ML	PF ₅₀	Average
X-1	Dolo	0.006	Pass	1	0.296	0.280	0.122	0.165
				2	0.289		0.155	
				3	0.255		0.219	
X-5	Grav	0.057	Borderline	1	0.278	0.333	0.382	0.406
				2	0.442		0.330	
				3	0.280		0.507	
X-7	LS	0.055	Borderline	1	0.268	0.313	0.176	0.205
				2	0.318		0.190	
				3	0.353		0.250	
X-12	LS	0.117	Fail	1	0.513	0.424	0.275	0.309
				2	0.370		0.321	
				3	0.388		0.331	
X-31	Dolo	0.010	Pass	1	0.435	0.435	0.046	0.046
				2				
				3				
X-32	Dolo	0.038	Pass	1	0.339	0.313	0.067	0.075
				2	0.288		0.082	
				3				
X-41	LS	0.021	Pass	1	0.570	0.570	0.774	0.774
				2				
				3				
X-42	Dolo	0.006	Pass	1	0.503	0.458	0.313	0.329
				2	0.495		0.352	
				3	0.376		0.322	
X-98	LS	0.074	Fail	1	0.264	0.226	0.193	0.154
				2	0.195		0.139	
				3	0.219		0.129	
X-167	LS	0.020	Pass	1	0.141	0.213	0.437	0.376
				2	0.237		0.355	
				3	0.261		0.337	
X-262	LS	0.033	Pass	1	0.269	0.233	0.103	0.105
				2	0.210		0.107	
				3	0.220		0.105	
X-263	Grav	0.073	Fail	1	0.220	0.220	0.631	0.631
				2				
				3				

Freeze/Thaw Failure Criteria: Pass : < 0.060, Fail : > 0.060

Table 6.5 WHFT 97 Mass Loss and Percent Fracture (continued)

Sample ID	Type of Rock	Freeze/Thaw		Mass Loss			Percent Fracture	
		Expansion (%)	Predicted Durability	Trial #	ML ₅₀	Average ML	PF ₅₀	Average
X-264	ACBF	0.008	Pass	1	0.829	0.881	0.301	0.299
				2	0.932		0.297	
				3				
X-275	Grav	0.029	Pass	1	0.229	0.201	0.350	0.329
				2	0.219		0.302	
				3	0.156		0.334	
X-277	Dolo	0.006	Pass	1	0.181	0.187	0.198	0.160
				2	0.178		0.151	
				3	0.202		0.131	
X-281	LS	0.066	Fail	1	0.384	0.300	0.182	0.161
				2	0.293		0.160	
				3	0.223		0.142	
X-282	Dolo	0.007	Pass	1	0.452	0.336	0.365	0.221
				2	0.264		0.134	
				3	0.293		0.164	
X-285	Grav	0.010	Pass	1	0.288	0.288	0.108	0.108
				2				
				3				
X-290	Dolo	0.004	Pass	1	0.285	0.257	0.280	0.257
				2	0.228		0.234	
				3				
X-305	LS	0.022	Pass	1	0.268	0.266	0.127	0.153
				2	0.262		0.144	
				3	0.268		0.188	
X-309	LS	0.085	Fail	1	0.309	0.239	0.076	0.080
				2	0.211		0.082	
				3	0.197		0.081	

Freeze/Thaw Failure Criteria: Pass : < 0.060, Fail : > 0.060

Table 6.6 WHFT 97 Individual HFI Results

Sample ID	Type of Rock	Freeze/Thaw		Percent Fracture			Hydraulic Fracture Index			
		Expansion (%)	Predicted Durability	Trial #	PF ₅₀	Average	10%	5%	2%	1.5%
X-1	Dolo	0.006	Pass	1	0.122	0.165	4095	2048	819	614
				2	0.155		3226	1613	645	484
				3	0.219		2284	1142	457	343
X-5	Grav	0.057	Borderline	1	0.382	0.406	1309	654	262	196
				2	0.330					
				3	0.507					
X-7	LS	0.055	Borderline	1	0.176	0.205	2841	1420	568	426
				2	0.190		2632	1316	526	395
				3	0.250					
X-12	LS	0.117	Fail	1	0.275	0.309	1818	909	364	273
				2	0.321		1558	779	312	234
				3	0.331		1511	755	302	227
X-31	Dolo	0.010	Pass	1	0.046	0.046	1087	5435	2174	1630
				2						
				3						
X-32	Dolo	0.038	Pass	1	0.067	0.075	7463	3731	1493	1119
				2	0.082		6098	3049	1220	915
				3						
X-41	LS	0.021	Pass	1	0.774	0.774	646	323	129	97
				2						
				3						
X-42	Dolo	0.006	Pass	1	0.313	0.329	1598	799	320	240
				2	0.352		1420	710	284	213
				3	0.322		1553	776	311	233
X-98	LS	0.074	Fail	1	0.193	0.154	2591	1295	518	389
				2	0.139		3597	1799	719	540
				3	0.129		3876	1938	775	581
X-167	LS	0.020	Pass	1	0.437	0.376	1143	572	229	171
				2	0.355		1408	704	282	211
				3	0.337		1484	742	297	223
X-262	LS	0.033	Pass	1	0.103	0.105	4864	2432	973	730
				2	0.107		4673	2336	935	701
				3	0.105		4762	2381	952	714
X-263	Grav	0.073	Fail	1	0.631	0.631	793	396	159	119
				2						
				3						

Freeze/Thaw Failure Criteria:
HFI Failure Criteria:

Pass : < 0.060, Fail : > 0.060
Pass : > 200, Fail : < 200

Table 6.6 WHFT 97 Individual HFI Results (continued)

Sample ID	Type of Rock	Freeze/Thaw		Percent Fracture			Hydraulic Fracture Index			
		Expansion (%)	Predicted Durability	Trial #	PF ₅₀	Avg.	10%	5%	2%	1.5%
X-264	ACBF	0.008	Pass	1	0.301	0.299	1661	831	332	249
				2	0.297		1684	842	337	253
				3						
X-275	Grav	0.029	Pass	1	0.350	0.329	1429	714	286	214
				2	0.302		1656	828	331	248
				3	0.334		1497	749	299	225
X-277	Dolo	0.006	Pass	1	0.198	0.160	2525	1263	505	379
				2	0.151		3311	1656	662	497
				3	0.131					
X-281	LS	0.066	Fail	1	0.182	0.161	2755	1377	551	413
				2	0.160		3125	1563	625	469
				3	0.142		3521	1761	704	528
X-282	Dolo	0.007	Pass	1	0.365	0.221	1368	684	274	205
				2	0.134		3731	1866	746	560
				3	0.164		3049	1524	610	457
X-285	Grav	0.010	Pass	1	0.108	0.108	4630	2315	926	694
				2						
				3						
X-290	Dolo	0.004	Pass	1	0.280	0.257	1786	893	357	268
				2	0.234		2137	1068	427	321
				3						
X-305	LS	0.022	Pass	1	0.127	0.153	3937	1969	787	591
				2	0.144		3472	1736	694	521
				3	0.188		2660	1330	532	399
X-309	LS	0.085	Fail	1	0.076	0.080	6579	3289	131	987
				2	0.082		6098	3049	122	915
				3	0.081		6173	3086	123	926

Freeze/Thaw Failure Criteria:
HFI Failure Criteria:

Pass : < 0.060, Fail : > 0.060
Pass : > 200, Fail : < 200

Table 6.7 WHFT 94 Average HFI Results

Sample ID	Type of Rock	Freeze/Thaw		Percent Fracture PF ₅₀	Hydraulic Fracture Index			
		Expansion (%)	Predicted Durability		10%	5%	2%	1.5%
X-1	Dolo	0.006	Pass	0.219	2283	1142	457	342
X-5	Grav	0.057	Borderline	0.405	1235	617	247	185
X-7	LS	0.055	Borderline	0.270	1852	926	370	278
X-12	LS	0.117	Fail	1.198	417	209	83	63
X-31	Dolo	0.010	Pass	0.630	794	397	159	119
X-32	Dolo	0.038	Pass	0.086	5814	2907	1163	872
X-41	LS	0.021	Pass	1.513	330	165	66	50
X-42	Dolo	0.006	Pass	0.464	1078	539	216	162
X-98	LS	0.074	Fail	0.303	1650	825	330	248
X-167	LS	0.020	Pass	0.389	1285	643	257	193
X-262	LS	0.033	Pass	0.482	1037	519	207	156
X-263	Grav	0.073	Fail	0.453	1104	552	221	166

Freeze/Thaw Failure Criteria:

Pass : < 0.060, Fail : > 0.060

HFI Failure Criteria:

Pass : > 200, Fail : < 200

Table 6.7 WHFT 94 Average HFI Results (continued)

Sample ID	Type of Rock	Freeze/Thaw		Percent Fracture PF ₅₀	Hydraulic Fracture Index			
		Expansion (%)	Predicted Durability		10%	5%	2%	1.5%
X-264	ACBF	0.008	Pass	4.469	72	40	21	18
X-275	Grav	0.029	Pass	0.480	1042	521	208	156
X-277	Dolo	0.006	Pass	0.614	814	407	163	122
X-281	LS	0.066	Fail	0.506	988	494	198	148
X-282	Dolo	0.007	Pass	0.434	1152	576	230	173
X-285	Grav	0.010	Pass	0.079	6329	3165	1266	949
X-290	Dolo	0.004	Pass	0.223	2242	1121	448	336
X-305	LS	0.022	Pass	0.223	2242	1121	448	336
X-309	LS	0.085	Fail	0.074	6757	3378	1351	1014

Freeze/Thaw Failure Criteria:

Pass : < 0.060, Fail : > 0.060

HFI Failure Criteria:

Pass : > 200, Fail : < 200

Table 6.8 WHFT 97 Average HFI Results

Sample ID	Type of Rock	Freeze/Thaw		Percent Fracture	Hydraulic Fracture Index			
		Expansion (%)	Predicted Durability	PF ₅₀	10%	5%	2%	1.5%
X-1	Dolo	0.006	Pass	0.165	3030	1515	606	455
X-5	Grav	0.057	Borderline	0.406	1232	616	246	185
X-7	LS	0.055	Borderline	0.205	2439	1220	488	366
X-12	LS	0.117	Fail	0.309	1618	809	324	243
X-31	Dolo	0.010	Pass	0.046	10870	5435	2174	1630
X-32	Dolo	0.038	Pass	0.075	6667	3333	1333	1000
X-41	LS	0.021	Pass	0.774	646	323	129	97
X-42	Dolo	0.006	Pass	0.329	1520	760	304	228
X-98	LS	0.074	Fail	0.154	3247	1623	649	487
X-167	LS	0.020	Pass	0.376	1330	665	266	199
X-262	LS	0.033	Pass	0.105	4762	2381	952	714
X-263	Grav	0.073	Fail	0.631	792	396	158	119

Freeze/Thaw Failure Criteria:

Pass : < 0.060, Fail : > 0.060

HFI Failure Criteria:

Pass : > 200, Fail : < 200

Table 6.8 WHFT 97 Average HFI Results (continued)

Sample ID	Type of Rock	Freeze/Thaw		Percent Fracture	Hydraulic Fracture Index			
		Expansion (%)	Predicted Durability	PF ₅₀	10%	5%	2%	1.5%
X-264	ACBF	0.008	Pass	0.299	1672	836	334	251
X-275	Grav	0.029	Pass	0.329	1520	760	304	228
X-277	Dolo	0.006	Pass	0.160	3125	1563	625	469
X-281	LS	0.066	Fail	0.161	3106	1553	621	466
X-282	Dolo	0.007	Pass	0.221	2262	1131	452	339
X-285	Grav	0.010	Pass	0.108	4630	2315	926	694
X-290	Dolo	0.004	Pass	0.257	1946	973	389	292
X-305	LS	0.022	Pass	0.153	3268	1634	654	490
X-309	LS	0.085	Fail	0.080	6250	3125	1250	938

Freeze/Thaw Failure Criteria:

Pass : < 0.060, Fail : > 0.060

HFI Failure Criteria:

Pass : > 200, Fail : < 200

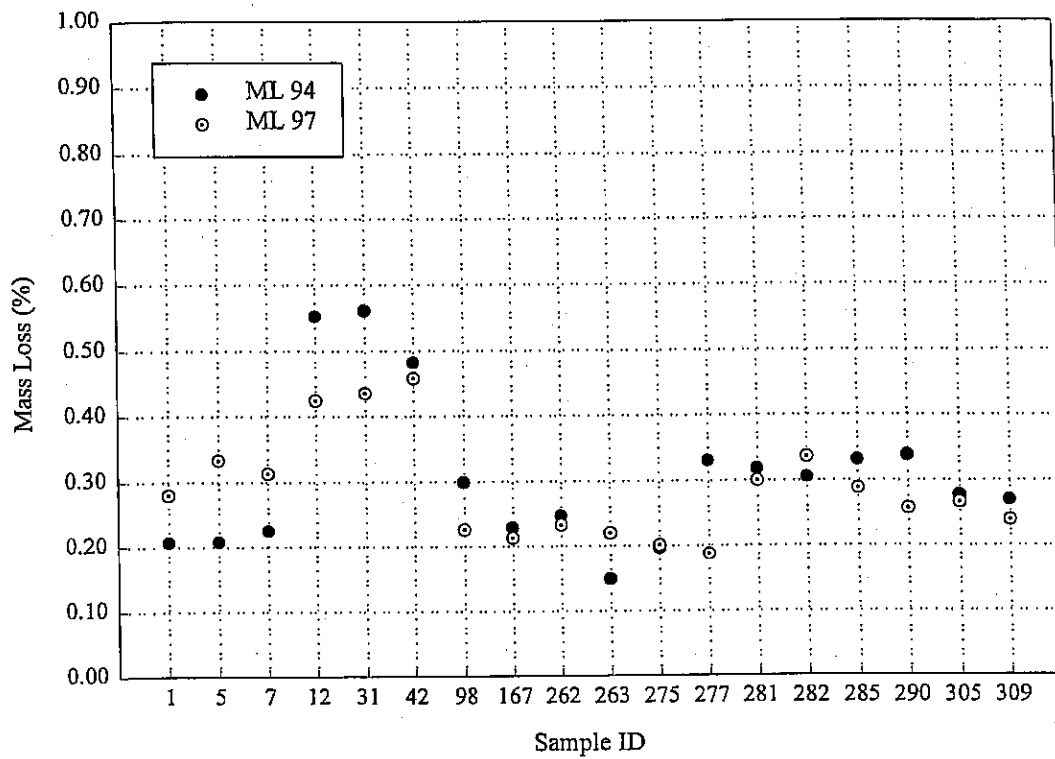


Fig. 6.1 Comparison of Mass Loss (ML)

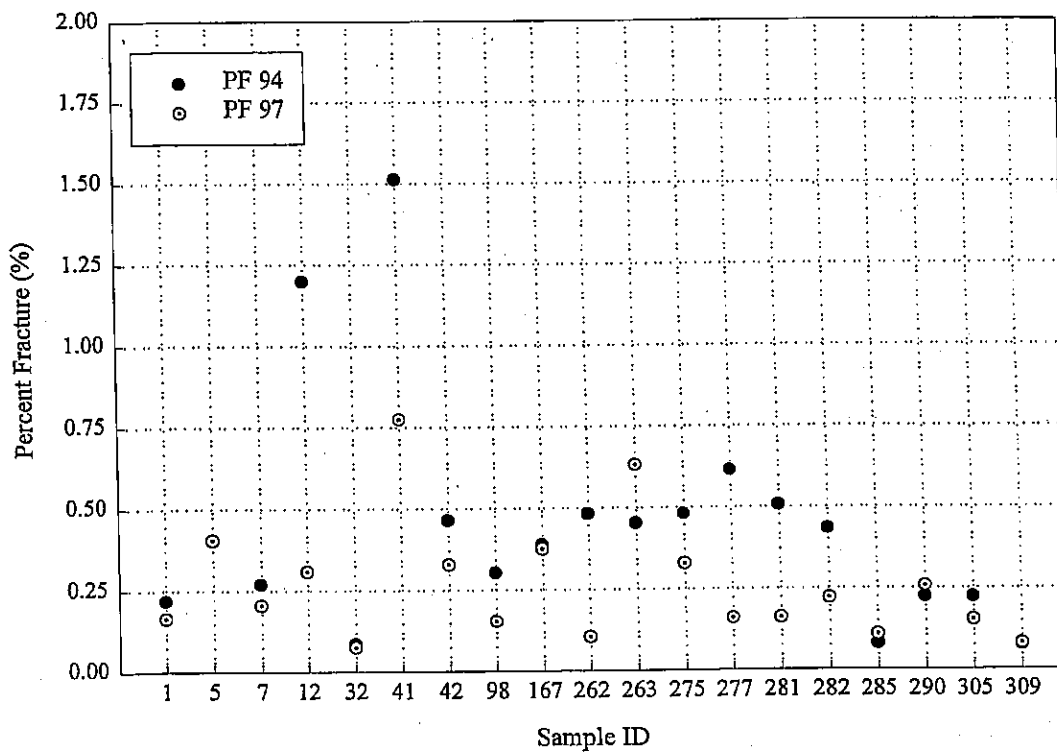


Fig. 6.2 Comparison of Percent Fracture (PF)

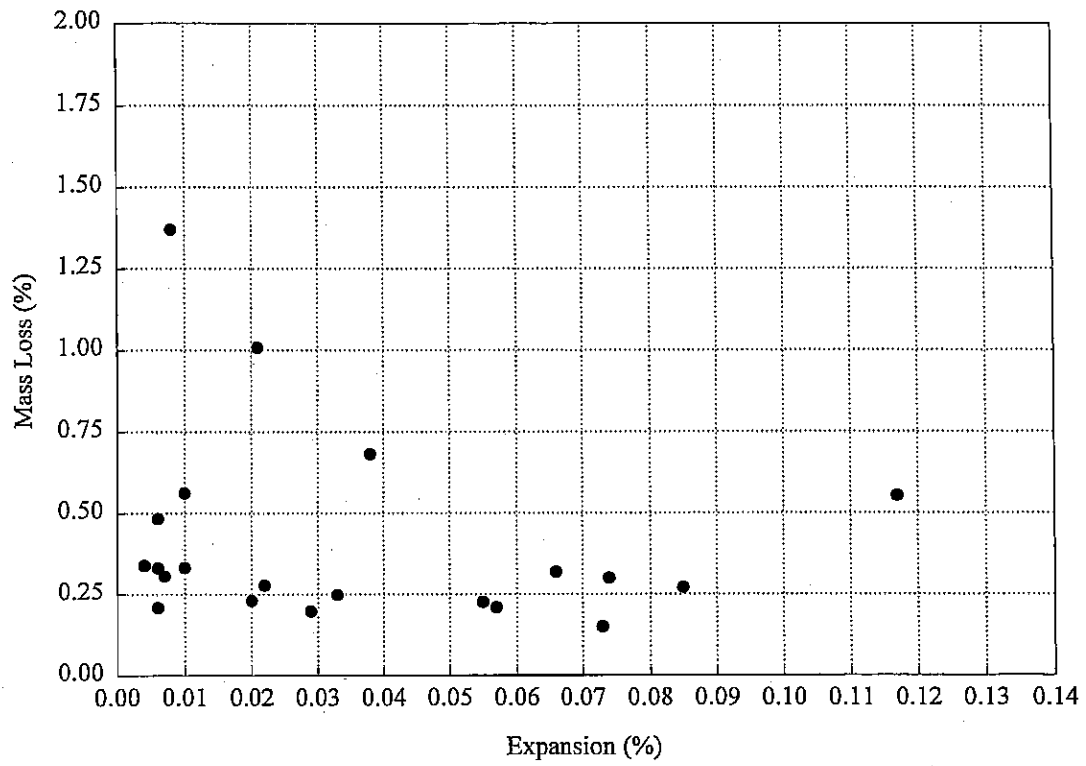


Fig. 6.3 WHFT 94 Mass Loss versus ASTM C666 (ILDOT modified) Percent Expansion

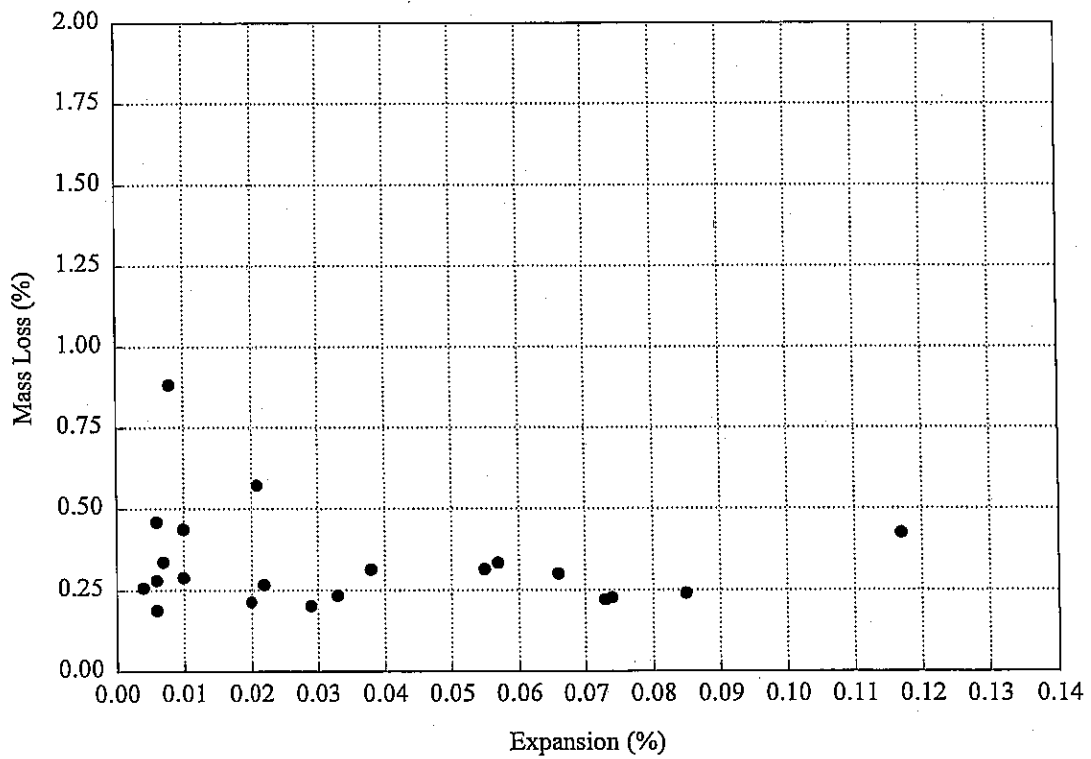


Fig. 6.4 WHFT 97 Mass Loss versus ASTM C666 (ILDOT modified) Percent Expansion

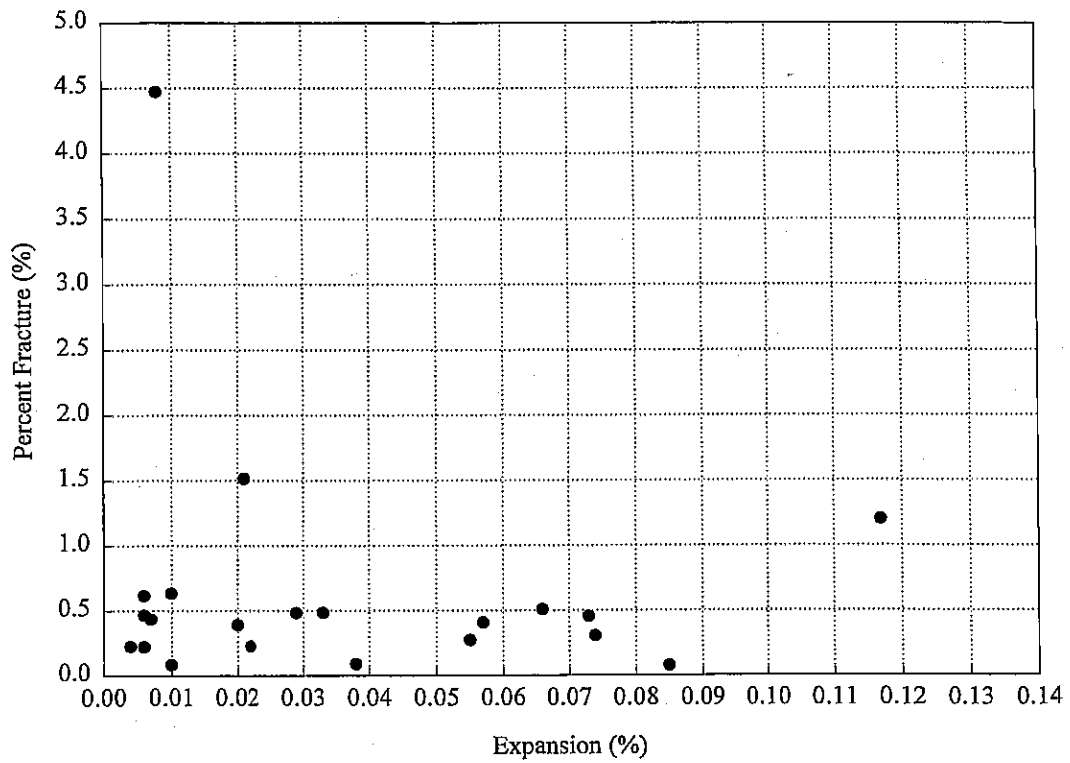


Fig. 6.5 WHFT 94 Percent Fracture versus ASTM C666 (ILDOT modified) Percent Expansion

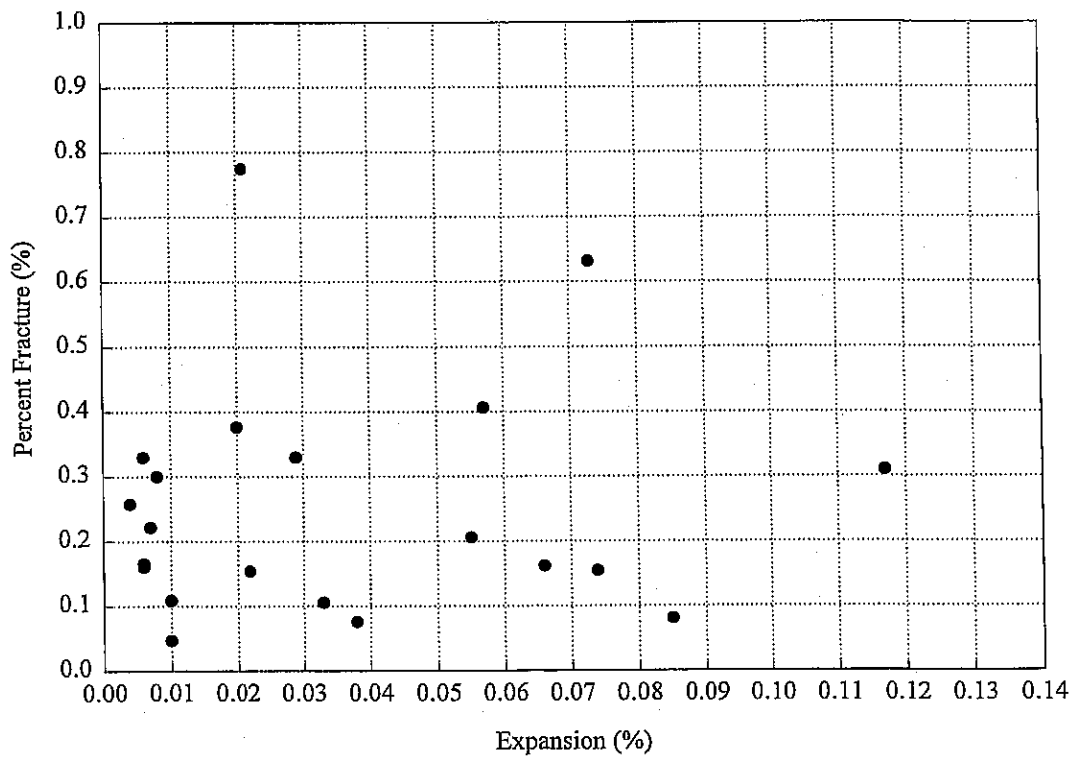


Fig. 6.6 WHFT 97 Percent Fracture versus ASTM C666 (ILDOT modified) Percent Expansion

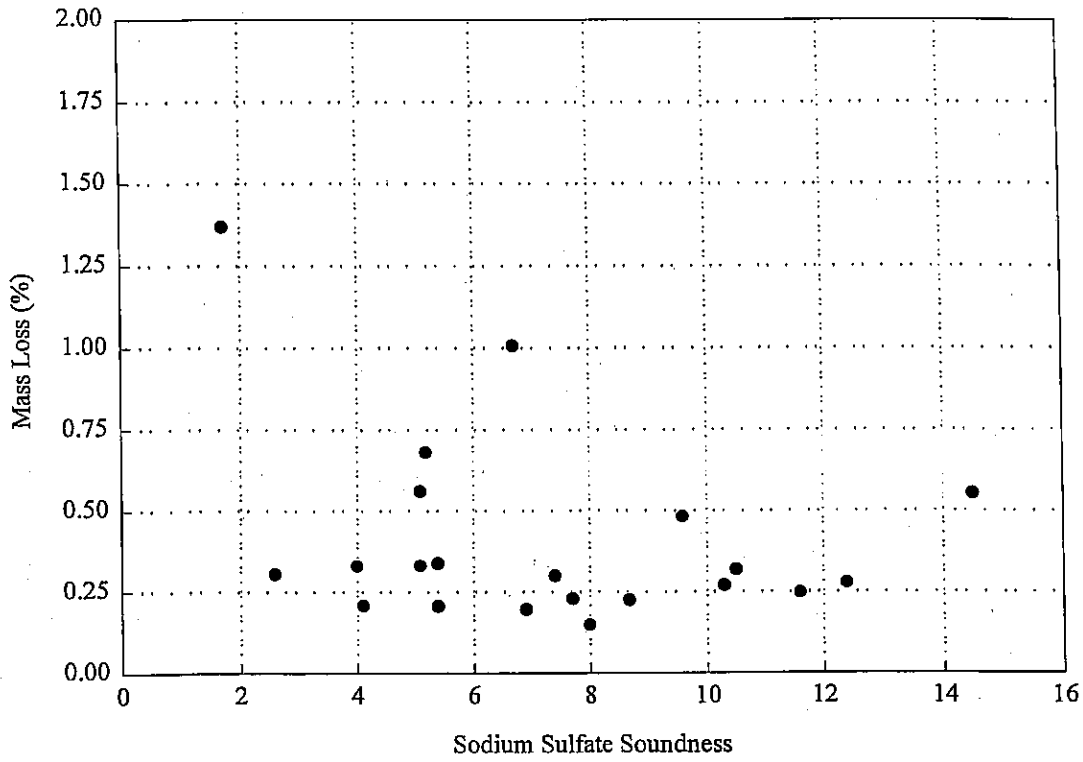


Fig. 6.7 WHFT 94 Mass Loss versus AASHTO T-104m Sodium Sulfate Soundness

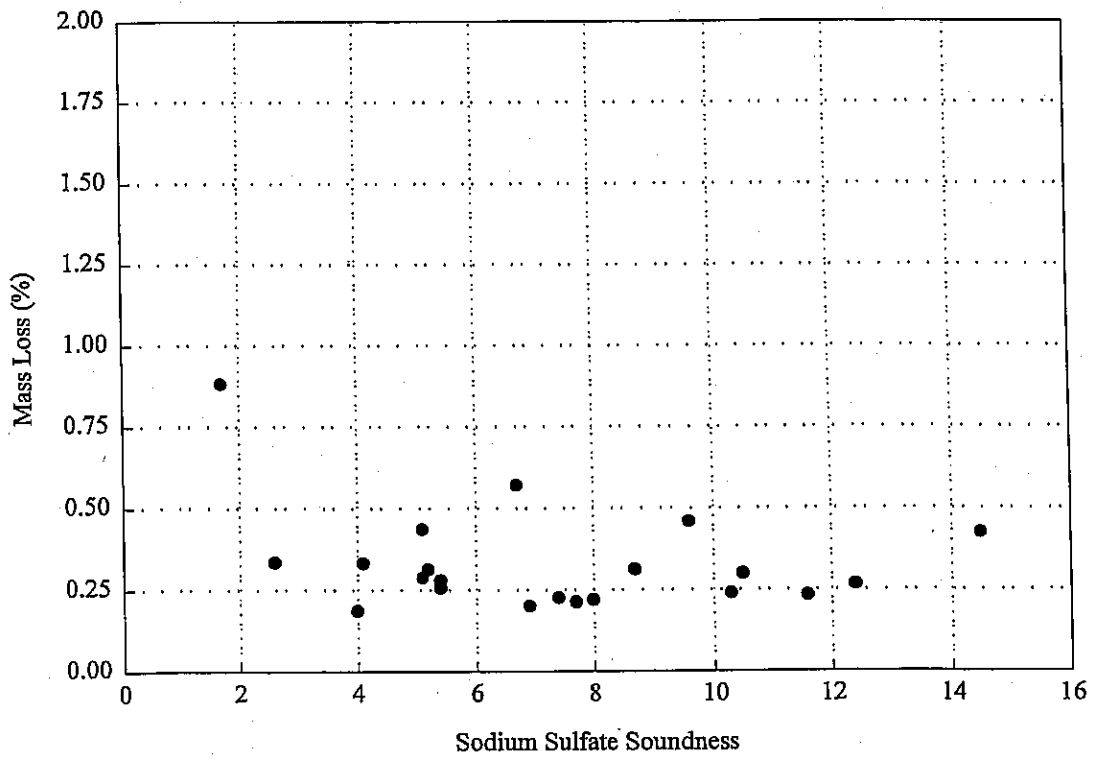


Fig. 6.8 WHFT 97 Mass Loss versus AASHTO T-104m Sodium Sulfate Soundness

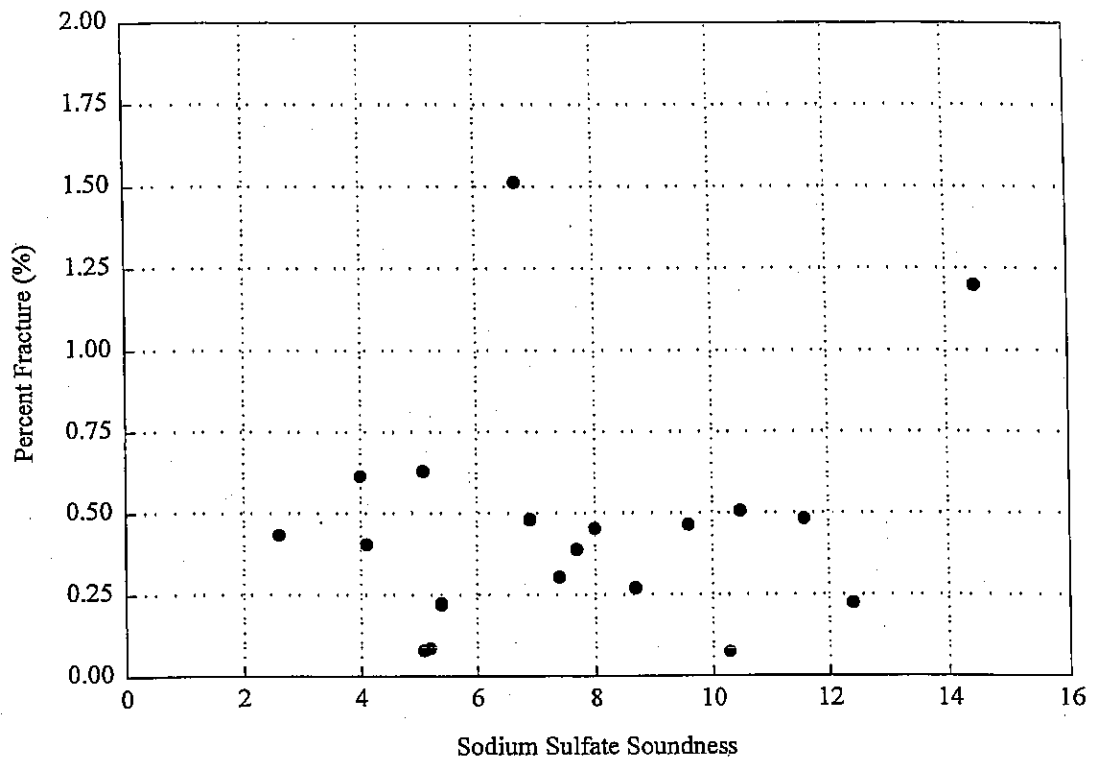


Fig. 6.9 WHFT 94 Percent Fracture versus AASHTO T-104m Sodium Sulfate Soundness

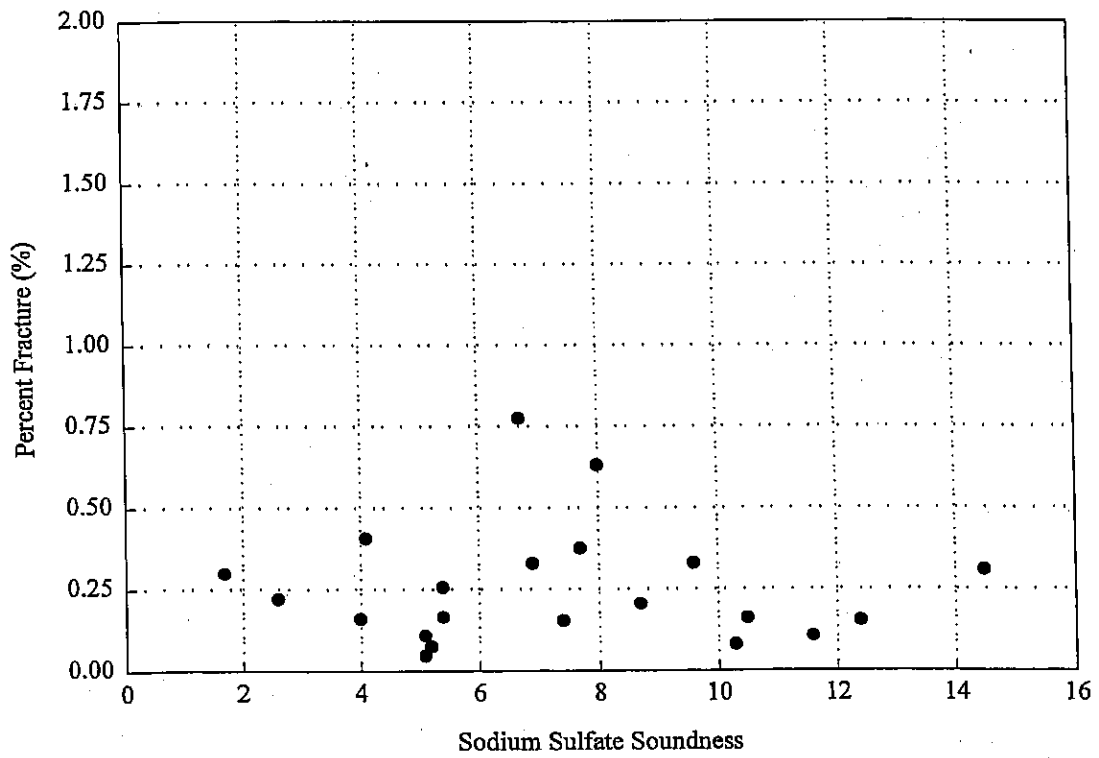


Fig. 6.10 WHFT 97 Percent Fracture versus AASHTO T-104m Sodium Sulfate Soundness

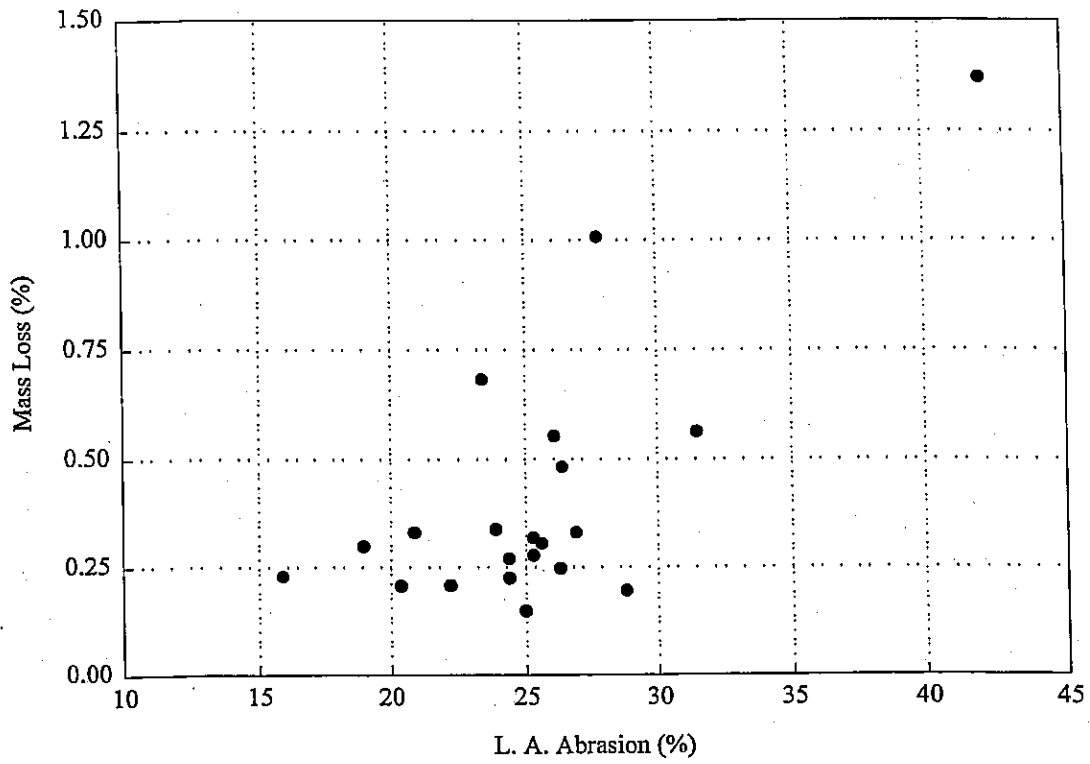


Fig. 6.11 WHFT 94 Mass Loss versus AASHTO T-96 L. A. Abrasion

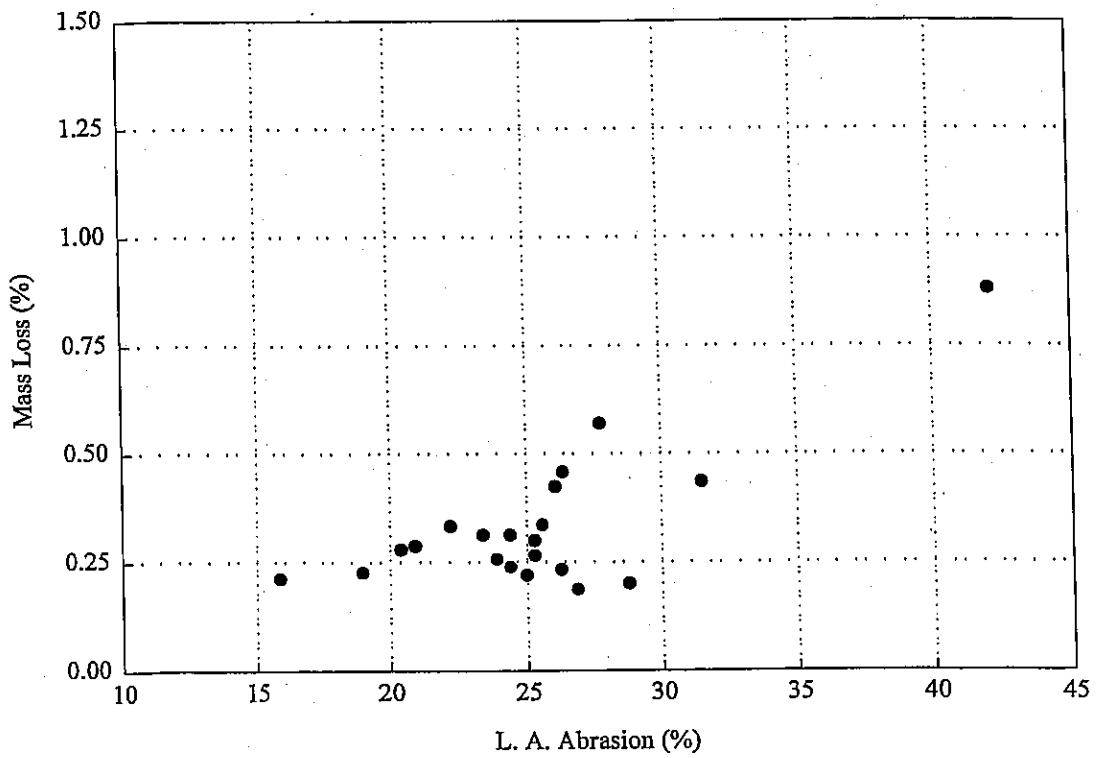


Fig. 6.12 WHFT 97 Mass Loss versus AASHTO T-96 L. A. Abrasion

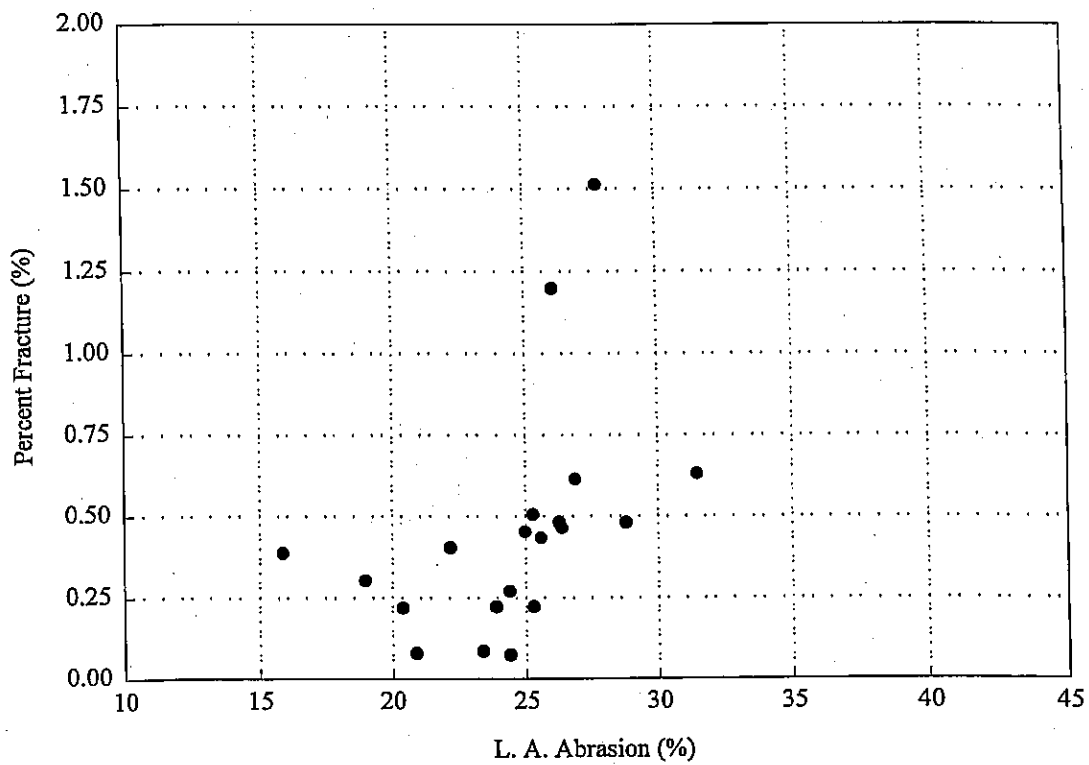


Fig. 6.13 WHFT 94 Percent Fracture versus AASHTO T-96 L. A. Abrasion

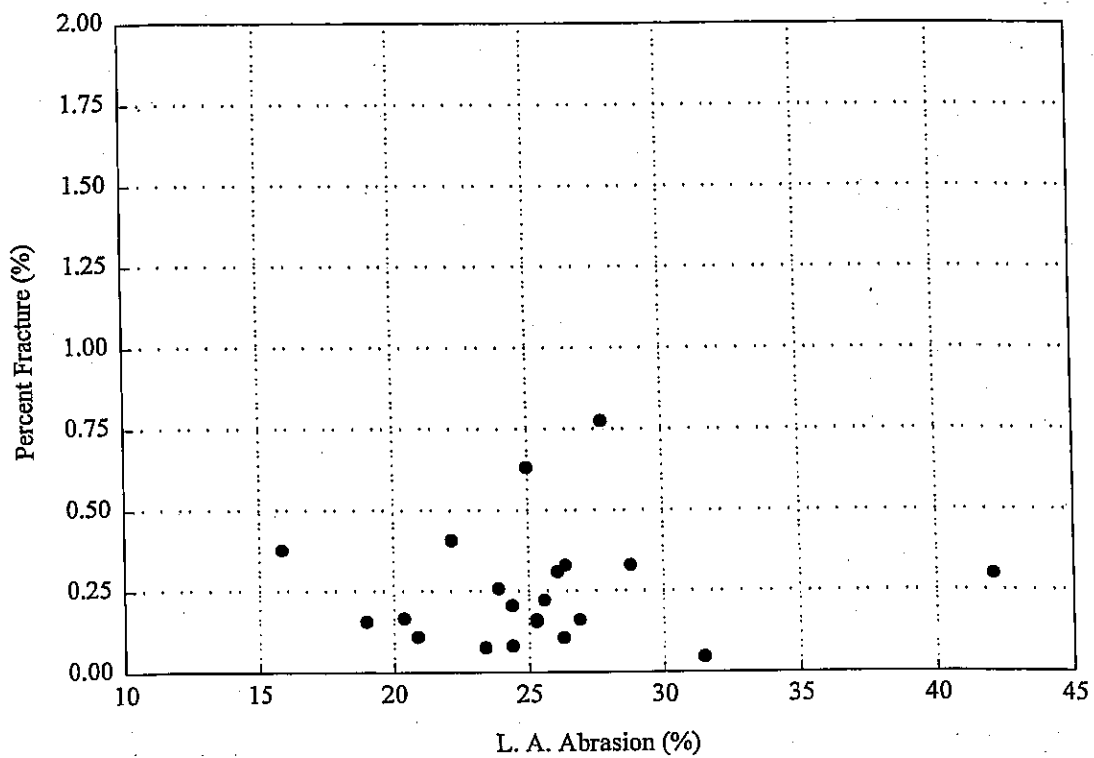


Fig. 6.14 WHFT 97 Percent Fracture versus AASHTO T-96 L. A. Abrasion

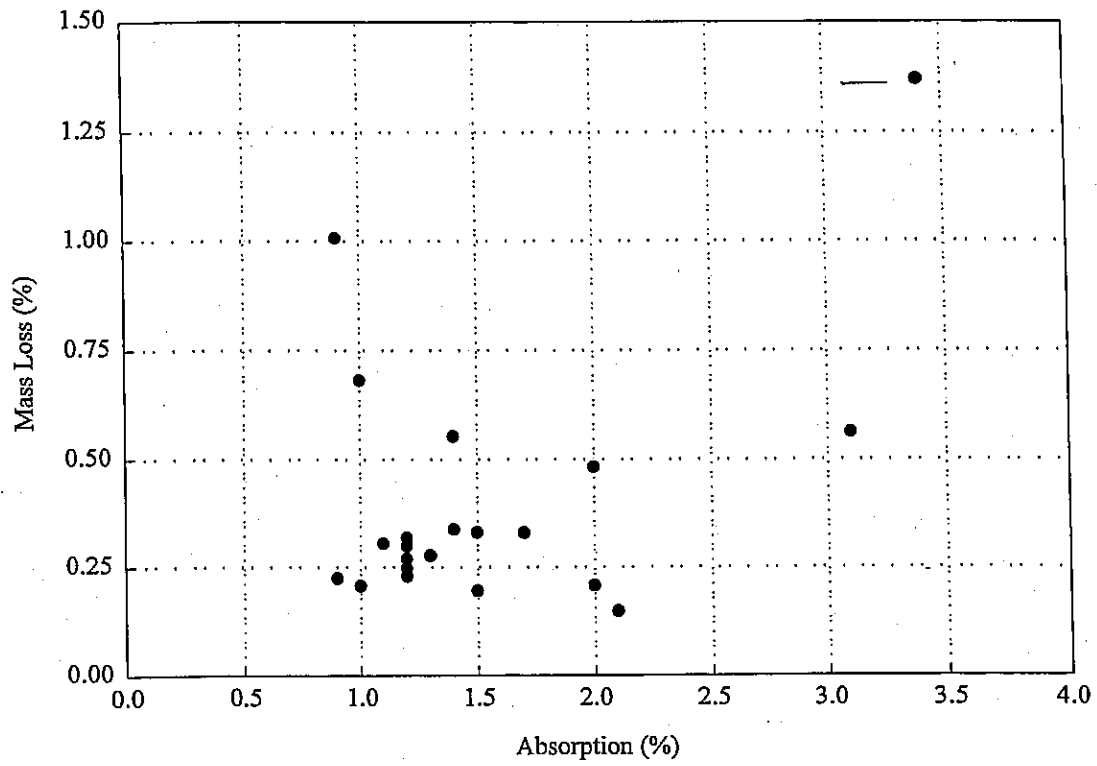


Fig. 6.15 WHFT 94 Mass Loss versus Percent Absorption

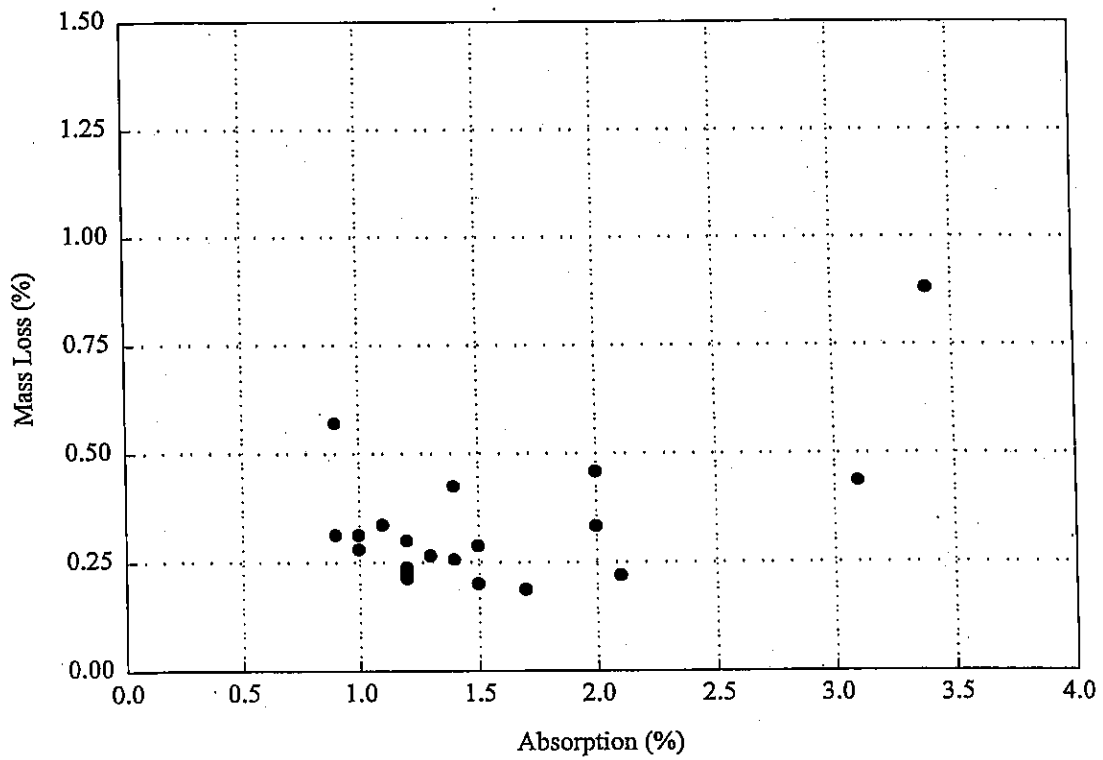


Fig. 6.16 WHFT 97 Mass Loss versus Percent Absorption

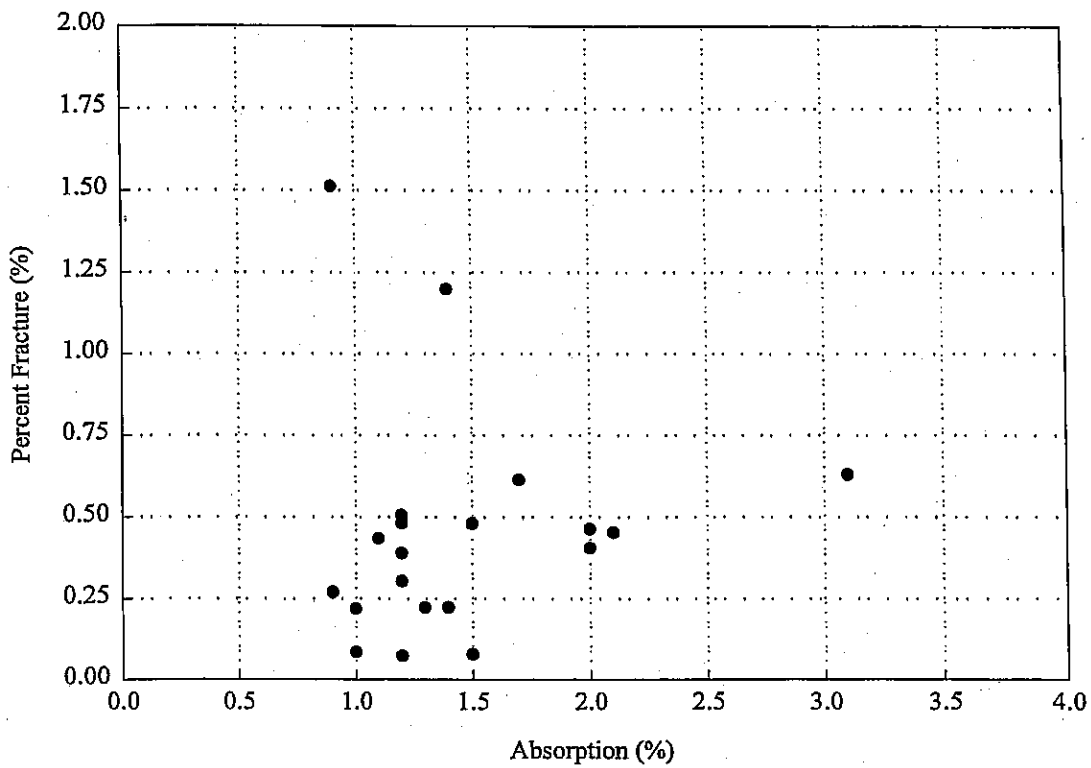


Fig. 6.17 WHFT 94 Percent Fracture versus Percent Absorption

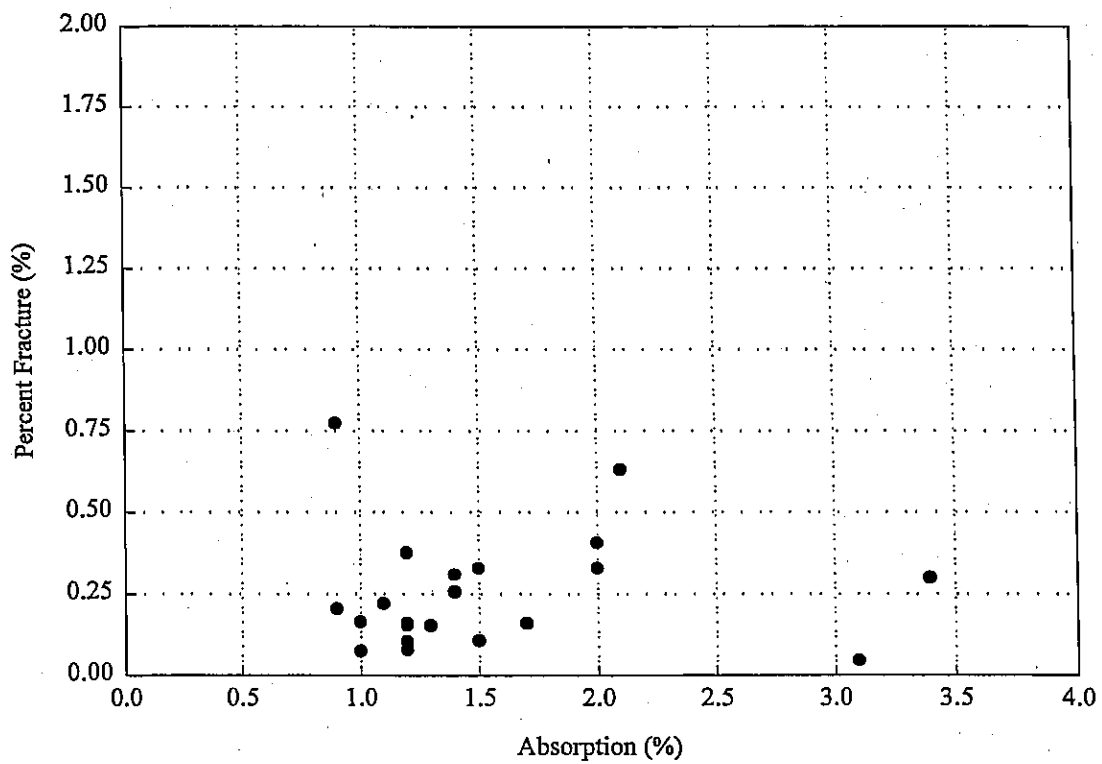


Fig. 6.18 WHFT 97 Percent Fracture versus Percent Absorption

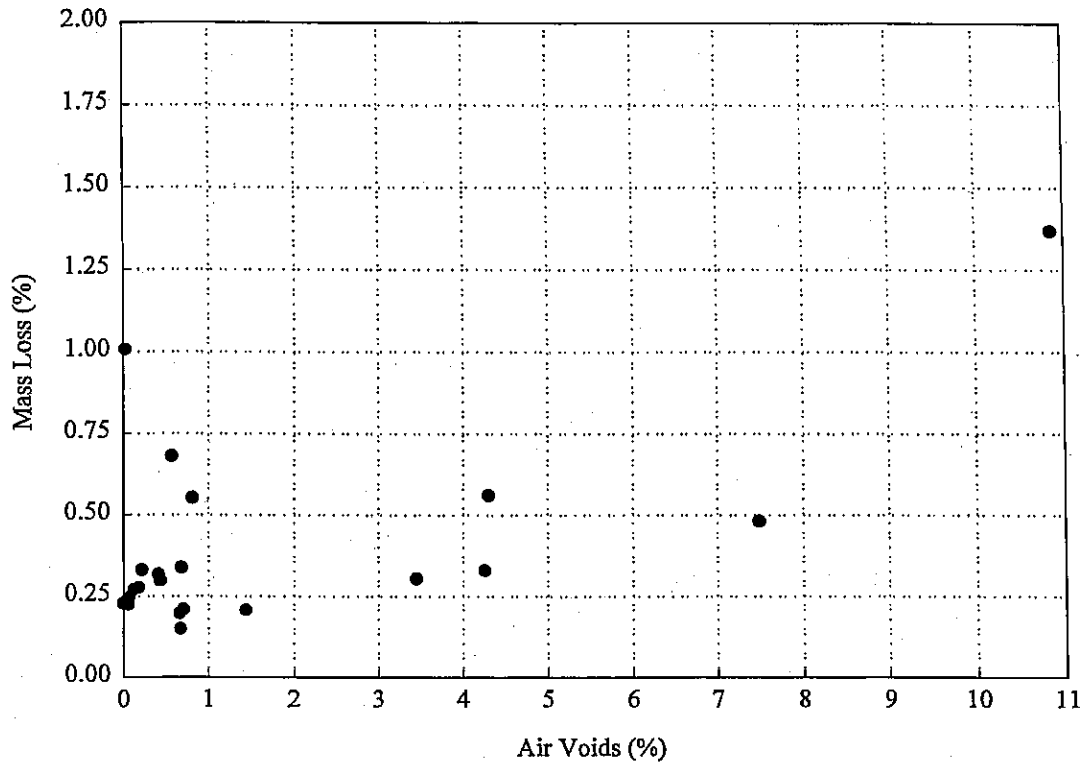


Fig. 6.19 WHFT 94 Mass Loss versus ASTM C457 Air Voids

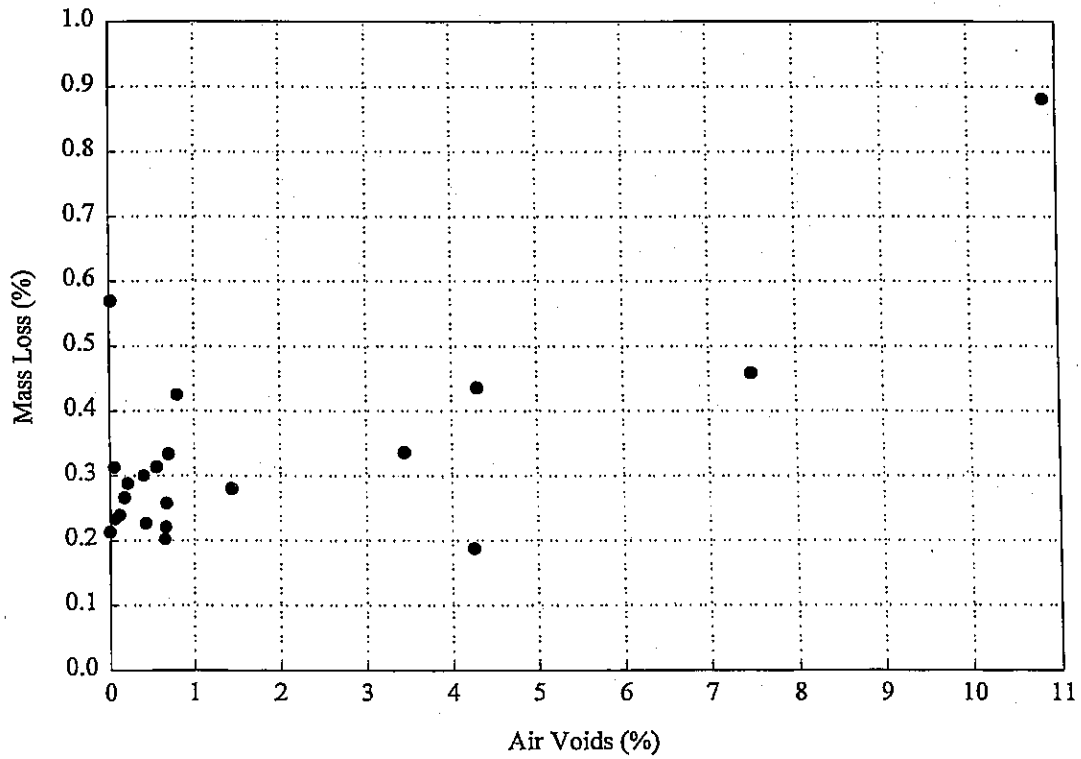


Fig. 6.20 WHFT 97 Mass Loss versus ASTM C457 Air Voids

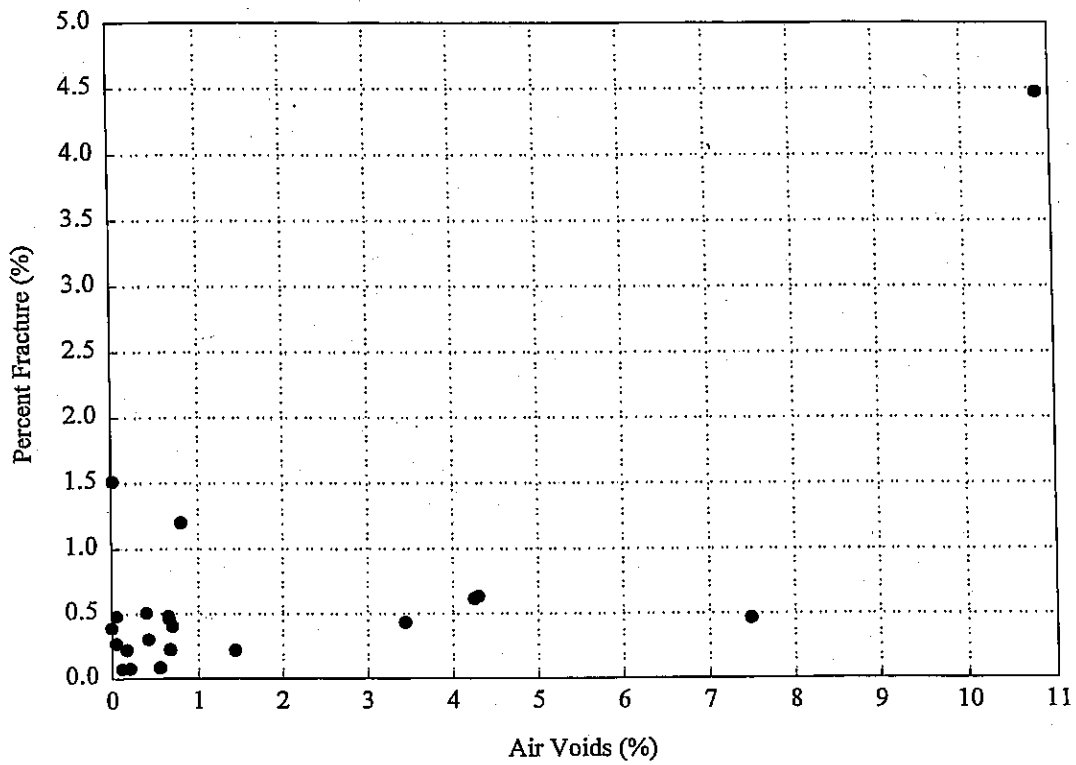
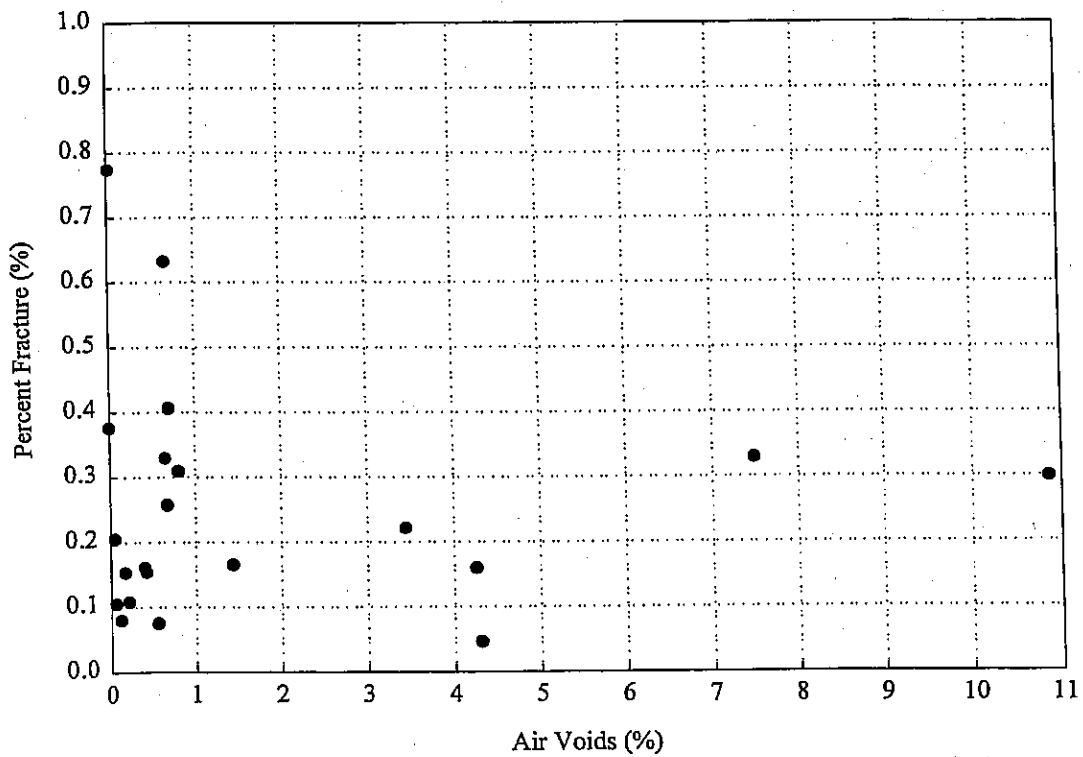


Fig. 6.21 WHFT 94 Percent Fracture versus ASTM C457 Air Voids



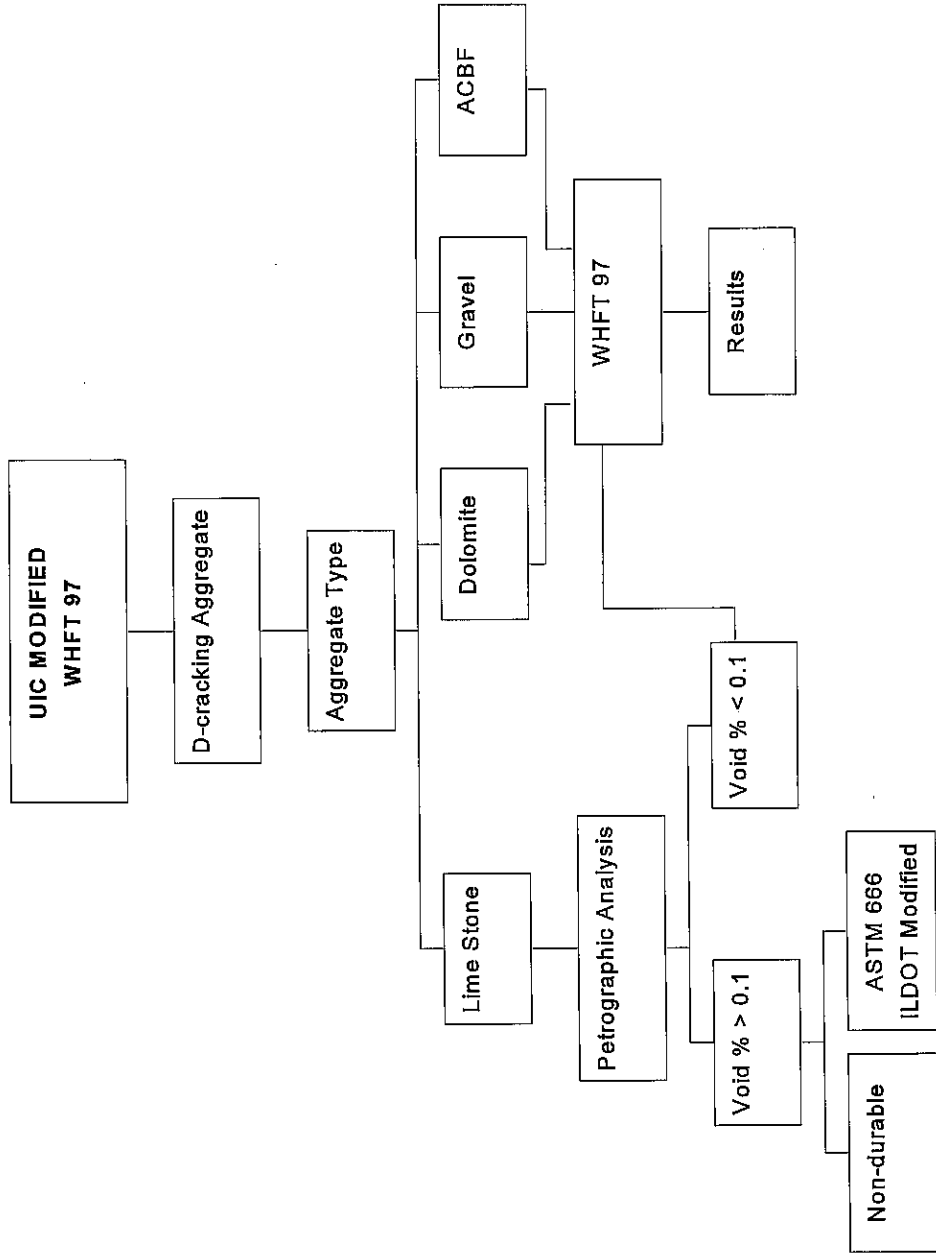


Fig. 6.23 Recommended WHFT 97 Procedure

Table 6.9 Comparison of Durability Factors Obtained by Freeze/Thaw, WHFT 94 and WHFT 97

Sample ID	Type Rock	Freeze/Thaw		WHFT 94		WHFT 97	
		Expansion (%)	Predicted Durability	2%		2%	
				HFI	Predicted Durability	HFI	Predicted Durability
X-1	Dolo	0.006	Pass	457	Pass	606	Pass
X-5	Grav	0.057	Borderline	247	Pass	246	Pass
X-7	LS	0.055	Borderline	370	Pass	488	Pass
X-12	LS	0.117	Fail	83	Fail	324	Pass
X-31	Dolo	0.010	Pass	159	Fail	2174	Pass
X-32	Dolo	0.038	Pass	1163	Pass	1333	Pass
X-41	LS	0.021	Pass	66	Fail	129	Fail
X-42	Dolo	0.006	Pass	216	Pass	304	Pass
X-98	LS	0.074	Fail	330	Pass	649	Pass
X-167	LS	0.020	Pass	257	Pass	266	Pass
X-262	LS	0.033	Pass	207	Pass	952	Pass
X-263	Grav	0.073	Fail	221	Pass	158	Fail
X-264	ACBF	0.008	Pass	21	Fail	334	Pass
X-275	Grav	0.029	Pass	208	Pass	304	Pass
X-277	Dolo	0.006	Pass	163	Fail	625	Pass
X-281	LS	0.066	Fail	198	Fail	621	Pass
X-282	Dolo	0.007	Pass	230	Pass	452	Pass
X-285	Grav	0.010	Pass	1266	Pass	926	Pass
X-290	Dolo	0.004	Pass	448	Pass	389	Pass
X-305	LS	0.022	Pass	448	Pass	654	Pass
X-309	LS	0.085	Fail	1351	Pass	1250	Pass

Freeze/Thaw Failure Criteria:

Pass : < 0.060, Fail : > 0.060

HFI Failure Criteria:

Pass : > 200, Fail : < 200

Table 6.10 WHFT 94 Correlation Coefficients

	Expansion (%)	Mass Loss (%)	Fracture (%)
Expansion (%)	1.0	-0.20	-0.12
Sulfate	-----	-0.30	-0.29
Abrasion (%)	-----	0.72	0.80
Absorption (%)	-----	0.46	0.61

Table 6.11 WHFT 97 Correlation Coefficients

	Expansion (%)	Mass Loss (%)	Fracture (%)
Expansion (%)	1.0	-0.18	0.08
Sulfate	-----	-0.28	-0.04
Abrasion (%)	-----	0.76	0.07
Absorption (%)	-----	0.58	0.03

Table 6.12 Relationship Between the Test Variables for WHFT 94

Linear Relationship	R²
ML (%) = -1.8398 [Exp (%)] + 0.4741	0.0399
ML (%) = -0.0267 [Snd] + 0.6032	0.0885
ML (%) = 0.0413 [Abr (%)] - 0.6357	0.5113
ML (%) = 0.2031 [Abs (%)] + 0.0962	0.2077
PF (%) = -3.6019 [Exp (%)] + 0.7716	0.0153
PF (%) = -0.0827 [Snd] + 1.2457	0.0847
PF (%) = 0.1466 [Abr (%)] - 3.0685	0.6457
PF (%) = 0.8628 [Abs (%)] - 0.6836	0.3746
Exponential Relationship	R²
ML (%) = 0.3876e ^{-3.3994 [Exp (%)]}	0.0387
ML (%) = 0.447e ^{-0.0362 [Snd]}	0.0461
ML (%) = 0.0628e ^{0.0671 [Abr (%)]}	0.385
ML (%) = 0.2141e ^{0.3072 [Abs (%)]}	0.1351
PF (%) = 0.4132e ^{-1.7482 [Exp (%)]}	0.0035
PF (%) = 0.4886e ^{-0.0315 [Snd]}	0.0118
PF (%) = 0.0162e ^{0.1255 [Abr (%)]}	0.4551
PF (%) = 0.1248e ^{0.7378 [Abs (%)]}	0.2634

ML: mass loss; PF: percent fracture; Exp: expansion; Snd: Sulfate soundness Abr: L.A. Abrasion;
Abs: absorption

Table 6.12 Relationship Between the Test Variables for WHFT 94 (continued)

Logarithmic Relationship	R²
ML (%) = -0.0602 Ln[Exp (%)] + 0.1792	0.0462
ML (%) = -0.2513 Ln[Snd] + 0.8785	0.1954
ML (%) = 0.9985 Ln[Abr (%)] - 2.7998	0.4184
ML (%) = 0.2693 Ln[Abs (%)] + 0.3117	0.1093
PF (%) = -0.1449 Ln[Exp (%)] + 0.0917	0.0267
PF (%) = -0.8979 Ln[Snd] + 2.3227	0.2495
PF (%) = 3.4318 Ln[Abr (%)] - 10.384	0.4941
PF (%) = 1.3168 Ln[Abs (%)] + 0.1697	0.2612
Power Relationship	R²
ML (%) = 0.2105 [Exp (%)] ^{-0.1285}	0.0598
ML (%) = 0.6811 [Snd] ^{-0.3661}	0.118
ML (%) = 0.0016 [Abr (%)] ^{1.671}	0.3333
ML (%) = 0.2982 [Abs (%)] ^{0.3932}	0.0663
PF (%) = 0.2734 [Exp (%)] ^{-0.0921}	0.0104
PF (%) = 0.992 [Snd] ^{-0.5015}	0.0748
PF (%) = 2E-5 [Abr (%)] ^{3.0882}	0.3847
PF (%) = 0.2531 [Abs (%)] ^{1.1898}	0.205

ML: mass loss; PF: percent fracture; Exp: expansion; Snd: Sulfate soundness Abr: L.A. Abrasion;
Abs: absorption

Table 6.13 Relationship Between the Test Variables for WHFT 97

Linear Relationship	R²
ML (%) = -0.891 [Exp (%)] + 0.3637	0.0329
ML (%) = -0.0132 [Snd] + 0.4285	0.0765
ML (%) = 0.0232 [Abr (%)] - 0.2563	0.5713
ML (%) = 0.1371 [Abs (%)] + 0.1212	0.3328
PF (%) = 0.4219 [Exp (%)] + 0.2394	0.0056
PF (%) = -0.0021 [Snd] + 0.27	0.0015
PF (%) = 0.0026 [Abr (%)] + 0.1898	0.0052
PF (%) = 0.0079 [Abs (%)] + 0.2423	0.0008
Exponential Relationship	R²
ML (%) = 0.3256e ^{-1.6501 [Exp (%)]}	0.0199
ML (%) = 0.3646e ^{-0.0236 [Snd]}	0.0428
ML (%) = 0.0895e ^{0.0487 [Abr (%)]}	0.4416
ML (%) = 0.1996e ^{0.28 [Abs (%)]}	0.2444
PF (%) = 0.192e ^{1.496 [Exp (%)]}	0.0047
PF (%) = 0.209e ^{-0.0044 [Snd]}	0.0004
PF (%) = 0.1856e ^{0.0034 [Abr (%)]}	0.0006
PF (%) = 0.2104e ^{-0.0249 [Abs (%)]}	0.0006

ML: mass loss; PF: percent fracture; Exp: expansion; Snd: Sulfate soundness Abr: L.A. Abrasion;
Abs: absorption

Table 6.13 Relationship Between the Test Variables for WHFT 97 (continued)

Logarithmic Relationship	R²
ML (%) = -0.0336 Ln[Exp (%)] + 0.2039	0.0507
ML (%) = -0.1375 Ln[Snd] + 0.5892	0.206
ML (%) = 0.5633 Ln[Abr (%)] - 1.4781	0.4688
ML (%) = 0.1979 Ln[Abs (%)] + 0.2609	0.2077
PF (%) = 0.0185 Ln[Exp (%)] + 0.325	0.0117
PF (%) = -0.0043 Ln[Snd] + 0.2625	0.0002
PF (%) = 0.0614 Ln[Abr (%)] + 0.0571	0.0042
PF (%) = 0.0162 Ln[Abs (%)] + 0.2486	0.0011
Power Relationship	R²
ML (%) = 0.236 [Exp (%)] ^{-0.0691}	0.0376
ML (%) = 0.5035 [Snd] ^{-0.2644}	0.1341
ML (%) = 0.0062 [Abr (%)] ^{1.2138}	0.3831
ML (%) = 0.267 [Abs (%)] ^{0.3885}	0.1409
PF (%) = 0.2322 [Exp (%)] ^{0.036}	0.0029
PF (%) = 0.2223 [Snd] ^{-0.0498}	0.0014
PF (%) = 0.1977 [Abr (%)] ^{0.0075}	4E-6
PF (%) = 0.2018 [Abs (%)] ^{0.0096}	2E-5

ML: mass loss; PF: percent fracture; Exp: expansion; Snd: Sulfate soundness Abr: L.A. Abrasion;
Abs: absorption

Table 6.14 Expansion and Mass Loss Repeatability Test Results

Sample ID	Type Rock	ASTM C666 Expansion** (ILDOT Modified)			WHFT 94 Mass Loss			WHFT 97 Mass Loss		
		Avg.	Std. Dev.	C.V. (%)	Avg.	Std. Dev.	C.V. (%)	Avg.	Std. Dev.	C.V. (%)
X-1	Dolo	0.0063	0.0015	24.12	0.2067	0.0089	4.34	0.2800	0.0219	7.83
X-5	Grav	0.0563	0.0138	24.49	0.2083	0.0643	30.85	0.3333	0.0941	28.23
X-7	LS	0.0547	0.0074	13.48	0.2253	0.0089	3.98	0.3130	0.0427	13.65
X-12	LS	0.1167	0.0153	13.12	0.5523	0.0737	13.34	0.4237	0.0779	18.38
X-31	Dolo	0.0103	0.0038	36.64	0.5607	0.0537	9.58	0.4350	---	---
X-32	Dolo	0.0380	0.0072	18.98	0.6807	0.4019	59.04	0.3135	0.0361	11.50*
X-41	LS	0.0213	0.0059	27.47	1.0067	0.1265	12.57	0.5700	---	---
X-42	Dolo	0.0063	0.0015	24.12	0.4823	0.0084	1.74	0.4580	0.0711	15.53
X-98	LS	0.0740	0.0104	14.11	0.2987	0.000006	0.19	0.2260	0.0350	15.50
X-167	LS	0.0203	0.0015	7.51	0.2290	0.0424	18.53*	0.2130	0.0635	29.81
X-262	LS	0.0330	0.0090	27.27	0.2473	0.0947	38.30	0.2330	0.0316	13.55
X-263	Grav	0.0727	0.0196	26.91	0.1490	0.0386	25.90	0.2200	---	---
X-264	ACBF	0.0077	0.0045	58.82	1.3687	0.1926	14.07	0.8805	0.0728	8.27*
X-275	Grav	0.0287	0.0146	51.07	0.1963	0.1697	86.42*	0.2013	0.0396	19.66
X-277	Dolo	0.0063	0.000006	9.12	0.3300	0.0481	14.59	0.1870	0.0131	6.99
X-281	LS	0.0663	0.0110	16.61	0.3183	0.0739	23.23	0.3000	0.0807	26.91
X-282	Dolo	0.0067	0.0015	22.91	0.3055	0.0856	28.01*	0.3363	0.1012	30.09
X-285	Grav	0.0107	0.0021	19.52	0.3310	0.1321	39.91	0.2880	---	---
X-290	Dolo	0.0043	0.0012	26.65	0.3380	0.1013	29.97	0.2565	0.0403	15.71*
X-305	LS	0.0220	0.0072	32.78	0.2773	0.0826	29.79	0.2660	0.0035	1.30
X-309	LS	0.0853	0.0071	8.31	0.2697	0.0579	21.46	0.2390	0.0610	25.53

* value based on the average of two trials

** test performed by ILDOT

Table 6.15 Expansion and Percent Fracture Repeatability Test Results

Sample ID	Type Rock	ASTM C666 Expansion** (ILDOT Modified)			WHFT 94 Percent Fracture			WHFT 97 Percent Fracture		
		Avg.	Std. Dev.	C.V. (%)	Avg.	Std. Dev.	C.V. (%)	Avg.	Std. Dev.	C.V. (%)
X-1	Dolo	0.0063	0.0015	24.12	0.2193	0.0419	19.09	0.1653	0.0493	29.83
X-5	Grav	0.0563	0.0138	24.49	0.4047	0.0787	19.44	0.4063	0.0910	22.39
X-7	LS	0.0547	0.0074	13.48	0.2703	0.0422	15.61	0.2053	0.0393	19.15
X-12	LS	0.1167	0.0153	13.12	1.1980	0.0940	7.84	0.3090	0.0299	9.67
X-31	Dolo	0.0103	0.0038	36.64	0.6297	0.0441	6.99	0.0460	---	---
X-32	Dolo	0.0380	0.0072	18.98	0.0860	0.0046	5.33	0.0745	0.0106	14.24*
X-41	LS	0.0213	0.0059	27.47	1.5130	0.3365	22.24	0.7740	---	---
X-42	Dolo	0.0063	0.0015	24.12	0.4640	0.1283	27.66	0.3290	0.0204	6.21
X-98	LS	0.0740	0.0104	14.11	0.3027	0.1451	47.95	0.1537	0.0344	22.41
X-167	LS	0.0203	0.0015	7.51	0.3890	0.0240	6.18*	0.3763	0.0533	14.16
X-262	LS	0.0330	0.0090	27.27	0.4823	0.0842	17.45	0.1050	0.0020	1.91
X-263	Grav	0.0727	0.0196	26.91	0.4527	0.0325	7.18	0.6310	---	---
X-264	ACBF	0.0077	0.0045	58.82	4.4690	2.2713	50.82	0.2990	0.0028	0.95*
X-275	Grav	0.0287	0.0146	51.07	0.4800	0.0600	12.50	0.3287	0.0244	7.44
X-277	Dolo	0.0063	0.00006	9.12	0.6137	0.7400	120.58	0.1600	0.0344	21.50
X-281	LS	0.0663	0.0110	16.61	0.5057	0.0823	16.27	0.1613	0.0200	12.42
X-282	Dolo	0.0067	0.0015	22.91	0.4335	0.0120	2.77*	0.2210	0.1256	56.84
X-285	Grav	0.0107	0.0021	19.52	0.0787	0.0059	7.45	0.1080	---	---
X-290	Dolo	0.0043	0.0012	26.65	0.2230	0.0101	4.55	0.2570	0.0325	12.66*
X-305	LS	0.0220	0.0072	32.78	0.2233	0.0578	25.90	0.1530	0.0315	20.58
X-309	LS	0.0853	0.0071	8.31	0.0743	0.0015	2.06	0.0797	0.0032	4.04

* value based on the average of two trials

** test performed by ILDOT

7. CONCLUSIONS AND RECOMMENDATIONS

A comprehensive literature review was conducted on the mechanism of freeze/thaw damage in concrete and existing test methods. A new, fully automated WHFT 97 apparatus was built and calibrated in accordance to the existing WHFT 94 apparatus. Twenty-one Illinois aggregates were tested with the WHFT 94 and WHFT 97 test apparatus to rapidly assess freeze/thaw durability of these aggregates in concrete. It was apparent that the percent fracture of the aggregate was dependent on the initial chamber pressure, the pressurized cycle duration and the pressure release rate. Correlation analyses were performed among the outputs of these tests and other existing test results.

7.1 Conclusions

Based on this study, the following conclusion can be drawn:

1. The WHFT 97 is completely automated in terms of controlling the entire testing procedure for each respective 10 cycles of operation, and requires minimal manual labor. A controlled interface is connected to the machine which provides a plot of the release for each cycle, hence good quality control of the system and much better results are expected.
2. Based on the comparison of the petrographic analysis and the percent expansion results, at constant total pore volume, the more the percentage of the small pore size, the less durable the aggregate.
3. The percent fracture (PF_{50}) for the three tests on the same aggregate sample show a wider variation using the WHFT 94 than the same sample tested on the WHFT 97. This clearly indicates that the larger sample tested provides more reliable results.

4. A comparison of WHFT to ASTM C 666 Method B (ILDOT modified) test results showed a lack of direct correlation across a vast majority of the 21 test samples. This lack of direct correlation precludes the use of the WHFT test as a direct replacement for the ASTM C 666 Method B test procedure.
5. The test data was also compared using the two test methods' failure modes, percent fracture (2%) for the WHFT 97 test and 0.060% maximum expansion for the ASTM C 666 Method B (ILDOT modified) test. This comparison showed 14 of 21 aggregates (67%) on the WHFT 94 and 16 of 21 aggregates (76%) on the WHFT 97 were identified correctly with respect to the ILDOT criteria. All the aggregate types (dolomite, gravel, ACBF slag) were successfully classified with the exception of one aggregate type, limestone. In addition, the WHFT 97 machine yielded more consistent results than the WHFT 94 machine in comparing results to the freeze-thaw test. It appears the WHFT 97 test may have the potential to be used as a screening test prior to ASTM freeze-thaw testing.
6. Based on repeatability of test results, the larger sample tested provides more reliable results. The WHFT 97 results show an average coefficient of variation (CV) of 16% for both mass loss and percent expansion. These same values are 24% and 21% on the WHFT 94. The coefficients of variation associated with some of the results from the WHFT testing were also high due to the fact that some (6) of the samples were only tested once or twice on the WHFT 97 machine.
7. In general, linear and logarithmic relationships between WHFT and the other test results yielded the highest coefficients of determination. For instance, a linear relationship between mass loss and percent abrasion produced the highest coefficients of 0.51 and 0.57 on the WHFT 94 and WHFT 97, respectively.

8. A draft screening procedure was developed based on aggregate type and petrographical analysis for use prior to the testing on the WHFT apparatus. The percentage of air voids in limestone is suggested as a way to identify limestones that must be tested in the WHFT 97 test. Based on the results obtained from the freeze-thaw test and petrographic analysis (Table 5.1), as the air void percentage exceeds 0.1, the limestone aggregate can be classified as non-durable and testing on the WHFT 97 machine is not necessary. If the air void percentage is less than 0.1, the aggregate should be tested to determine its susceptibility to D-cracking. However, this procedure for limestones was based on extremely limited samples and will require additional research on a wider range of durable and non-durable rock types to achieve validation.
9. Overall, the WHFT test method needs further modification to yield better correlation for reliability and test applicability for durability assessment.

7.2 Recommendations

To validate and extend the work presented, the following is recommended:

1. Conduct tests using the WHFT 97 apparatus with a higher initial pressure. This will help determine if a higher initial pressure will increase the percent fracture. However, above some unknown pressure, the strength of all aggregates, D-cracking susceptible and non-susceptible, will be exceeded, making it impossible to differentiate between materials.
2. Conduct tests using the WHFT 97 with longer pressurization cycle duration. Two minutes has proven to be a short time for the aggregate pore pressure to be in equilibrium with the external pressure. Therefore, it is suggested that all consecutive pressurization cycles be 5 minutes long. This increase in cycle duration could indeed increase the percent fracture and mass loss, and more accurately correlate with percent expansion. If this new procedure produced a significant increase in percent fracture, the number of cycles could be decreased

to only 10, hence making it a four-day test instead of 8.

3. Conduct testing on a wider range of aggregate sources based on freeze and thaw factors, i.e., ranging from very high D-cracking susceptible aggregates (non-durable aggregates) to non-susceptible D-cracking aggregates (durable aggregates). This is due to the fact that, based on the results obtained, most of the Illinois aggregates tested were not D-cracking susceptible. The aggregates that failed using the freeze-thaw method were close to being classified as durable. More aggregates should be tested that correspond to the characteristics observed in the Kansas DOT aggregate sample. This parametric study will be of great importance in specifying and optimizing the ML and HFI critical limits.

REFERENCES

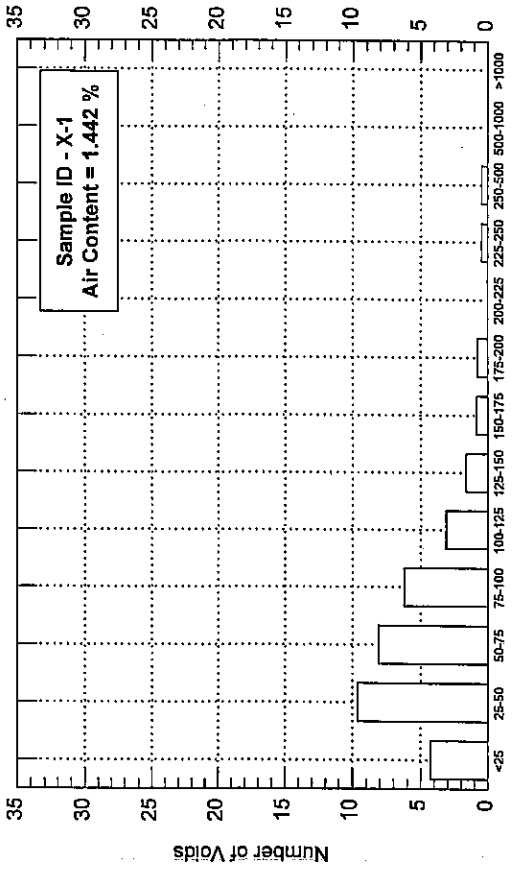
1. Stark, D., "Characteristics and Utilization of Coarse Aggregates Associated with D-cracking," Research and Development Bulletin RD047.01P, Portland Cement Association, Skokie, Illinois, 1976, 7 pp.
2. Domaschuk, L., Hermanson, G., and Ganapathy, G., "D-Cracking of Concrete Pavements in Manitoba," Tribune Des Transports, Vol. 3-2, Canada.
3. Rhoades, R. and Mielenz, R.C., "Petrography of Concrete Aggregates," Proc. ACI Vol. 42, No. 6, p. 581, 1956.
4. Sweet, H.S., "Research on Concrete Durability as Affected by Coarse Aggregates," Proc. ASTM, Vol. 48, p. 988, 1948.
5. Schuster, R.L. and McLaughlin, J.F., "A study of Chert and Shale Gravel in Concrete," HRB Bull., No. 305, pp. 51-75, 1961.
6. Kaneuji, M., Winslow, D.N., and Dolch, W.L., "The Relationship between an Aggregate's Pore Size Distribution and Its Freeze-Thaw Durability in Concrete," Cement and Concrete Research, Vol. 10, No. 3, pp. 433-441, 1980.
7. Lewis, D.W., Dolch, W.L., and Woods, K.B., "Porosity Determinations and the Significance of Pore Characteristics of Aggregates," Proc. ASTM, Vol. 53, p. 449, 1953.
8. Hiltrop, C.L. and Lemish J., "Relationship of Pore-Size Distribution and other Rock Properties to Serviceability of Some Carbonate Aggregates," Highway Research Board Bull. 239, pp. 1-23, 1960.
9. Gonnerman, H.F. and Ward, G.W., "Studies on the Soundness and Durability of Aggregates and Concrete," Pit and Quarry, No. 12, September 9, 1931.
10. Stark, D. and Klieger, P., "Effect of Maximum Size of Coarse Aggregate on D-Cracking in Concrete Pavements," 33-43, Washington D.C., 1973.
11. Traylor, M.L., "Efforts to Eliminate D-Cracking in Illinois," Transportation Research Record 853, TRB. National Research Council, Washington, D.C., 1982. pp. 9-14.
12. Janssen, D.J. and Almond, D.K., "The Washington Hydraulic Test for Concrete Aggregates Exposed to Freezing and Thawing," Second CANMET/ACI International Conference on Durability of Concrete, Montreal, Canada, August 1991, pp. 265-293.

13. Whiting, D.A. and Nagi, M., "Interlaboratory Evaluation of AASHTO TP12 Hydraulic Fracture of Concrete Aggregates," Final Report, FHWA Contract DTFH61-94-C-00119/Task N, August 1998.
14. Alford, T.E. and Janssen, D.J., "Calibrating the Washington Hydraulic Fracture Apparatus," Transportation Research Board, No. 1486, pp. 142-148, Washington D.C., 1995.
15. Janssen, D.J. and Almond, D.K., "Comparison of Four Aggregates Using the Washington Hydraulic Fracture Test," Transportation Research Record No. 1301, Washington State Transportation Center, pp. 57-67, 1991.
16. Janssen, D.J. and Snyder, M.B., "Resistance of Concrete Freezing and Thawing," Report No. SHRP-C-391, Strategic Highway Research Program, National Research Council, Washington D.C., 1994.
17. Winslow, D.N., "The Rate of Absorption of Aggregates," Cement, Concrete, and Aggregates, CCAGDP, Vol. 9, No. 2, pp. 154- 158, 1987.
18. Hossain, M. and Zubery, M.H., "Correlation of KDOT and SHRP's Washington Hydraulic Fracture Index (WHFI) Aggregate Durability Test Methods," Report No. K-TRAN: Kansas State University-94-5, 1996.
19. Micromeritics, "Mercury Intrusion Porosimetry and Typical Pore Size Distributions," Micromeritics Instrument Corporation, Georgia, 1981.
20. Kaneuji, M., "Correlation Between Pore Size Distribution and Freeze Thaw Durability of Coarse Aggregates in Concrete," Joint Highway Research Project, Report No. JHRP -78- 15, August 1978.
21. Almond, D., "A Test for Identifying Aggregates Susceptible to freeze-Thaw Damage," M.S. Thesis, University of Washington, 1990.
22. Shakoor, A., "Evaluation of Methods for Predicting Durability Characteristics of Argillaceous Carbonate Aggregates for Highway Pavements," Ph.D. Thesis, Purdue University, 1982.
23. Lindgren, M.N., "The Prediction of Freeze-Thaw Durability of Coarse Aggregates in Concrete by Mercury Intrusion Porosimetry," M.S. Thesis, Purdue University, 1980.
24. Shakoor, A. and Scholer, C.F., "Comparison of Aggregate Pore Characteristics as Measured by Mercury Intrusion Porosimeter and Iowa Pore Index Tests," ACI Journal, Vol. 82, No. 4, pp. 453-458, 1985.

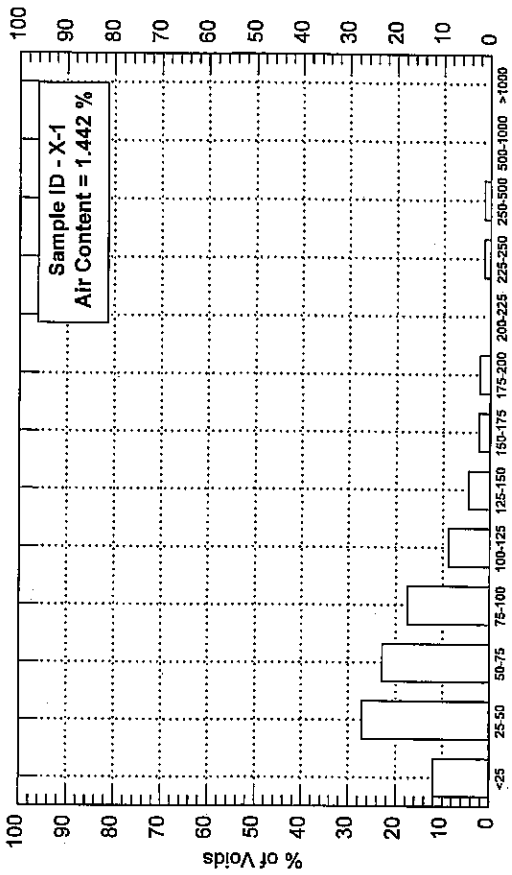
25. Winslow, D.W. and Diamond, S., " A Mercury Porosimetry Study of the Evolution of Porosity in Portland Cement," *Journal of Materials, ASTM*, Vol.5, No. 3, p. 564, 1970.
26. Neumann, A.W, and Good R.J., "Techniques of Measuring Contact Angles," *Surface and Colloid Science*, Vol. 11, pp. 31-89, 1979.
27. Winslow, D.N., "Advances in Experimental Techniques for Mercury Intrusion Porosimetry," *Surface and Colloid Science*, Vol. 13, pp. 259-282, 1984.
28. Good, R.J., " The Contact Angle of Mercury on the Internal Surface of Porous Bodies," *Surface and Colloid Science*, Vol. 13, pp. 283-287, 1984.
29. Walker, R.D., "Relationship Between Aggregate Pore Characteristics and Durability of Concrete Exposed to Freezing and Thawing," *Highway Research Record* 226 p. 441, 1949.

APPENDIX A
Petrographic Analysis

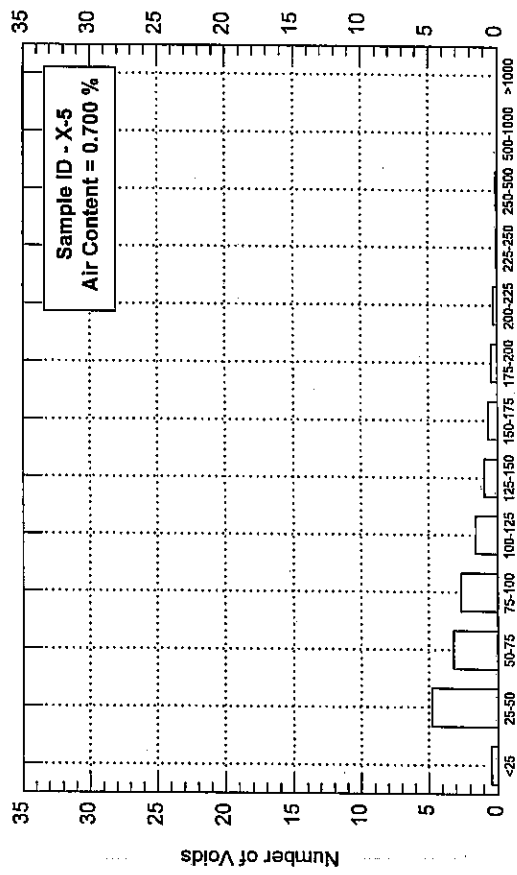




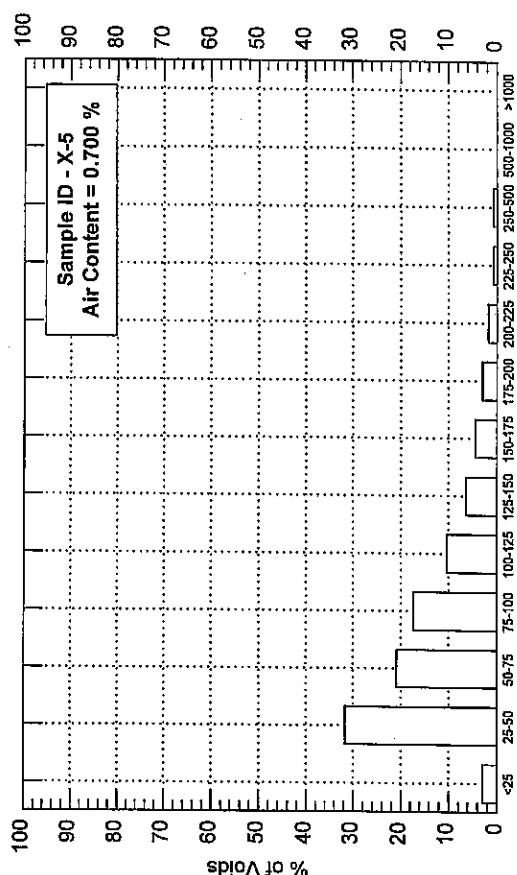
Size Range of Air Voids (microns)



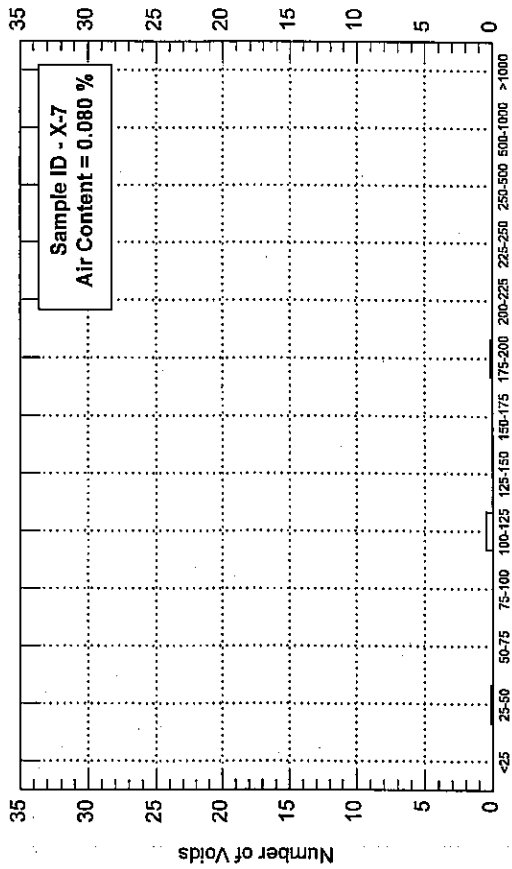
Size Range of Air Voids (microns)



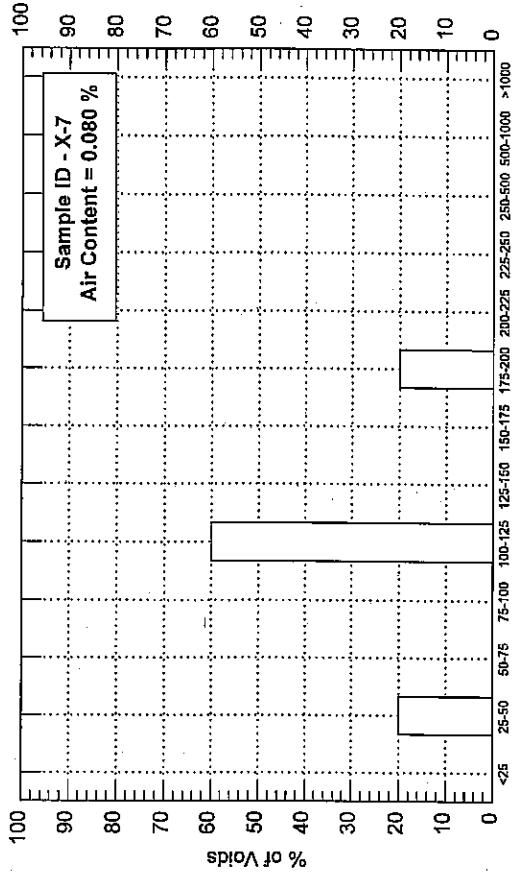
Size Range of Air Voids (microns)



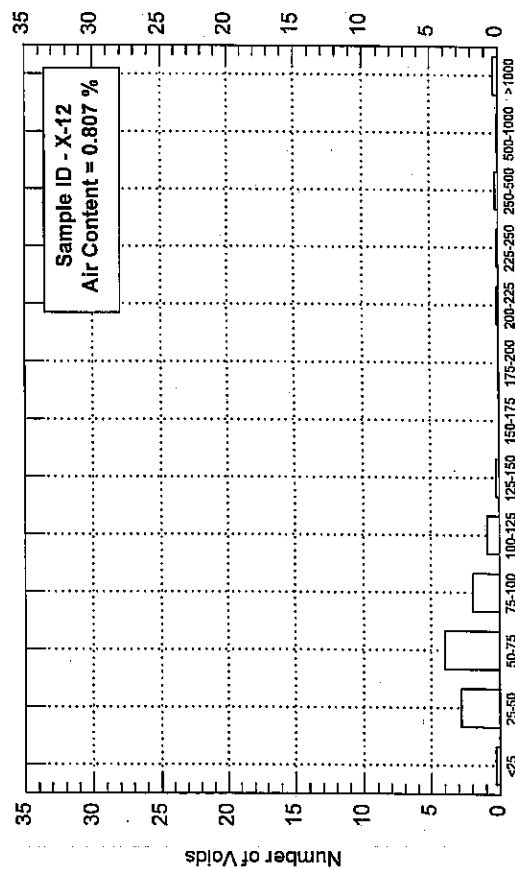
Size Range of Air Voids (microns)



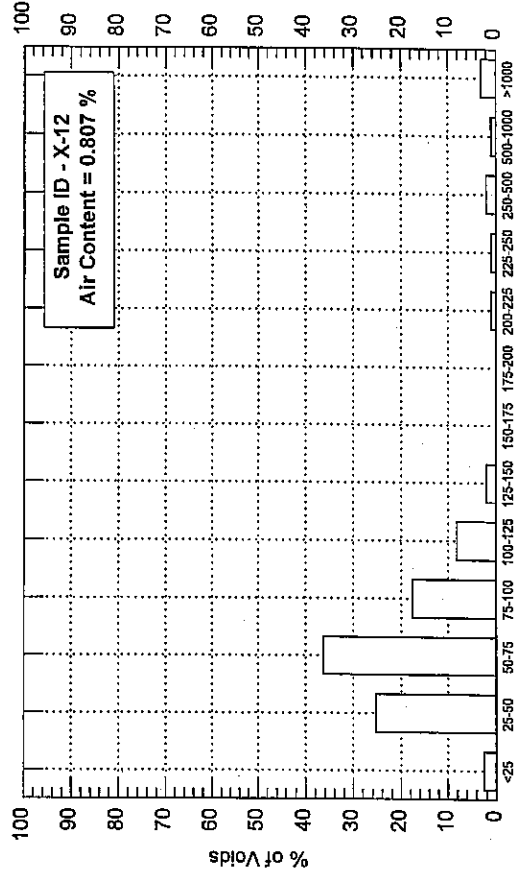
Size Range of Air Voids (microns)



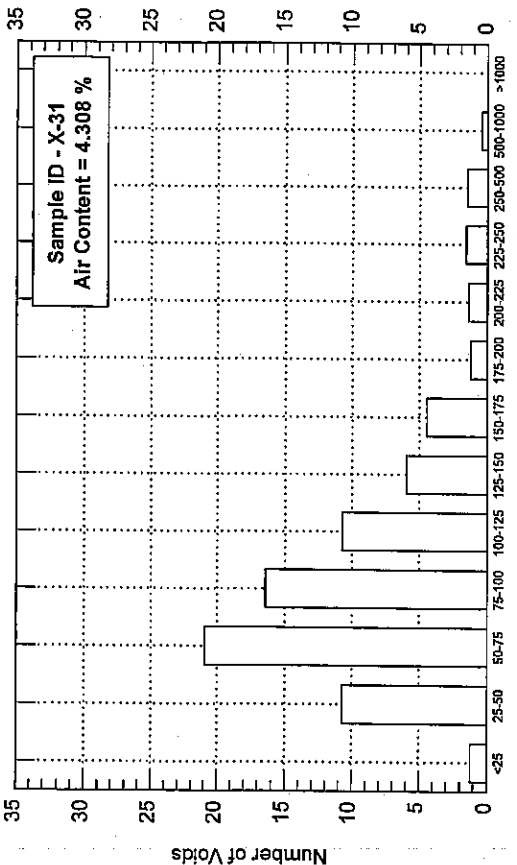
Size Range of Air Voids (microns)



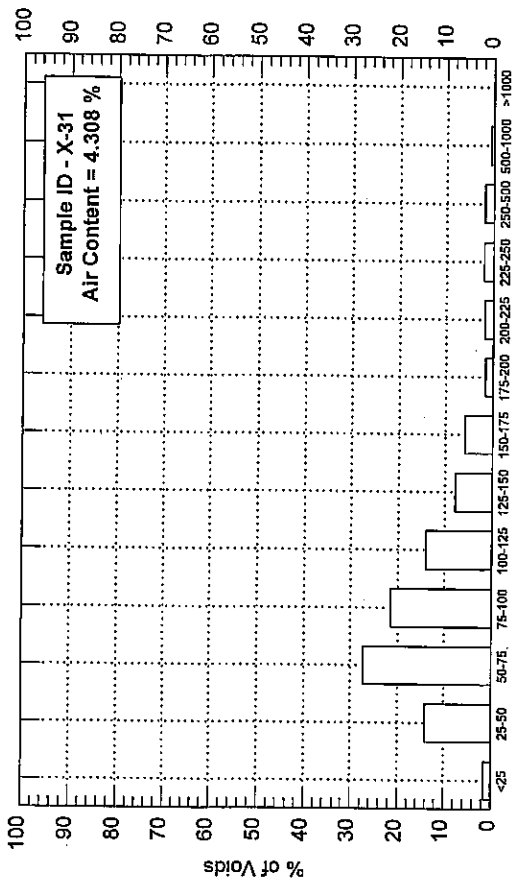
Size Range of Air Voids (microns)



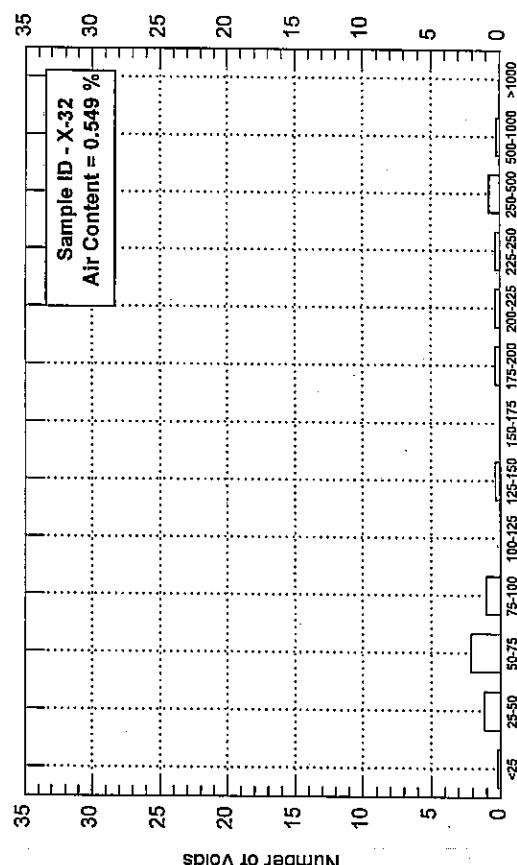
Size Range of Air Voids (microns)



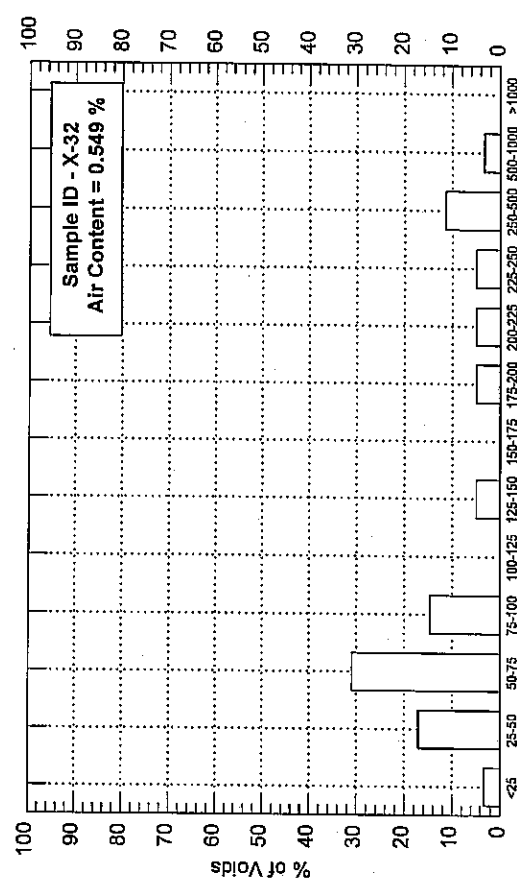
Size Range of Air Voids (microns)



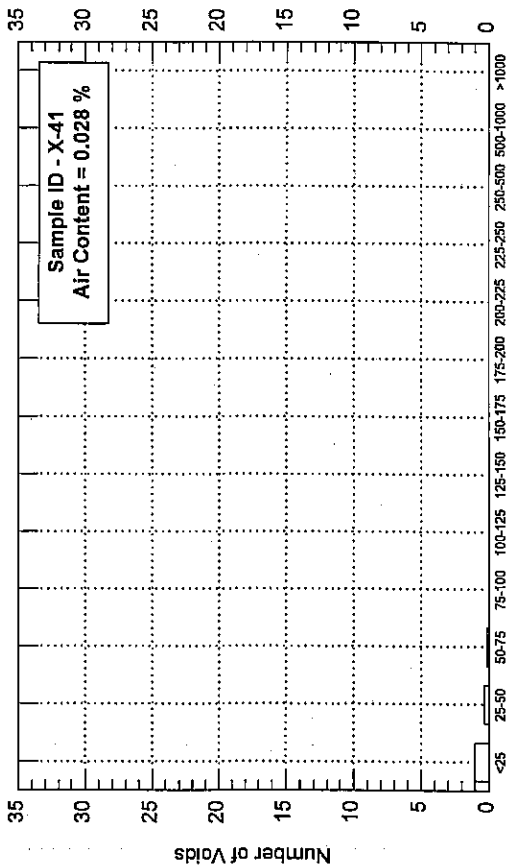
Size Range of Air Voids (microns)



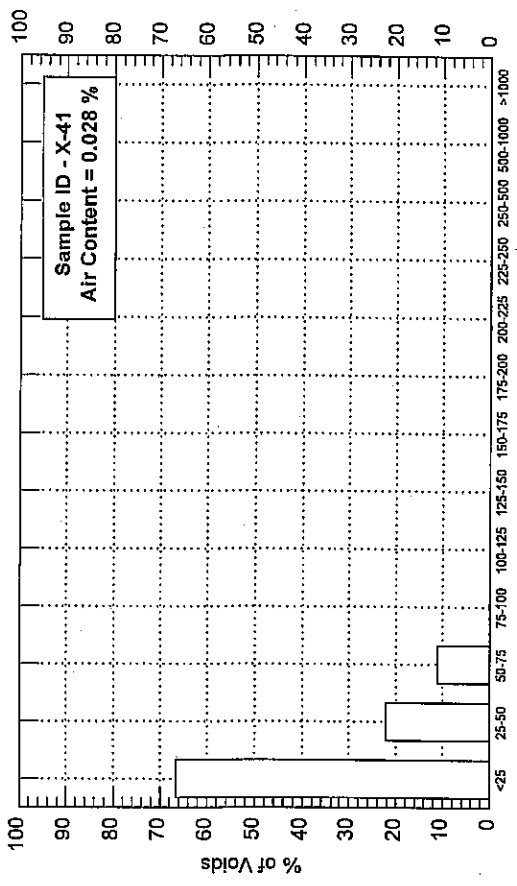
Size Range of Air Voids (microns)



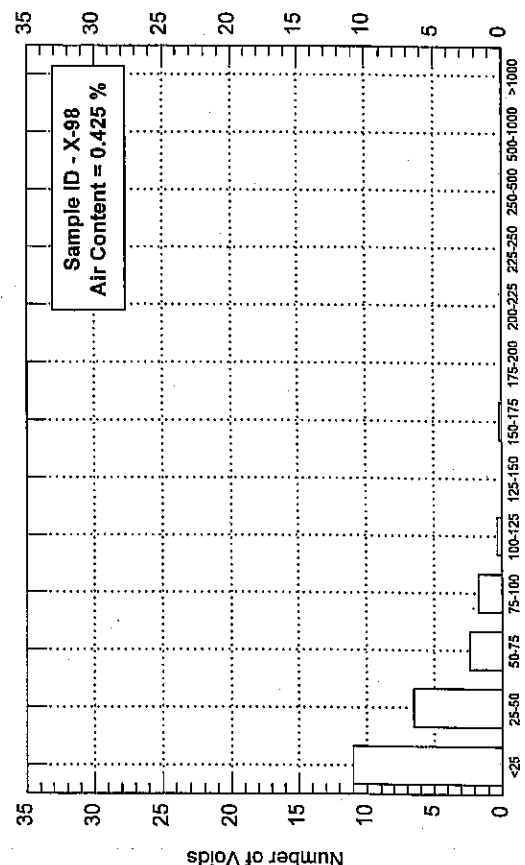
Size Range of Air Voids (microns)



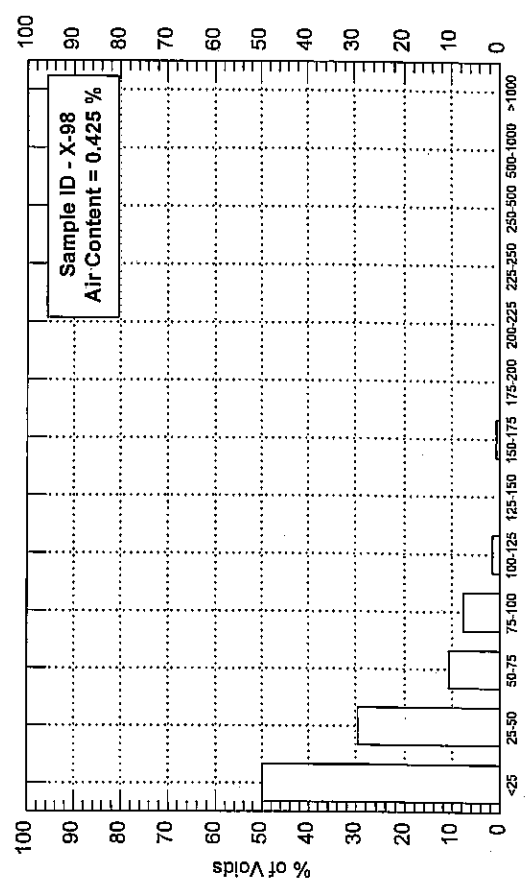
Size Range of Air Voids (microns)



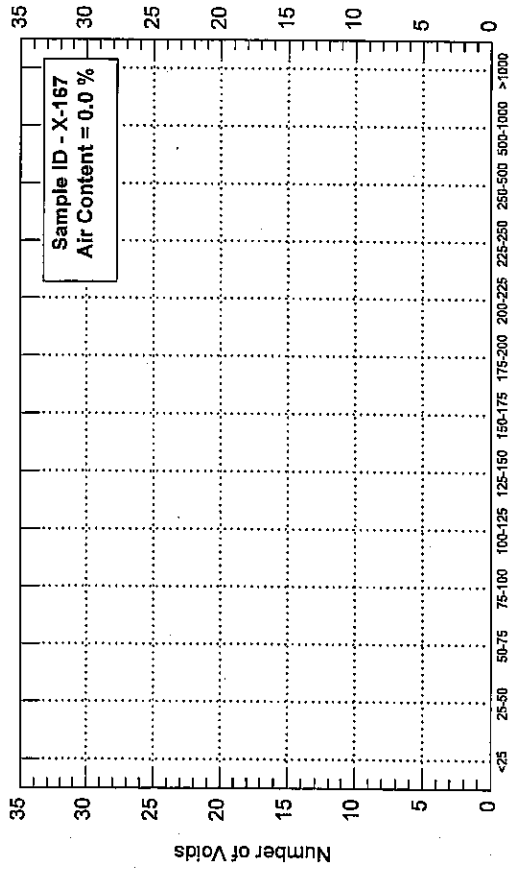
Size Range of Air Voids (microns)



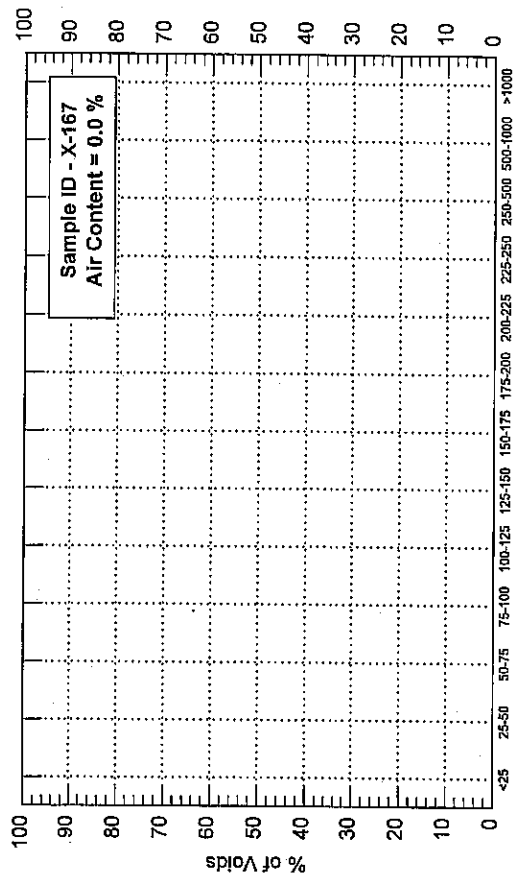
Size Range of Air Voids (microns)



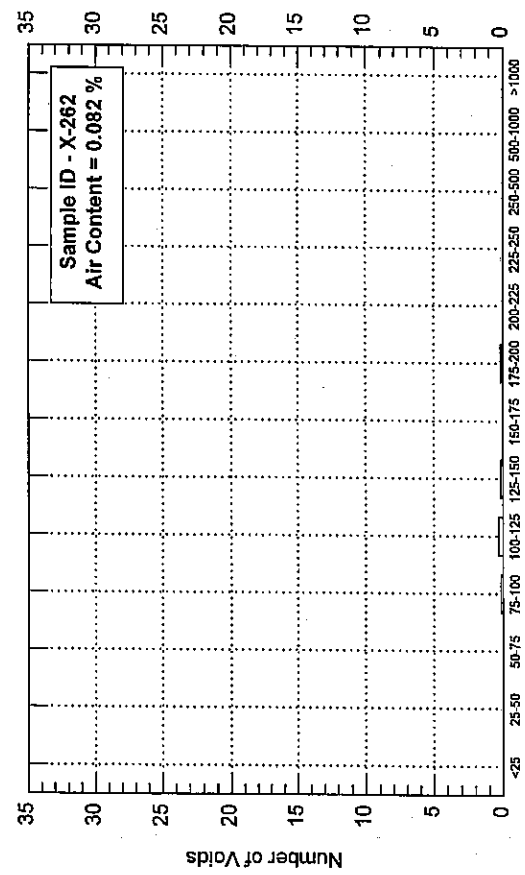
Size Range of Air Voids (microns)



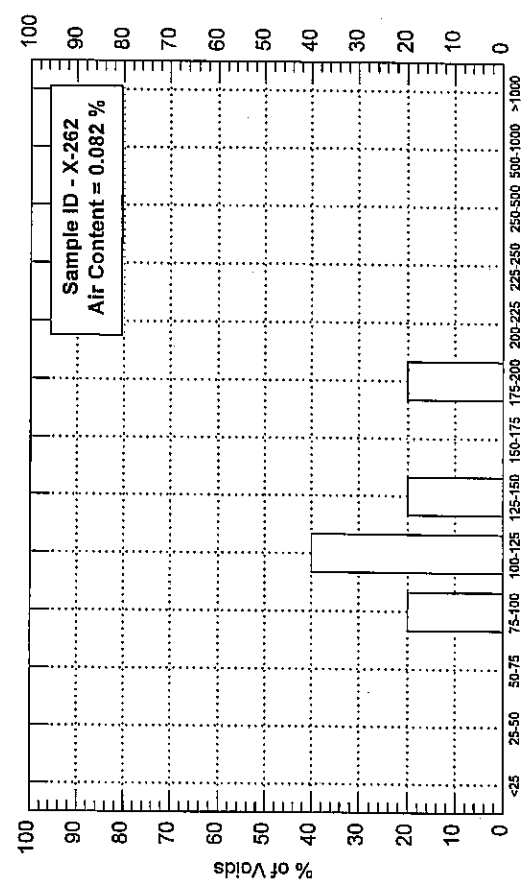
Size Range of Air Voids (microns)



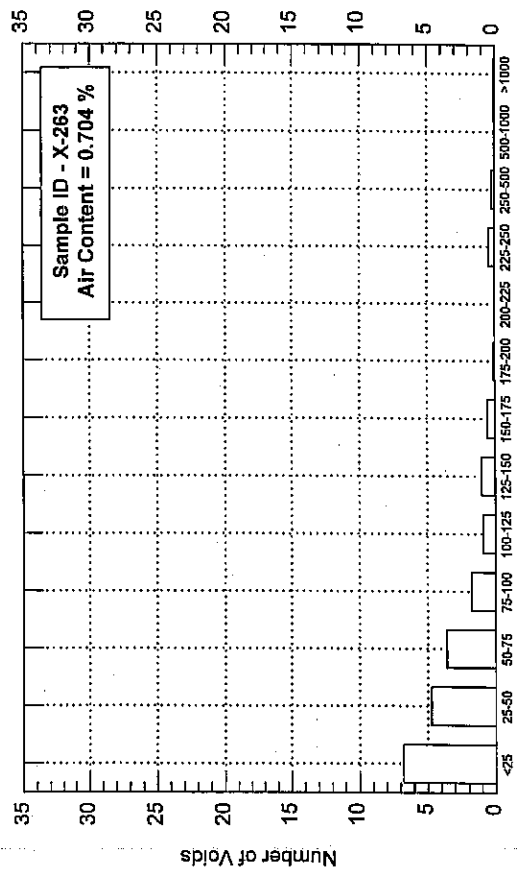
Size Range of Air Voids (microns)



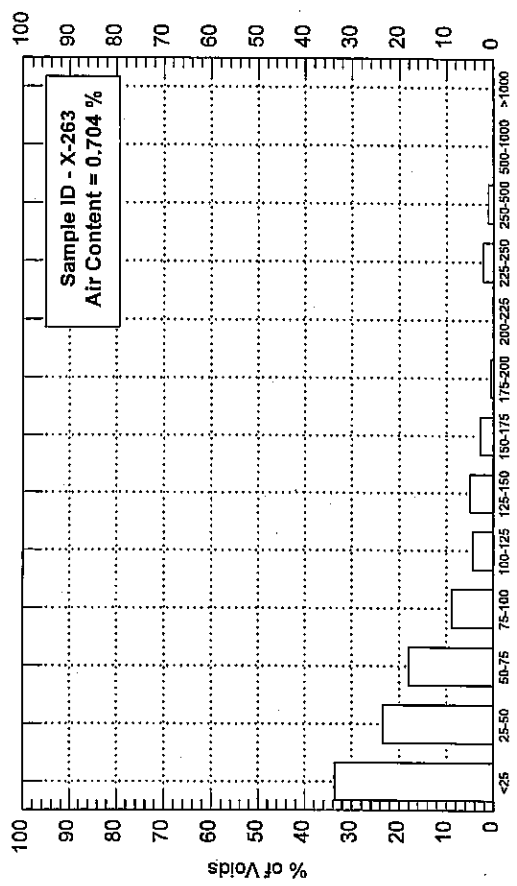
Size Range of Air Voids (microns)



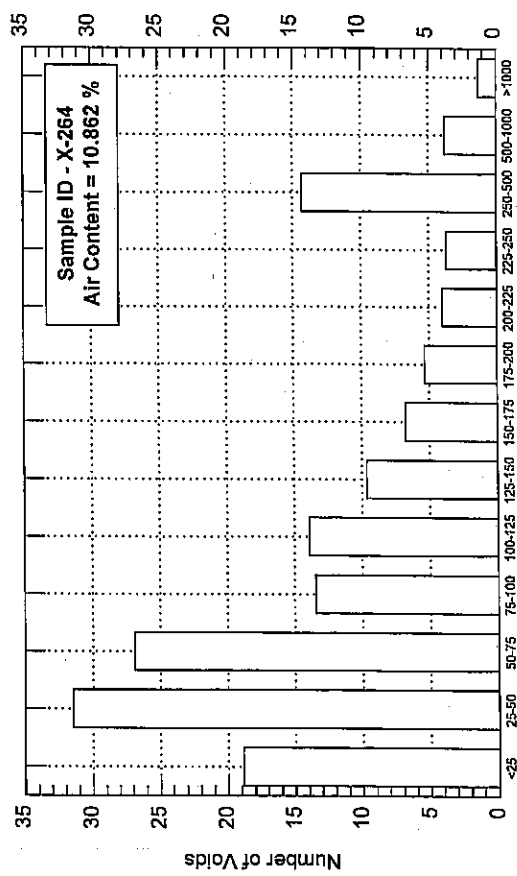
Size Range of Air Voids (microns)



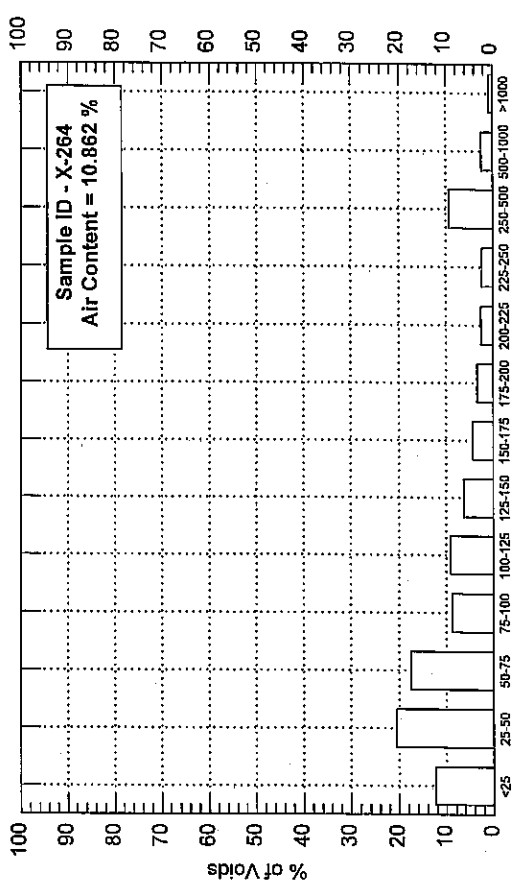
Size Range of Air Voids (microns)



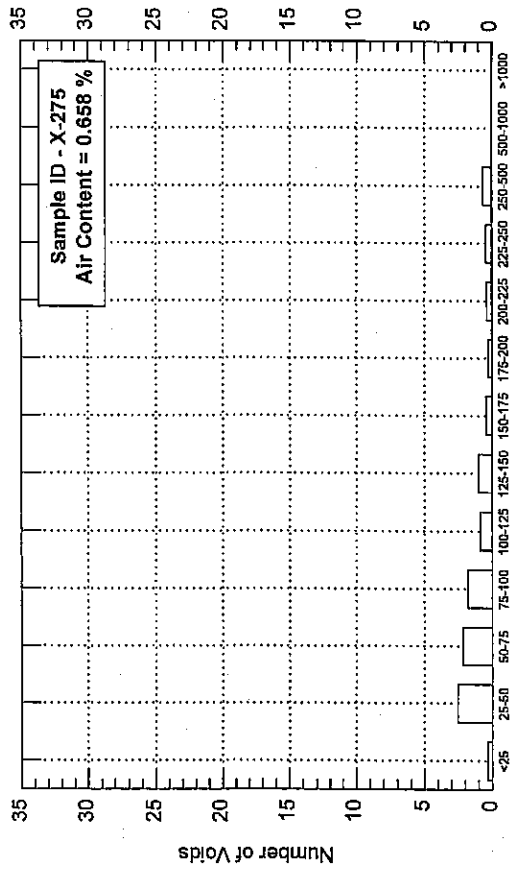
Size Range of Air Voids (microns)



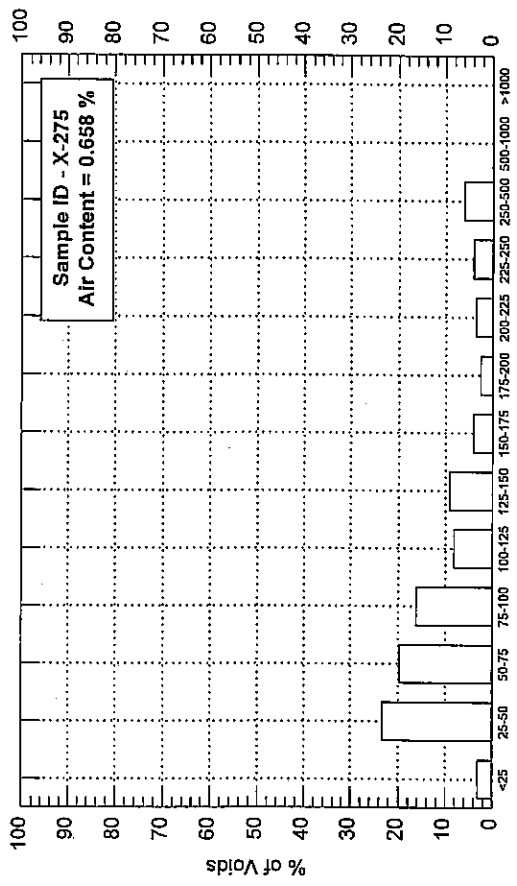
Size Range of Air Voids (microns)



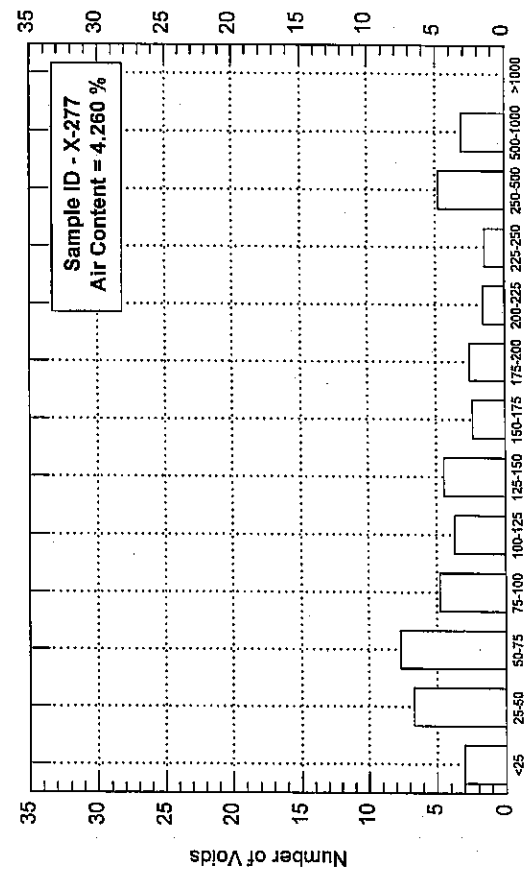
Size Range of Air Voids (microns)



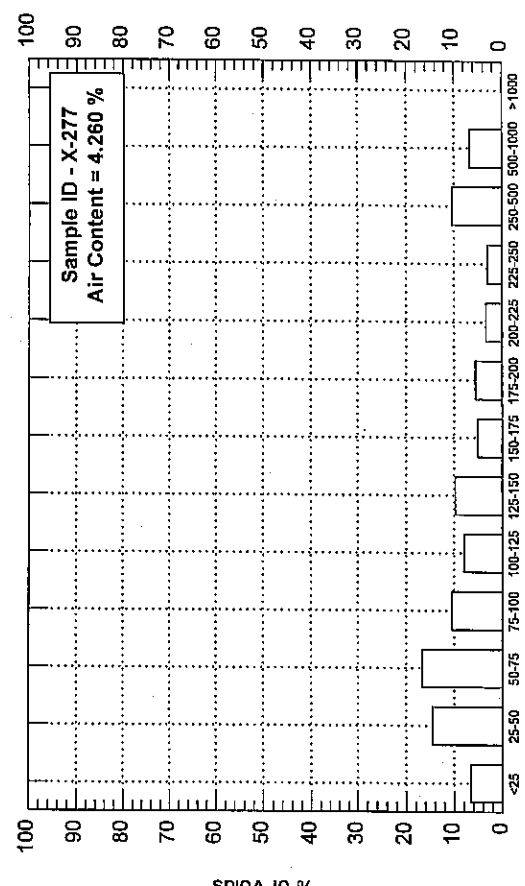
Size Range of Air Voids (microns)



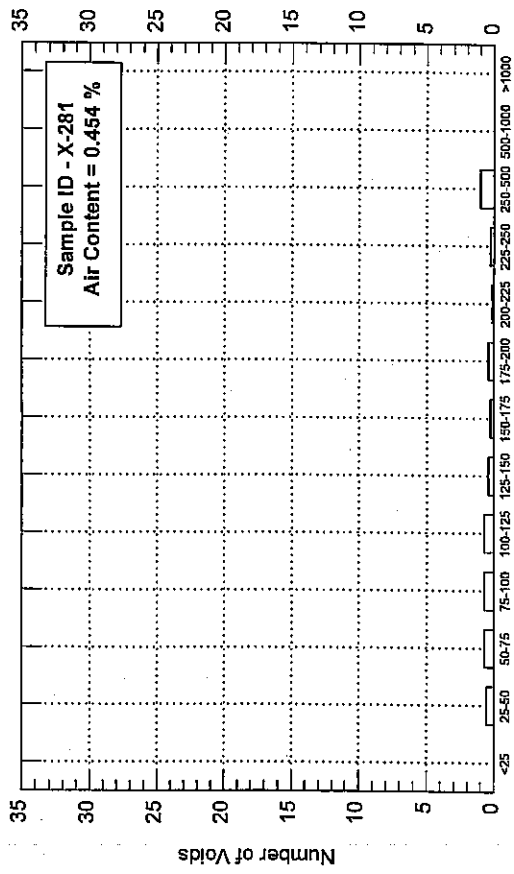
Size Range of Air Voids (microns)



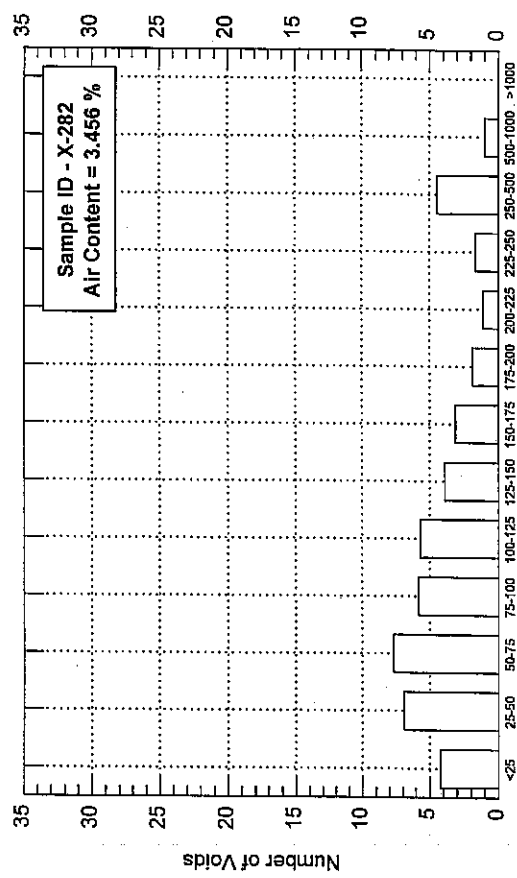
Size Range of Air Voids (microns)



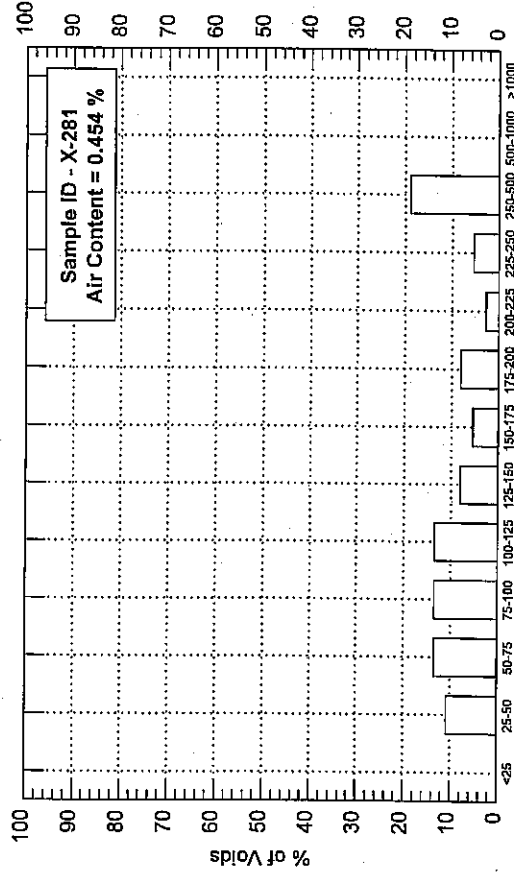
Size Range of Air Voids (microns)



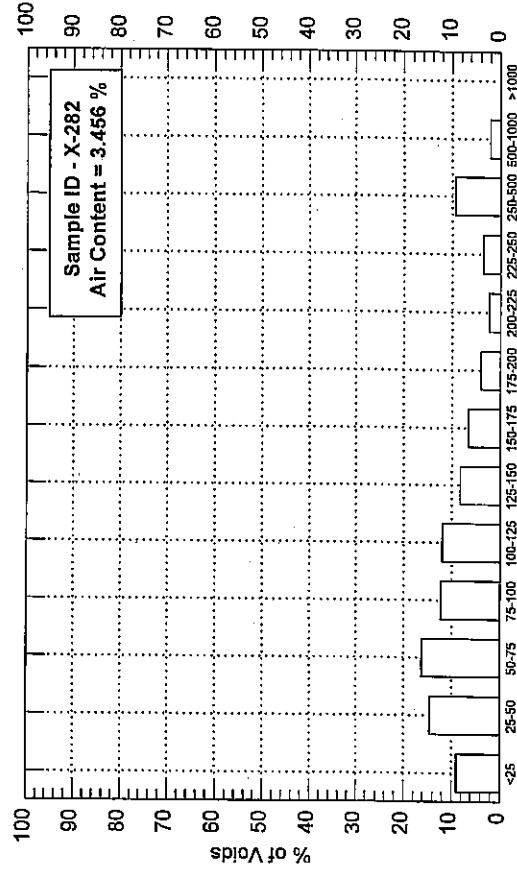
Size Range of Air Voids (microns)



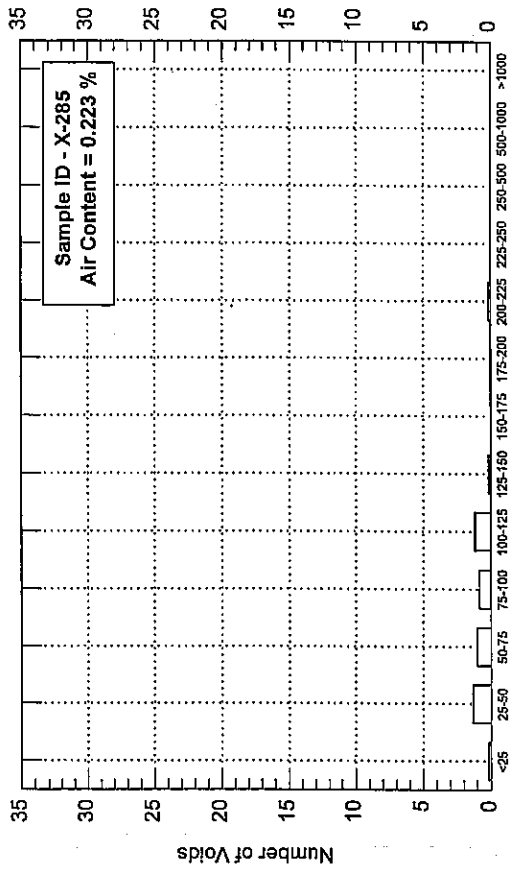
Size Range of Air Voids (microns)



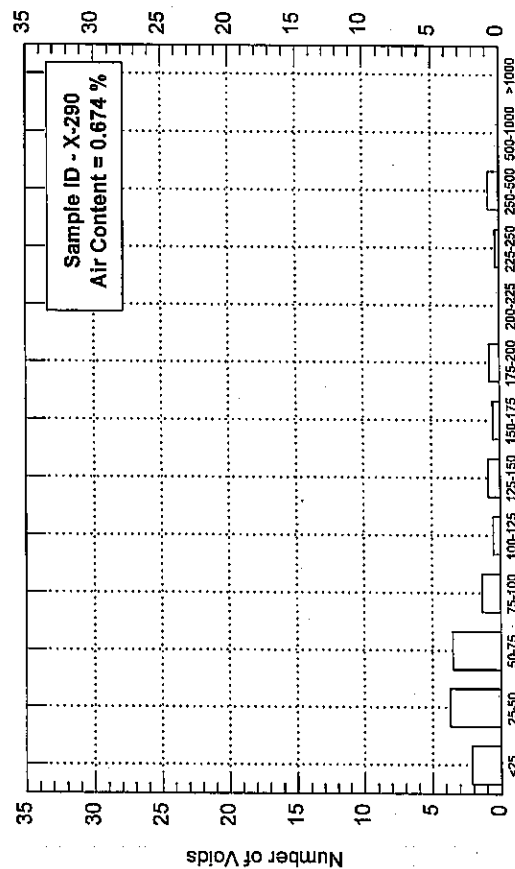
Size Range of Air Voids (microns)



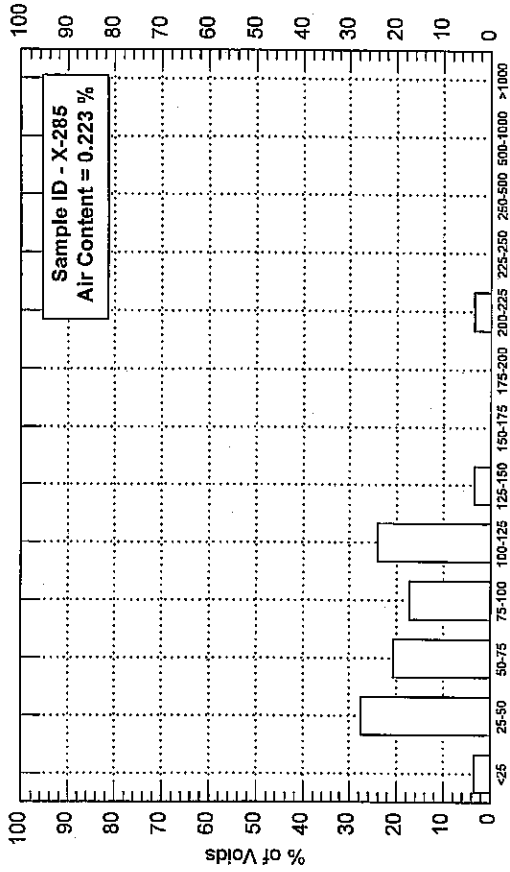
Size Range of Air Voids (microns)



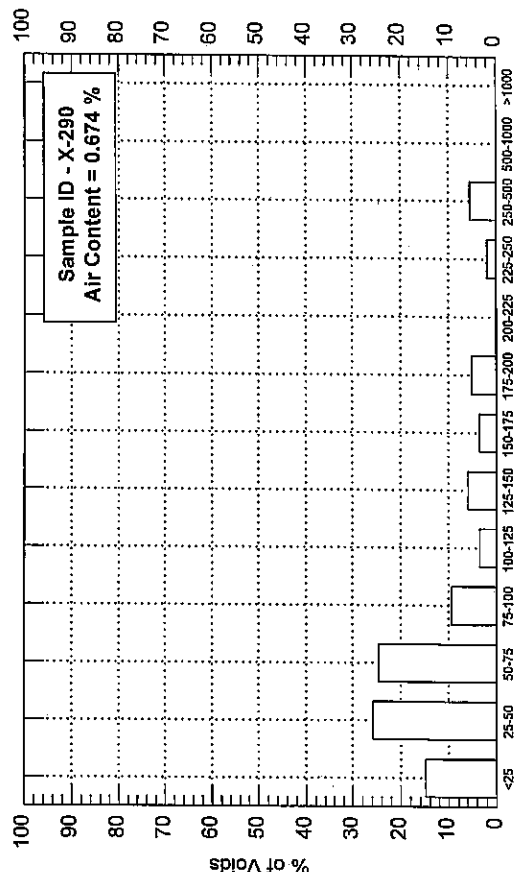
Size Range of Air Voids (microns)



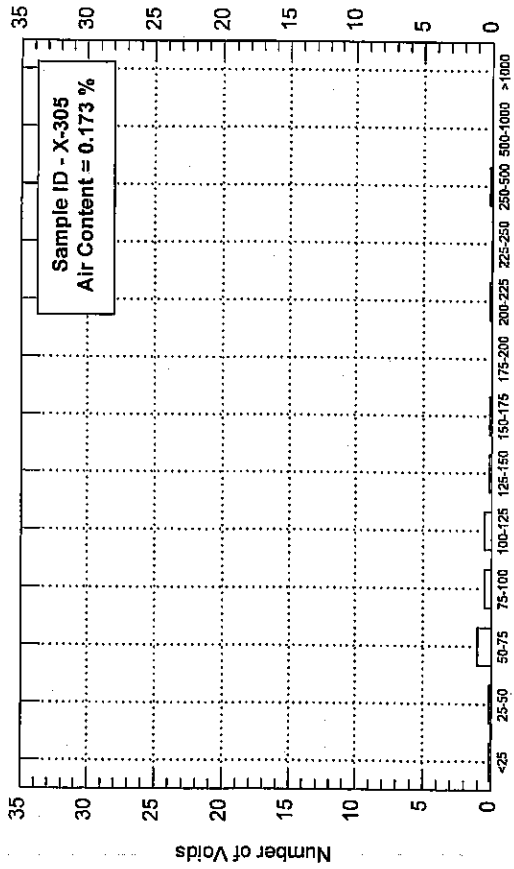
Size Range of Air Voids (microns)



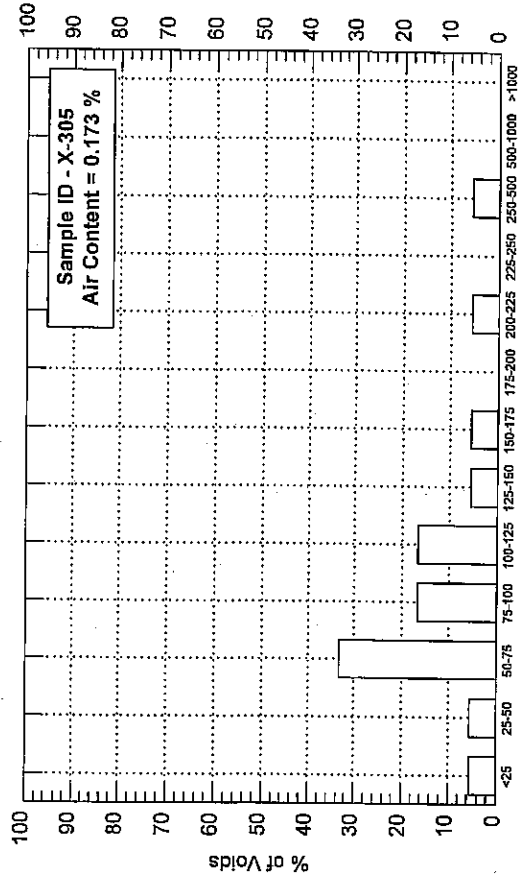
Size Range of Air Voids (microns)



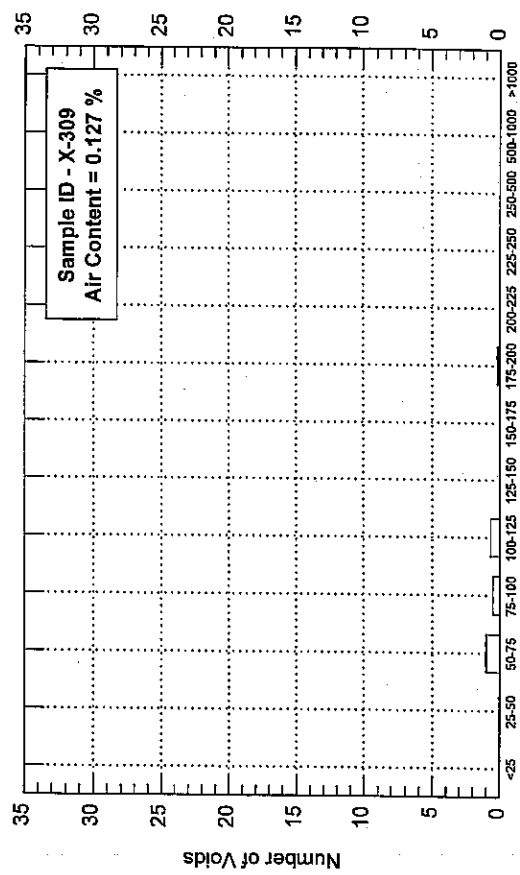
Size Range of Air Voids (microns)



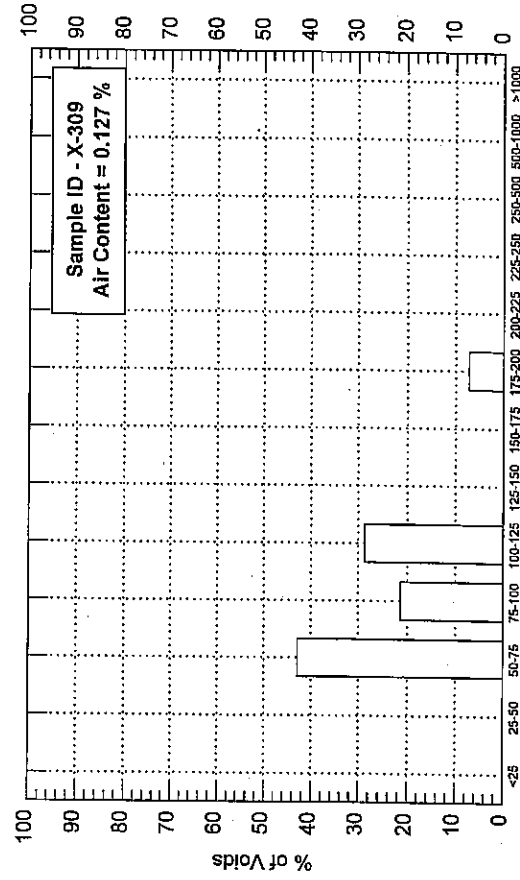
Size Range of Air Voids (microns)



Size Range of Air Voids (microns)



Size Range of Air Voids (microns)



Size Range of Air Voids (microns)

LINEAR TRAVERSE DATA -- LINE STATISTICS REPORT

Originator- Prof.Mohsen A. Issa
 Operator--- Cyro
 Date----- 01/20/99
 File----- X-264B30
 Sample ID- X-264B30
 Project #- ITRC

Data reported in Millimeters (mm).

Total Travel Executed----- 25.4 cm
 Total Area Covered----- 1.5 Sq. cm
 Total Void Length----- 4.0 cm
 Total Number of Voids----- 406

Line	Line Lgth	Num Vds	Average Vd Lgth	Std Dev	Coef Var	Line	Line Lgth	Num Vds	Average Vd Lgth	Std Dev	Coef Var
1	12.700	12	0.122	0.098	80.5%	2	12.700	14	0.144	0.149	103.9%
3	12.700	22	0.058	0.083	141.9%	4	12.772	24	0.064	0.068	105.5%
5	12.700	17	0.080	0.100	124.3%	6	12.700	10	0.116	0.147	126.7%
7	10.992	16	0.095	0.132	138.9%	8	0.468	2	0.132	0.000	N/A
9	1.240	2	0.054	0.000	N/A	10	12.700	18	0.114	0.182	160.0%
11	12.700	10	0.218	0.284	130.1%	12	12.700	16	0.086	0.052	60.5%
13	12.700	21	0.119	0.165	138.4%	14	12.700	20	0.115	0.144	125.2%
15	12.700	23	0.095	0.095	99.9%	16	12.700	28	0.090	0.102	113.1%
17	12.700	23	0.083	0.118	141.9%	18	12.700	34	0.101	0.110	109.2%
19	12.700	19	0.103	0.089	86.0%	20	12.700	25	0.062	0.062	99.3%
21	12.700	27	0.115	0.107	92.9%	22	12.628	23	0.106	0.148	139.3%

Note: Only lines with one or more voids shown in list.

Total Average Void Size= 0.099 (Avg. Chord Intercept)
 Total Standard Deviation= 0.123
 Total Coefficient of Variation= 123.6%

ACCUMULATED LINEAR TRAVERSE DATA

Originator- Prof.Mohsen A. Issa
 Operator--- Cyro
 Date----- 01/20/99
 File----- X-264B30
 Assumed Paste Content = 75.0%

Sample ID- X-264B30
 Project #- ITRC

Total Travel Executed----- 25.4 cm
 Total Area Covered----- 1.5 Sq. cm
 Total Void Length----- 4.0 cm
 Total Number of Voids----- 406

Void Size Breakdown (microns)

Voids less than 25-----	103	(25.37%)
Voids 25 to 50-----	85	(20.94%)
Voids 50 to 75-----	65	(16.01%)
Voids 75 to 100-----	28	(6.90%)
Voids 100 to 125-----	27	(6.65%)
Voids 125 to 150-----	18	(4.43%)
Voids 150 to 175-----	15	(3.69%)
Voids 175 to 200-----	14	(3.45%)
Voids 200 to 225-----	2	(0.49%)
Voids 225 to 250-----	6	(1.48%)
Voids 250 to 500-----	34	(8.37%)
Voids 500 to 1000-----	9	(2.22%)
Voids 1000 and greater -----	0	(0.00%)

LINEAR TRAVERSE CALCULATIONS

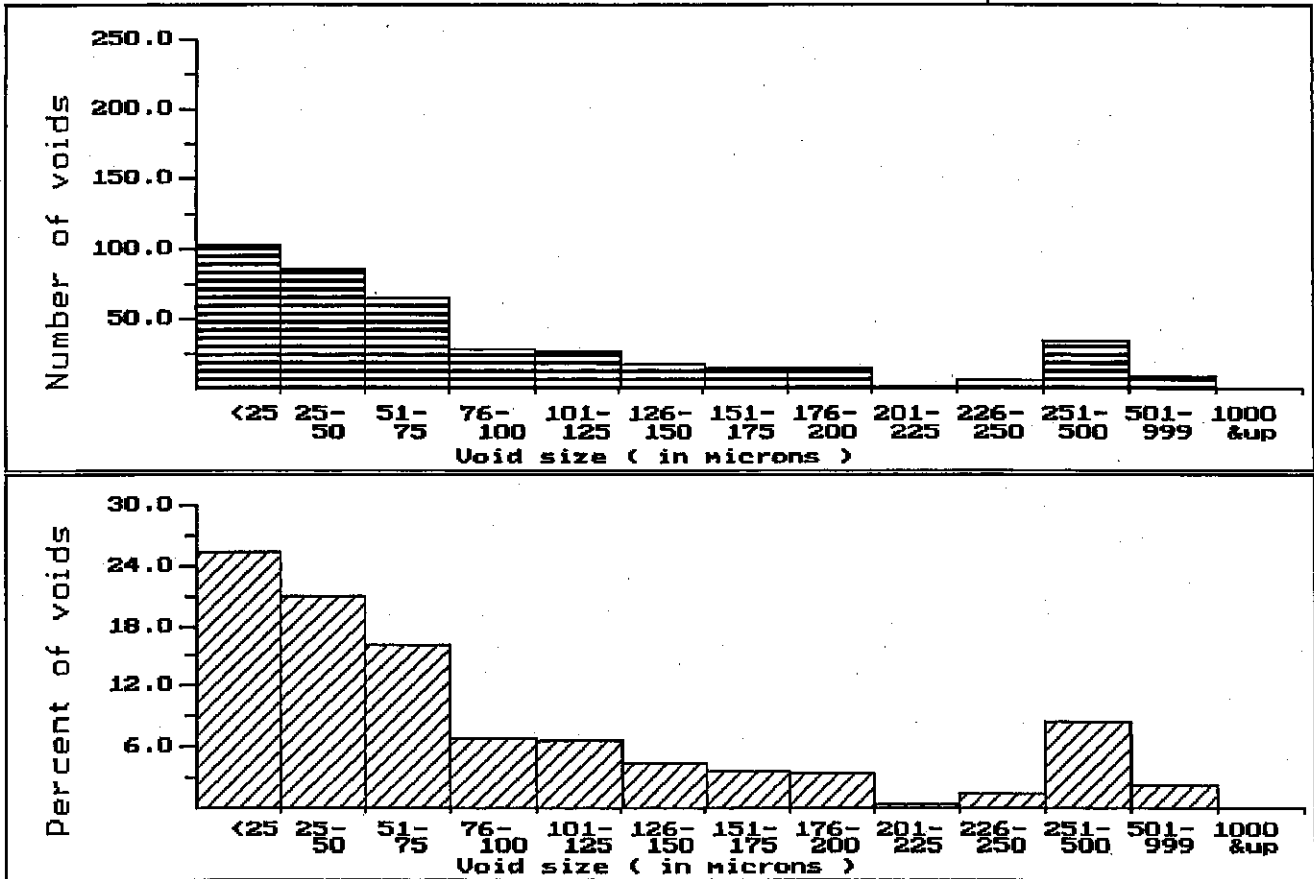
Average Chord Intercept----- 0.0992 mm
 Voids per mm----- 1.60
 Specific Surface (1/mm)----- 40.3
 Paste to Air Ratio----- 4.73
 Air Content----- 15.85 %

ACCUMULATED LINEAR TRAVERSE DATA

Originator- Prof.Mohsen A. Issa
 Operator--- Cyro
 Date----- 01/20/99
 File----- X-264B30
 Assumed Paste Content = 75.0%

Sample ID- X-264B30
 Project #- ITRC

Linear Traverse Bin-Width Bar Graph

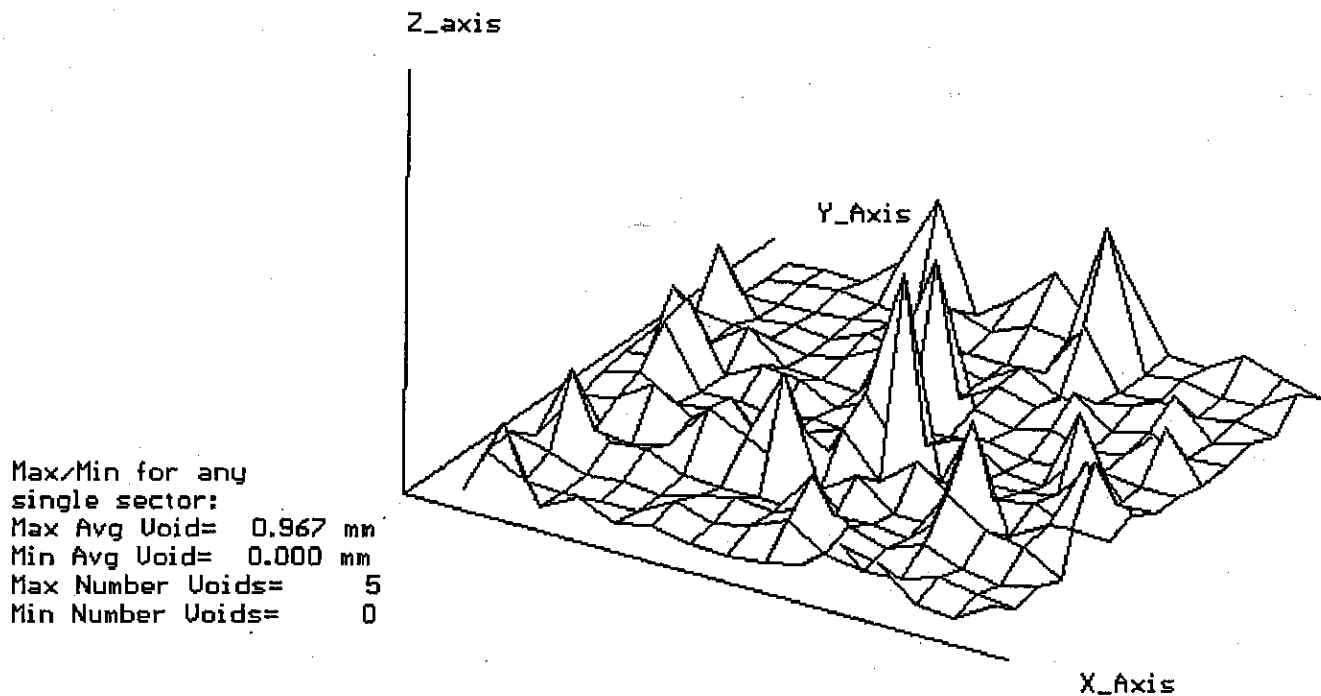


ACCUMULATED LINEAR TRAVERSE DATA -- SURFACE PLOT

Originator- Prof.Mohsen A. Issa
Operator--- Cyro
Date----- 01/20/99
File----- X-264B30
Assumed Paste Content = 75.0%

Sample ID- X-264B30
Project #- ITRC

Simulated 3D Surface Plot of Average Void Size per Sector.
Sample is divided into a 15 x 15 sector matrix . Peaks show relative average void size in any one sector.



Sector width (x-axis)= 0.847 mm Sector depth (y-axis)= 0.847 mm

APPENDIX B
WHFT

1. WHFT 1994

1.1 General Description

The procedure described in the WHFT method is intended to aid in the identification of D-cracking susceptible aggregates. WHFT relies on the pressure differential between the inside and outside of the aggregate pieces to cause D-cracking susceptible pieces to fracture. Aggregates that exhibit a high percentage of fracturing under repeated pressurization cycles are considered to be more likely to cause D-cracking in field applications. The relatively short time (approximately 8 working days) required for completion of this procedure makes it appropriate for use as a screening test to identify questionable aggregates requiring additional (more time consuming) testing, such as the AASHTO T161 test prior to final approval. It is recommended that aggregates with HFI of greater than 75 are not susceptible to D-cracking. If for any aggregate this value of HFI falls below 75, then before rejecting the aggregates, it is suggested to perform the freezing and thawing test.

1.2 Procedure

The procedure for the WHFT method is described as follows. Duplicate specimens should be run to obtain acceptable variability.

1.2.1 Sample Preparation

1. Separate the sample into appropriate size (passing the 31.5 mm (1¼ in.) but retained on the 19 mm (¾ in.) sieves or passing the 19 mm (¾ in.) but retained on the 13 mm (½ in.) sieves). Usually a sample size of approximately 3.2 kg (7.0 lb) is needed for each test.
2. Thoroughly wash the aggregates and dry to a constant mass at a temperature of $120^{\circ}\text{C} \pm 5^{\circ}\text{C}$ ($250^{\circ}\text{F} \pm 9^{\circ}\text{F}$) for 2 hours and allow the aggregates to cool to room temperature.
3. Place the aggregate specimen in silane solution for 30 seconds \pm 5 seconds. Make sure that all aggregate pieces are covered. Remove the specimen from the silane solution and allow the excess solution to drain for 5 minutes.
4. Dry the specimen to a constant mass at a temperature of $120^{\circ}\text{C} \pm 5^{\circ}\text{C}$ ($250^{\circ}\text{F} \pm 9^{\circ}\text{F}$) for overnight and allow to cool to room temperature.

5. Place enough of the specimen into the tumbler to fill it approximately half way and tumble for 1 minute.
6. Separate out any pieces passing the 9.5 mm ($\frac{3}{8}$ in.) sieve. Repeat for the remainder of the specimen.
7. Determine the mass (say m_0) to the nearest gram and carefully count the number of pieces (say n_0) retained on the 9.5 mm ($\frac{3}{8}$ in.) sieve.

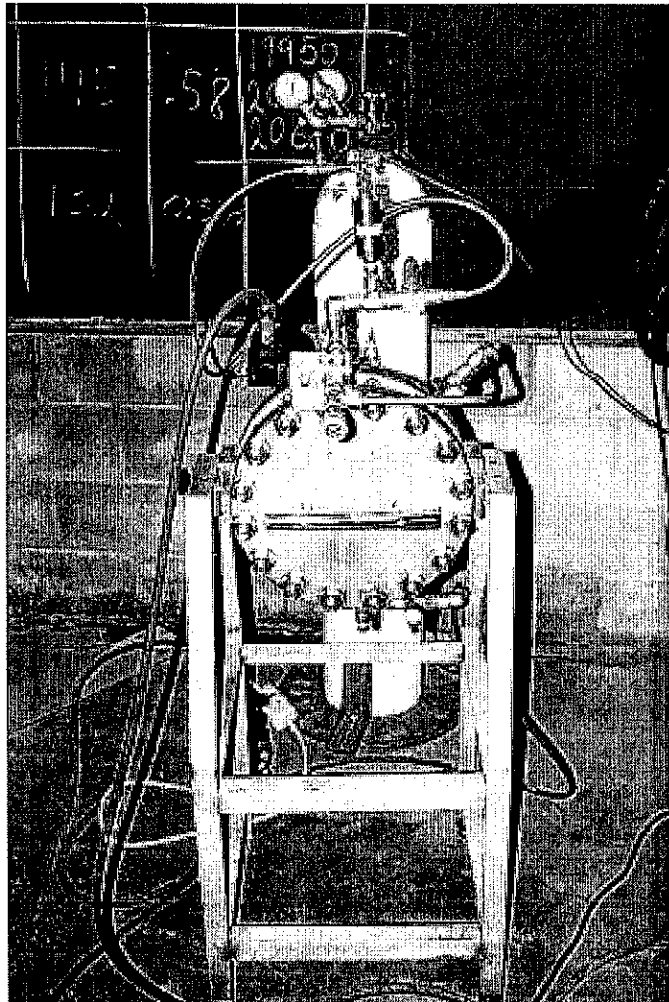


Fig. B.1 WHFT 1994 Apparatus

1.2.2 Chamber Assembly

1. With the bottom plate in a horizontal position with the inside facing up, wipe the machined surface with a cloth to remove any rock chips. Place the o-ring on the bottom plate so that it is a circular shape and symmetrical on the machined surface.
2. Carefully wipe any rock chips and/or dirt from the o-ring groove in the cylinder assembly, and set the cylinder assembly onto the bottom plate so that the o-ring is completely captured in the o-ring channel. The cylinder assembly should be aligned so that a line from the fill assembly to the pressure release assembly is perpendicular to the pivot axis of the pivot stand.
3. Place the aggregate specimen into the pressure cylinder and spread the aggregates around to a uniform thickness (The cylinder holds a specimen of approximately 3 to 4 kg). For the first testing of an aggregate specimen, use a straight edge across the open end of the cylinder assembly to check for any particles that extends above the top edge of the cylinder. Remove any pieces touched by the straight edge and subtract both their mass and number from the initial specimen mass and count. For subsequent pressurization of the specimen, rearrange any protruding pieces so that they all fit into the chamber.
4. Clean the o-ring channel and insert the o-ring.
5. Place the top plate onto the pressure cylinder and align the holes in the 2 end plates.
6. Insert the bolts into the holes in the bottom plate, and through the top plate. Do the holes closest to the pivot assembly first, and the remaining bolts after those closest to the pivot assembly are in. The top plate may need to be moved around slightly in order to insert the first bolts. Place nuts on all the bolts.
7. Tighten the nuts to 6.8 to 9.1 N-m (60 to 80 lb-in.) in the following pattern:
 - (a) Tighten two nuts on opposite sides of the pressure cylinder (nuts 1 and 9 if the nuts are numbered consecutively going around the cylinder).
 - (b) Tighten the nuts on each side, midway between the nuts already tightened (nuts 5 and 13).

- (c) Tighten nuts 3, 7, 11, 15.
 - (d) Tighten the remaining nuts.
 - (e) Check the nuts to make sure none have loosened as the o-rings were compressed. Retighten any loose nuts, and re-check all nuts for tightness.
8. Rotate the apparatus from the filling (horizontal) to the testing (vertical) position.
 9. Attach the drain line to the pressure release connector.
 10. Turn on the air pressure, and adjust the regulator to 655 kPa (95 psi).
 11. Open the fill valve and open the pressure release valve by turning the switch on the solenoid to on. Fill the chamber with water by turning on the water source.
 12. After the chamber is full (excess water is coming out of the drain line, which is connected to the pressure release valve), fill the copper drain pipe by opening the drain valve and allowing water to flow through the copper line connecting the drain assembly to the pressure release assembly. Close the drain valve.
 13. Remove any air bubbles in the chamber by pivoting the chamber back and forth while vigorously tapping the end plates with a rubber mallet (this loosens air bubbles adhering to aggregate pieces). After the chamber has been pivoted back and forth at least 3 times with no additional air coming out the drain line, shut off the water source.
 14. Close the fill valve, close the pressure release valve by turning the switch on the solenoid off, and disconnect the drain line. The chamber should be tilted so that the quick-disconnect on the pressure release assembly is pointing about 5° below horizontal.

1.2.3 Chamber Pressurization

1. Close the pressure isolation valve and open the main valve on the nitrogen tank. Set the pressure regulator to 7930 kPa (1150 psi).

2. Pressurize the chamber for 5 minutes \pm 5 seconds by opening the pressure isolation valve. Slightly adjust the pressure regulator as necessary to maintain the required pressure of 7930 kPa (1150 psi). At about 4.5 minutes, close the pressure valve to isolate the chamber from the compressed nitrogen.
3. After 5 minutes \pm 5 seconds of pressurization release the pressure by opening the pressure release valve with a rate of 224,000 kPa/sec (32510 psi/sec) for a duration of 0.01 second. Wear ear protection while releasing the pressure.
4. The drain line is reconnected and the chamber is refilled with water. Do the same treatment as before to remove air bubbles.
5. Pressurize the chamber for 2 minutes \pm 3 seconds and release the pressure as before.
6. Repeat step 4 and 5 eight additional times.

1.2.4 Chamber Opening

1. Turn off the valve on the nitrogen tank and open the drain valve. Drain water from the pressure chamber by slowly opening the pressure valve and allowing the compressed gas in the line to force the water out of the chamber.
2. Unbolt the chamber and remove the specimen. Dry the specimen to a constant mass at a temperature of 120°C \pm 5°C (250°F \pm 9°F) over night and allow the aggregates to cool to room temperature.
3. Place enough of the specimen into the tumbler to fill it approximately half way and tumble for 1 minute. Repeat with the remaining portion of the specimen.
4. Separate out any pieces passing the 9.5 mm (3/8 in.) sieve but retained on the No. 4 sieve.
5. Weigh and count the material retained on both sieves. Record the mass of the specimen retained on the 9.5 mm (3/8 in.) sieve after "i" pressurization cycles (say m_i) and the mass of the cumulative specimen passing the 9.5 mm (3/8 in.) sieve but retained on the No. 4 sieve

after "i" pressurization cycles to the nearest gram (say m_{4_i}). Count the number of pieces retained on the 9.56 mm ($\frac{3}{8}$ in.) sieve after "i" pressurization cycles (say n_i) and the number of the cumulative specimen passing the 9.5 mm ($\frac{3}{8}$ in.) sieve but retained on the No. 4 sieve after "i" pressurization cycles (say n_{4_i}).

6. Repeat steps 5.1.3.2-1 through 5.1.3.4-5 for 4 more sets of cycles to complete a total of 50 pressurization cycles.
7. Finally, calculate percent fracture (PF), percent mass loss (PML) and hydraulic fracture index (HFI) as described in the report.

2. WHFT 1997

2.1 General Description

This Washington Hydraulic Fracture Test (WHFT 97) is a modified version of the 1994 apparatus (Fig. B.2). It contains the following changes to facilitate the operation of this test: (1) WHFT 97 has a larger chamber with a 254 mm (10 in.) inside diameter and a 30.5 cm (12 in.) height. (2) Operator and handling time is reduced by using pressure to hold the chamber lid down instead of 16 high strength bolts. (3) Air driven water is used instead of the Nitrogen gas to pressurize the chamber. (4) The machine is fully automated in terms of controlling the entire testing procedure for each respective 10 cycles of operation. (5) It has a more accurate controlled release rate. (6) A controlled interface is connected to the machine that reads pressure and temperature, hence good quality control of the system and much better results are expected. (7) The computer interface will provide a plot of the release for each cycle.

2.2 Data Acquisition System

The designed system aims at both high accurate data acquisition and full computer control over the experiment during its active stage. At the initial stage of an experiment, an operator would setup the time table. This includes entering the number of cycles, pressurization time per cycle, time between cycles, and maximum allowable pressure. During the active stage of the experiment, the system operates on an air line valve to build up the pressure, and an outlet valve to release the pressure. This would be based on the time table, maximum pressure and data readings.

This controlled interface is connected to the machine that reads pressure and temperature (Fig. C.5), hence good quality control of the system and much better results are expected. The computer interface will also provide a plot of the release for each cycle. The following is a list of the data acquisition parts:

The software used for this data acquisition system is called Labview. It is a fully development system for Windows 95/NT/3.1

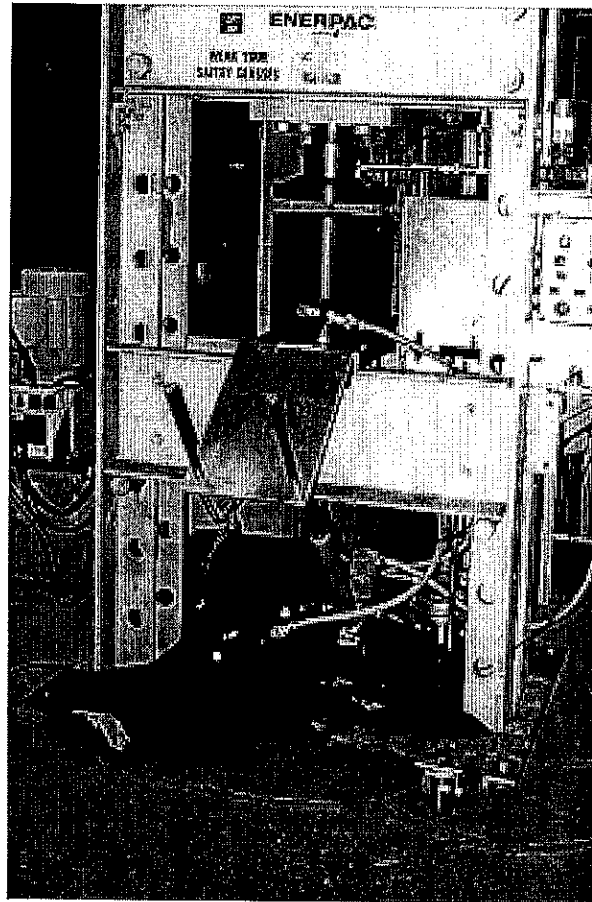


Fig. B.2 - WHFT 1997 Apparatus

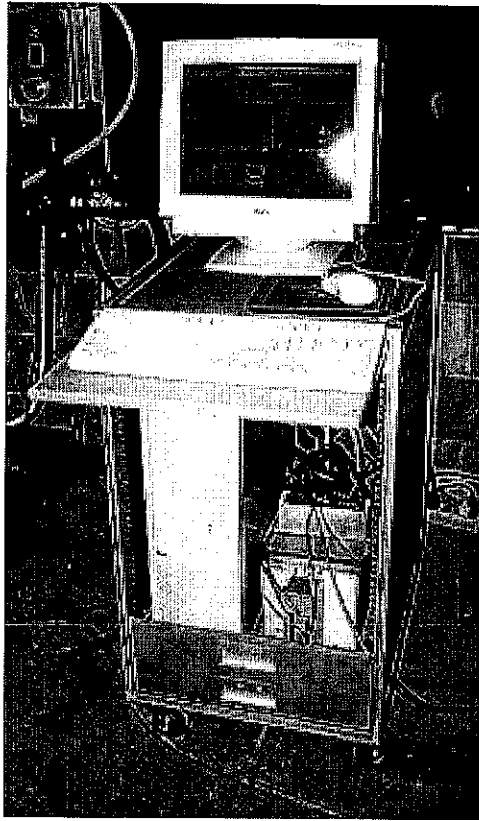


Fig. B.3 Data Acquisition System

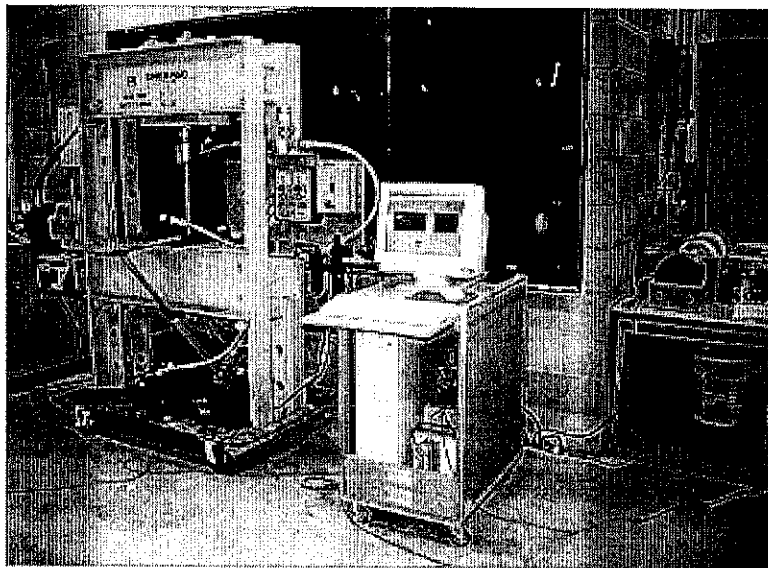


Fig. B.4 WHFT 1997 Setup

2.2 Procedure

2.2.1 Sample Preparation

1. Separate the sample into appropriate size (passing the 31.5 mm (1¼ in.) but retained on the 19 mm (¾ in.) sieves or passing the 19 mm (¾ in.) but retained on the 13 mm (½ in.) sieves). Usually a sample size of approximately 16 kg (35 lb) is needed for each test.
2. The aggregate specimen should be thoroughly washed and dried for 24 hours at a temperature of $120^{\circ}\text{C} \pm 5^{\circ}\text{C}$ ($250^{\circ}\text{F} \pm 9^{\circ}\text{F}$), and allowed to cool to room temperature.
3. Place the aggregate specimen in the silane solution making sure that all aggregate pieces are covered. Allow the specimen to remain in the silane solution for 30 seconds \pm 5 seconds.
4. Remove the specimen from the silane solution and allow the excess solution to drain for five minutes.
5. Dry the specimen for 24 hours at a temperature of $120^{\circ}\text{C} \pm 5^{\circ}\text{C}$ ($250^{\circ}\text{F} \pm 9^{\circ}\text{F}$), and allow to cool to room temperature.
6. Place enough of the specimen into the tumbler to fill it approximately half way and tumble for 1 minute. Separate out any pieces passing the 9.5 mm (¾ in.) Sieve. Repeat for the remaining portion of the specimen. Determine the mass to the nearest gram and count the number of pieces retained on the 9.5 mm (¾ in.) sieve. Record these numbers as the initial mass and number of particles, m_0 and n_0 , respectively.

2.2.2 Chamber Assembly

1. Place the specimen into the pressure chamber.
2. Slide the chamber into position.
3. Attach the inlet hose to the quick disconnect fitting located towards the bottom of the chamber.

4. Fill the reservoir up with distilled water. Add 80 ml of TBP and 8 ml of PPG to the water and mix very well. These admixtures are used to minimize the amount of entrapped air bubbles inside the pressurized chamber.
5. Fill the chamber with water by pressing the de-watering pump button. Press the button again to stop the pump when water reaches the top of the chamber.
6. Close the fill valve.
7. Place the o-ring around the top of the chamber.
8. Start the hydraulic system and slowly increase the loading by pressing the advancing button on the control center until the loading head touches the lid. Make sure that the chamber is perfectly aligned with the lid.
9. Increase the loading until the machine maintains a controlled reading of 50986 kPa (7400 psi). The loading will stop automatically when this load is achieved.
10. Open the release solenoid valve by pulling on the red button located at the upper right hand corner of the control board, and by turning it on using the computer interface.
11. Turn on the valve on the air tank to activate the air driven pump, and open the air supply valve, which is connected to the air pressure regulator to allow water to run through the inlet pipes. Make sure the chamber and fill valves are open.
12. Press the de-watering pump button to continue filling the chamber with water. The chamber is full when the outlet clear pipe shows a minimum amount of air bubbles in the flow.

2.2.3 Chamber Pressurization

The machine is fully automated in terms of controlling the entire testing procedure for each respective 10 cycles of operation. The data acquisition system is programmed to run the procedure of 10 cycles of pressurizing and release without stopping. The total time for ten cycles is about 35 minutes.

1. On the operating screen of the Labview software, close the outlet solenoid.
2. Press the run button found in the upper left hand corner of the computer screen. A small window will pop open. Open the timetable which will be used during testing.
3. Enter the specimen ID on the computer screen. At this point, everything is ready for starting the pressurization cycles.
4. Press the START DAQ button on the computer screen. Then name the file of the sample being tested.
5. By pressing ENTER key, the chamber will start building up pressure.
6. When the pressure reaches 7925 kPa (1150 psi) the inlet solenoid will close automatically.
7. Pressurize the chamber for 5 minutes \pm 5 seconds.
8. After 5 minutes \pm 5 seconds of pressurization, the outlet solenoid valve will open automatically to release the pressure in the chamber. At the time of release, pressure versus time data will be collected to control the release rate.
9. At this point the inlet solenoid valve will open to refill the chamber with water.
10. The outlet solenoid will close and re-pressurize the chamber after a total elapsed time of 1 minute \pm 5 seconds without pressure. The computer interface should automatically build up the pressure back to 7925 kPa (1150 psi). This pressurization time is 2 minutes \pm 5 seconds.
11. After 2 minutes \pm 5 seconds of pressurization, the outlet solenoid will open and release the pressure in the chamber.
12. The data acquisition system will repeat step 5.2.5.3-5 through 5.2.5.3-7 eight additional times for a total of 10 pressurization cycles.

2.2.4 Chamber Opening

1. Drain the water from the chamber by opening the drain valve.
2. Release the pressure on the chamber lid by slowly decreasing the applied load. Make sure no pressure is in the chamber by inspecting the pressure gauges.
3. Disconnect the inlet hose from the bottom quick disconnect fitting of the chamber.
4. Carefully slide the chamber from under the loading device, and remove the aggregates from inside the chamber.
5. Dry the specimen to a constant mass at a temperature of $120^{\circ}\text{C} \pm 5^{\circ}$ ($250^{\circ}\text{F} \pm 9^{\circ}\text{F}$), and allow it to cool to room temperature.
6. Place enough of the specimen into the tumbler to fill it approximately half way, and tumble for $1 \text{ minute} \pm 5 \text{ seconds}$. Repeat with the remaining portion of the specimen.
7. Separate out any pieces passing the 9.5 mm ($\frac{3}{8}$ in.) sieve but retained on the 4.75 mm (No. 4) sieve.
8. Determine the masses of pieces retained on the 9.5 mm ($\frac{3}{8}$ in.) sieve and cumulative pieces passing the 9.5 mm and retained on the 4.75 mm (No. 4) sieve particles to the nearest gram. Record these value as m_i and m_{4_i} , respectively for the "i" number of pressurization cycles completed.
9. Count the number of pieces retained on the 9.5 mm ($\frac{3}{8}$ in.) sieve and record this number as n_i . Count the cumulative number of pieces passing the 9.5 mm ($\frac{3}{8}$ in.) sieve but retained on the 4.75 mm (No. 4) sieve and record this number as n_{4_i} .
10. Repeat steps 5.2.5.2-1 through 5.2.5.4-9 for a total of 50 pressurization cycles.
11. Finally, calculate percent fracture (PF), percent mass loss (PML) and hydraulic fracture index (HFI) as described in the report.

APPENDIX C
Results



Table C.1 X-1 Daily Data Sheet

Trial #	WHFT 94				WHFT 97				
	1	2	3	Total	1	2	3	Total	
Date Treated	8/23/98	8/23/98	8/23/98	8/23/98	7/26/98	9/20/98	9/20/98	9/20/98	
initial m_0 , g	3237.0	3231.0	3216.0	9684.0	16073.0	15419.5	15303.5	46796.0	
initial n_0	617	614	585	1816	3275	2904	2969	9148	
Date Pressurized	8/24/98	8/24/98	8/24/98	8/24/98	7/27/98	9/21/98	9/21/98	9/21/98	
10 Cycles	m_{10} , g	3235.5	3228.5	3214.0	9678.0	16062.0	15408.0	15292.5	46762.5
	$m_{4_{10}}$, g	0.0	0.5	0.0	0.5	0.0	2.5	1.5	4.0
	PML_{10}	0.046	0.062	0.062	0.057	0.068	0.058	0.062	0.063
	n_{10}	618	615	585	1818	3275	2904	2968	9147
	$n_{4_{10}}$	0	1	0	1	0	3	2	5
	PF_{10}	0.162	0.244	0.000	0.138	0.000	0.052	0.000	0.016
Date Pressurized	8/25/98	8/25/98	8/25/98	8/25/98	7/28/98	9/22/98	9/22/98	9/22/98	
20 Cycles	m_{20} , g	3234.0	3227.0	3211.5	9672.5	16051.0	15393.5	15280.5	46725.0
	$m_{4_{20}}$, g	0.0	0.5	1.0	1.5	1.0	4.0	4.0	9.0
	PML_{20}	0.093	0.108	0.109	0.103	0.131	0.143	0.124	0.132
	n_{20}	618	615	585	1818	3275	2902	2968	9145
	$n_{4_{20}}$	0	1	2	3	1	5	6	12
	PF_{20}	0.162	0.244	0.171	0.193	0.015	0.017	0.067	0.033
Date Pressurized	8/26/98	8/26/98	8/26/98	8/26/98	7/29/98	9/23/98	9/23/98	9/23/98	
30 Cycles	m_{30} , g	3232.5	3226.0	3210.5	9669.0	16039.0	15382.5	15273.5	46695.0
	$m_{4_{30}}$, g	0.5	0.5	1.0	2.0	2.5	6.5	5.0	14.0
	PML_{30}	0.124	0.139	0.140	0.134	0.196	0.198	0.163	0.186
	n_{30}	618	615	585	1818	3274	2902	2968	9144
	$n_{4_{30}}$	1	1	2	4	3	10	8	21
	PF_{30}	0.243	0.244	0.171	0.220	0.015	0.103	0.101	0.071
Date Pressurized	8/27/98	8/27/98	8/27/98	8/27/98	7/30/98	9/24/98	9/24/98	9/24/98	
40 Cycles	m_{40} , g	3231.0	3224.5	3209.0	9664.5	16031.0	15374.5	15263.0	46668.5
	$m_{4_{40}}$, g	0.5	0.5	1.0	2.0	3.0	7.5	9.0	19.5
	PML_{40}	0.170	0.186	0.187	0.181	0.243	0.243	0.206	0.231
	n_{40}	618	615	585	1818	3274	2902	2968	9144
	$n_{4_{40}}$	1	1	2	4	4	13	14	31
	PF_{40}	0.243	0.244	0.171	0.220	0.031	0.155	0.202	0.126
Date Pressurized	8/28/98	8/28/98	8/28/98	8/28/98	7/31/98	9/25/98	9/25/98	9/25/98	
50 Cycles	m_{50} , g	3230.0	3223.5	3208.5	9662.0	16022.0	15367.5	15255.0	46644.5
	$m_{4_{50}}$, g	0.5	0.5	1.0	2.0	3.5	7.5	9.5	20.5
	PML_{50}	0.201	0.217	0.202	0.207	0.296	0.289	0.255	0.280
	n_{50}	618	615	585	1818	3275	2902	2968	9145
	$n_{4_{50}}$	1	1	2	4	8	13	15	36
	PF_{50}	0.243	0.244	0.171	0.220	0.122	0.155	0.219	0.164
HFI	2057	2047	2925	2270	4094	3227	2284	3049	

Source: ILDOT

Chamber psi: 1150

Size: 1/2"

Tested by: Mark Bendok

Table C.2 X-5 Daily Data Sheet

Trial #	WHFT 94				WHFT 97				
	1	2	3	Total	1	2	3	Total	
Date Treated	8/9/98	8/9/98	10/26/98	8/9/98	9/13/98	12/6/98	12/6/98	12/6/98	
initial m_0 , g	2900.0	2916.0	3220.5	9036.5	16005.0	16056.5	16085.0	48146.5	
initial n_0	478	550	562	1590	2747	2727	2959	8433	
Date Pressurized	8/10/98	8/10/98	10/27/98	8/10/98	9/14/98	12/7/98	12/7/98	12/7/98	
10 Cycles	m_{10} , g	2899.5	2914.0	3217.0	9030.5	15990.5	16029.5	16063.5	48083.5
	$m_{4_{10}}$, g	0.0	0.0	1.0	1.0	3.0	2.0	3.5	8.5
	PML_{10}	0.017	0.069	0.078	0.055	0.072	0.156	0.112	0.113
	n_{10}	479	551	564	1594	2746	2727	2959	8432
	$n_{4_{10}}$	0	0	2	2	6	2	5	13
	PF_{10}	0.209	0.182	0.534	0.314	0.073	0.037	0.084	0.065
Date Pressurized	8/11/98	8/11/98	10/28/98	8/11/98	9/15/98	12/8/98	12/8/98	12/8/98	
20 Cycles	m_{20} , g	2898.5	2912.0	3214.5	9025.0	15982.0	16018.0	16050.5	48050.5
	$m_{4_{20}}$, g	0.0	1.0	1.0	2.0	3.0	4.0	8.5	15.5
	PML_{20}	0.052	0.103	0.155	0.105	0.125	0.215	0.162	0.167
	n_{20}	479	550	564	1593	2749	2727	2959	8435
	$n_{4_{20}}$	0	2	2	4	6	5	13	24
	PF_{20}	0.209	0.182	0.534	0.314	0.182	0.092	0.220	0.166
Date Pressurized	8/12/98	8/12/98	10/29/98	8/12/98	9/16/98	12/9/98	12/9/98	12/9/98	
30 Cycles	m_{30} , g	2897.0	2909.0	3212.5	9018.5	15972.5	16002.0	16034.5	48009.0
	$m_{4_{30}}$, g	0.5	2.5	2.0	5.0	3.0	6.5	13.0	22.5
	PML_{30}	0.086	0.154	0.186	0.144	0.184	0.299	0.233	0.239
	n_{30}	479	550	563	1592	2749	2728	2958	8435
	$n_{4_{30}}$	1	3	3	7	6	9	22	37
	PF_{30}	0.314	0.273	0.445	0.346	0.182	0.202	0.338	0.243
Date Pressurized	8/13/98	8/13/98	10/30/98	8/13/98	9/17/98	12/10/98	12/10/98	12/10/98	
40 Cycles	m_{40} , g	2896.0	2907.5	3212.0	9015.5	15965.5	15990.0	16023.0	47978.5
	$m_{4_{40}}$, g	0.5	3.0	2.0	5.5	6.5	7.0	18.0	31.5
	PML_{40}	0.121	0.189	0.202	0.172	0.206	0.371	0.274	0.284
	n_{40}	479	550	563	1592	2749	2729	2957	8435
	$n_{4_{40}}$	1	5	3	9	9	11	30	50
	PF_{40}	0.314	0.455	0.445	0.409	0.237	0.275	0.439	0.320
Date Pressurized	8/14/98	8/14/98	10/31/98	8/14/98	9/18/98	12/11/98	12/11/98	12/11/98	
50 Cycles	m_{50} , g	2895.5	2906.5	3210.0	9012.0	15952.5	15978.0	16019.0	47949.5
	$m_{4_{50}}$, g	0.5	3.0	2.0	5.5	8.0	7.5	21.0	36.5
	PML_{50}	0.138	0.223	0.264	0.210	0.278	0.442	0.280	0.333
	n_{50}	479	550	563	1592	2752	2730	2955	8437
	$n_{4_{50}}$	1	5	3	9	11	12	38	61
	PF_{50}	0.314	0.455	0.445	0.409	0.382	0.330	0.507	0.409
HFI	1593	1100	1124	1223	1308	1515	986	1222	

Source: ILDOT

Chamber psi: 1150

Size: 1/2"

Tested by: Mark Bendok

Table C.3 X-7 Daily Data Sheet

Trial #	WHFT 94				WHFT 97				
	1	2	3	Total	1	2	3	Total	
Date Treated	8/23/98	8/23/98	8/23/98	8/23/98	9/13/98	9/13/98	12/6/98	12/6/98	
initial m_0 , g	3245.0	3257.5	3260.0	9762.5	16041.0	16042.0	16009.0	48092.0	
initial n_0	606	626	616	1848	2844	3150	3001	8995	
Date Pressurized	8/24/98	8/24/98	8/24/98	8/24/98	9/14/98	9/14/98	12/7/98	12/7/98	
10 Cycles	m_{10} , g	3241.5	3255.5	3258.0	9755.0	16032.0	16026.5	15994.0	48052.5
	$m_{4_{10}}$, g	1.0	0.5	0.0	1.5	0.0	1.5	0.5	2.0
	PML_{10}	0.077	0.046	0.061	0.061	0.056	0.087	0.091	0.078
	n_{10}	607	626	617	1850	2845	3150	3001	8996
	$n_{4_{10}}$	1	1	0	2	0	2	2	4
	PF_{10}	0.248	0.080	0.162	0.162	0.035	0.032	0.033	0.033
Date Pressurized	8/25/98	8/25/98	8/25/98	8/25/98	9/15/98	9/15/98	12/8/98	12/8/98	
20 Cycles	m_{20} , g	3240.0	3254.0	3256.0	9750.0	16019.5	16013.0	15980.0	48012.5
	$m_{4_{20}}$, g	1.0	0.5	0.5	2.0	1.5	3.0	2.0	6.5
	PML_{20}	0.123	0.092	0.107	0.108	0.125	0.162	0.169	0.152
	n_{20}	607	626	617	1850	2845	3150	3003	8998
	$n_{4_{20}}$	1	1	1	3	2	4	6	12
	PF_{20}	0.248	0.080	0.244	0.189	0.070	0.063	0.167	0.100
Date Pressurized	8/26/98	8/26/98	8/26/98	8/26/98	9/16/98	9/16/98	12/9/98	12/9/98	
30 Cycles	m_{30} , g	3239.0	3252.5	3254.5	9746.0	16011.5	16001.5	15975.0	47988.0
	$m_{4_{30}}$, g	1.0	0.5	0.5	2.0	1.5	6.5	3.0	11.0
	PML_{30}	0.154	0.138	0.153	0.149	0.175	0.212	0.194	0.193
	n_{30}	607	627	617	1851	2845	3150	3003	8998
	$n_{4_{30}}$	1	2	1	4	2	7	8	17
	PF_{30}	0.248	0.319	0.244	0.271	0.070	0.111	0.200	0.128
Date Pressurized	8/27/98	8/27/98	8/27/98	8/27/98	9/17/98	9/17/98	12/10/98	12/10/98	
40 Cycles	m_{40} , g	3237.5	3251.0	3253.5	9742.0	16000.5	15992.5	15960.5	47953.5
	$m_{4_{40}}$, g	1.0	0.5	0.5	2.0	3.0	6.5	3.5	13.0
	PML_{40}	0.200	0.184	0.184	0.190	0.234	0.268	0.281	0.261
	n_{40}	607	627	617	1851	2845	3150	3004	8999
	$n_{4_{40}}$	1	2	1	4	6	7	9	22
	PF_{40}	0.248	0.319	0.244	0.271	0.141	0.111	0.250	0.167
Date Pressurized	8/28/98	8/28/98	8/28/98	8/28/98	9/18/98	9/18/98	12/11/98	12/11/98	
50 Cycles	m_{50} , g	3236.5	3250.0	3252.0	9738.5	15992.0	15983.0	15949.0	47924.0
	$m_{4_{50}}$, g	1.0	0.5	0.5	2.0	6.0	8.0	3.5	17.5
	PML_{50}	0.231	0.215	0.230	0.225	0.268	0.318	0.353	0.313
	n_{50}	607	627	617	1851	2845	3151	3004	9000
	$n_{4_{50}}$	1	2	1	4	8	10	9	27
	PF_{50}	0.248	0.319	0.244	0.271	0.176	0.190	0.250	0.206
HFI	2020	1565	2053	1848	2844	2625	2001	2431	

Source: ILDOT

Chamber psi: 1150

Size: 1/2"

Tested by: Mark Bendok

Table C.4 X-12 Daily Data Sheet

Trial #	WHFT 94				WHFT 97				
	1	2	3	Total	1	2	3	Total	
Date Treated	8/30/98	8/30/98	8/30/98	8/30/98	6/21/98	10/4/98	10/4/98	10/4/98	
initial m_0 , g	3227.5	3212.5	3253.0	9693.0	15890.5	15940.0	15859.0	47689.5	
initial n_0	558	575	622	1755	2908	2804	3024	8736	
Date Pressurized	8/31/98	8/31/98	8/31/98	8/31/98	6/22/98	10/5/98	10/5/98	10/5/98	
10 Cycles	m_{10} , g	3218.5	3205.5	3247.5	9671.5	15864.5	15915.5	15833.0	47613.0
	$m_{4_{10}}$, g	2.5	1.5	1.0	5.0	5.0	6.0	4.5	15.5
	PML_{10}	0.201	0.171	0.138	0.170	0.132	0.116	0.136	0.128
	n_{10}	556	576	621	1753	2902	2804	3020	8726
	$n_{4_{10}}$	12	8	5	25	12	13	8	33
	PF_{10}	0.717	0.870	0.241	0.598	0.000	0.232	0.000	0.074
Date Pressurized	9/1/98	9/1/98	9/1/98	9/1/98	6/23/98	10/6/98	10/6/98	10/6/98	
20 Cycles	m_{20} , g	3214.0	3198.0	3244.5	9656.5	15843.5	15900.0	15810.5	47554.0
	$m_{4_{20}}$, g	3.0	3.0	1.0	7.0	7.5	9.0	10.5	27.0
	PML_{20}	0.325	0.358	0.231	0.304	0.249	0.194	0.240	0.228
	n_{20}	557	572	623	1752	2902	2800	3022	8724
	$n_{4_{20}}$	14	14	5	33	19	22	19	60
	PF_{20}	1.075	0.696	0.563	0.769	0.120	0.250	0.248	0.206
Date Pressurized	9/2/98	9/2/98	9/2/98	9/2/98	6/24/98	10/7/98	10/7/98	10/7/98	
30 Cycles	m_{30} , g	3207.5	3194.0	3242.0	9643.5	15826.5	15886.5	15793.5	47506.5
	$m_{4_{30}}$, g	6.5	3.5	1.0	11.0	9.5	11.0	15.0	35.5
	PML_{30}	0.418	0.467	0.307	0.397	0.343	0.267	0.318	0.309
	n_{30}	556	574	623	1753	2901	2799	3016	8716
	$n_{4_{30}}$	18	16	5	39	22	25	30	77
	PF_{30}	1.254	1.217	0.563	0.997	0.138	0.267	0.231	0.212
Date Pressurized	9/3/98	9/3/98	9/3/98	9/3/98	6/25/98	10/8/98	10/8/98	10/8/98	
40 Cycles	m_{40} , g	3205.0	3190.5	3238.5	9634.0	15808.5	15878.5	15785.0	47472.0
	$m_{4_{40}}$, g	7.0	4.0	2.0	13.0	11.5	11.5	15.0	38.0
	PML_{40}	0.480	0.560	0.384	0.475	0.444	0.314	0.372	0.376
	n_{40}	555	574	622	1751	2898	2799	3016	8713
	$n_{4_{40}}$	19	17	8	44	26	26	30	82
	PF_{40}	1.165	1.304	0.643	1.026	0.103	0.285	0.231	0.206
Date Pressurized	9/4/98	9/4/98	9/4/98	9/4/98	6/26/98	10/9/98	10/9/98	10/9/98	
50 Cycles	m_{50} , g	3202.5	3188.5	3231.5	9622.5	15791.0	15869.5	15780.0	47440.5
	$m_{4_{50}}$, g	7.0	4.0	6.0	17.0	18.0	11.5	17.5	47.0
	PML_{50}	0.558	0.623	0.476	0.552	0.513	0.370	0.388	0.424
	n_{50}	555	574	622	1751	2898	2800	3016	8714
	$n_{4_{50}}$	19	17	14	50	36	26	36	98
	PF_{50}	1.165	1.304	1.125	1.197	0.275	0.321	0.331	0.309
HF1	429	383	444	418	1818	1558	1512	1618	

Source: ILDOT

Chamber psi: 1150

Size: 1/2"

Tested by: Mark Bendok

Table C.5 X-31 Daily Data Sheet

Trial #	WHFT 94				WHFT 97			
	1	2	3	Total	1	2	3	Total
Date Treated	8/30/98	8/30/98	8/30/98	8/30/98	8/2/98			
initial m_0 , g	3036.5	3241.0	3062.0	9339.5	16327.5			16327.5
initial n_0	605	607	614	1826	3293			3293
Date Pressurized	8/31/98	8/31/98	8/31/98	8/31/98	8/3/98			
10 Cycles	m_{10} , g	3032.0	3237.0	3060.0	9329.0	16307.0		16307.0
	$m_{4_{10}}$, g	0.0	0.0	0.0	0.0	1.5		1.5
	PML_{10}	0.148	0.123	0.065	0.112	0.116		0.116
	n_{10}	606	607	614	1827	3293		3293
	$n_{4_{10}}$	0	0	0	0	2		2
	PF_{10}	0.165	0.000	0.000	0.055	0.030		0.030
Date Pressurized	9/1/98	9/1/98	9/1/98	9/1/98	8/4/98			
20 Cycles	m_{20} , g	3024.0	3235.0	3058.0	9317.0	16289.0		16289.0
	$m_{4_{20}}$, g	4.5	0.0	0.0	4.5	2.0		2.0
	PML_{20}	0.263	0.185	0.131	0.193	0.224		0.224
	n_{20}	604	607	614	1825	3293		3293
	$n_{4_{20}}$	4	0	0	4	3		3
	PF_{20}	0.165	0.000	0.000	0.055	0.046		0.046
Date Pressurized	9/2/98	9/2/98	9/2/98	9/2/98	8/5/98			
30 Cycles	m_{30} , g	3020.0	3232.0	3054.0	9306.0	16276.0		16276.0
	$m_{4_{30}}$, g	6.0	0.5	0.0	6.5	2.0		2.0
	PML_{30}	0.346	0.262	0.261	0.289	0.303		0.303
	n_{30}	604	607	614	1825	3293		3293
	$n_{4_{30}}$	6	1	0	7	3		3
	PF_{30}	0.331	0.082	0.000	0.137	0.046		0.046
Date Pressurized	9/3/98	9/3/98	9/3/98	9/3/98	8/6/98			
40 Cycles	m_{40} , g	3018.0	3219.0	3050.0	9287.0	16262.5		16262.5
	$m_{4_{40}}$, g	6.0	4.0	0.5	10.5	2.0		2.0
	PML_{40}	0.412	0.555	0.376	0.450	0.386		0.386
	n_{40}	605	606	616	1827	3293		3293
	$n_{4_{40}}$	6	10	2	18	3		3
	PF_{40}	0.496	0.659	0.489	0.548	0.046		0.046
Date Pressurized	9/4/98	9/4/98	9/4/98	9/4/98	8/7/98			
50 Cycles	m_{50} , g	3014.5	3216.5	3044.0	9275.0	16254.5		16254.5
	$m_{4_{50}}$, g	6.5	4.5	1.0	12.0	2.0		2.0
	PML_{50}	0.510	0.617	0.555	0.562	0.435		0.435
	n_{50}	605	606	616	1827	3293		3293
	$n_{4_{50}}$	7	10	4	21	3		3
	PF_{50}	0.579	0.659	0.651	0.630	0.046		0.046
HFI	864	759	768	794	10977			10977

Source: ILDOT

Chamber psi: 1150

Size: 1/2"

Tested by: Mark Bendok

Table C.6 X-32 Daily Data Sheet

Trial #	WHFT 94				WHFT 97				
	1	2	3	Total	1	2	3	Total	
Date Treated	6/4/98	6/4/98	10/26/98	6/4/98	8/2/98	9/20/98	9/20/98	9/20/98	
initial m_0 , g	3020.0	3060.0	3206.0	9286.0	16018.0	16088.5	16140.0	48246.5	
initial n_0	586	613	549	1748	3336	2988	3063	9387	
Date Pressurized	6/5/98	6/5/98	10/27/98	6/5/98	8/3/98	9/21/98	9/21/98	9/21/98	
10 Cycles	m_{10} , g	3002.0	3040.0	3203.5	9245.5	16003.5	16070.0	16121.0	48194.5
	$m_{4_{10}}$, g	3.0	5.5	0.5	9.0	1.0	3.5	7.0	11.5
	PML_{10}	0.497	0.474	0.062	0.339	0.084	0.093	0.074	0.084
	n_{10}	586	611	549	1746	3336	2986	3059	9381
	$n_{4_{10}}$	2	7	1	10	1	4	8	13
	PF_{10}	0.171	0.245	0.091	0.172	0.015	0.000	0.000	0.005
Date Pressurized	6/6/98	6/6/98	10/28/98	6/6/98	8/4/98	9/22/98	9/22/98	9/21/98	
20 Cycles	m_{20} , g	3000.0	3033.0	3202.0	9235.0	15988.5	16058.5	16105.0	48152.0
	$m_{4_{20}}$, g	3.0	5.5	0.5	9.0	2.5	4.5	12.5	19.5
	PML_{20}	0.563	0.703	0.109	0.452	0.169	0.159	0.139	0.155
	n_{20}	586	611	549	1746	3335	2986	3059	9380
	$n_{4_{20}}$	2	7	1	10	5	5	13	23
	PF_{20}	0.171	0.245	0.091	0.172	0.045	0.017	0.082	0.048
Date Pressurized	6/7/98	6/7/98	10/29/98	6/7/98	8/5/98	9/23/98	9/23/98	9/23/98	
30 Cycles	m_{30} , g	2999.0	3029.0	3200.5	9228.5	15977.0	16050.0	16100.5	48127.5
	$m_{4_{30}}$, g	3.0	7.0	0.5	10.5	4.5	6.0	12.5	23.0
	PML_{30}	0.596	0.784	0.156	0.506	0.228	0.202	0.167	0.199
	n_{30}	586	609	549	1744	3334	2986	3059	9379
	$n_{4_{30}}$	2	8	1	11	8	7	13	28
	PF_{30}	0.171	0.000	0.091	0.086	0.060	0.050	0.082	0.064
Date Pressurized	6/8/98	6/8/98	10/30/98	6/8/98	8/6/98	9/24/98	9/24/98	9/24/98	
40 Cycles	m_{40} , g	2992.0	3021.0	3200.0	9213.0	15964.0	16038.5	16091.0	48093.5
	$m_{4_{40}}$, g	4.0	8.0	0.5	12.5	6.5	7.5	12.5	26.5
	PML_{40}	0.795	1.013	0.172	0.652	0.297	0.264	0.226	0.262
	n_{40}	585	609	549	1743	3335	2985	3059	9379
	$n_{4_{40}}$	3	9	1	13	11	9	13	33
	PF_{40}	0.085	0.082	0.091	0.086	0.135	0.050	0.082	0.091
Date Pressurized	6/9/98	6/9/98	10/31/98	6/9/98	8/7/98	9/25/98	9/25/98	9/25/98	
50 Cycles	m_{50} , g	2992.0	3021.0	3198.0	9211.0	15951.0	16025.0	16081.0	48057.0
	$m_{4_{50}}$, g	4.0	8.0	0.5	12.5	8.5	9.0	12.5	30.0
	PML_{50}	0.795	1.013	0.234	0.673	0.365	0.339	0.288	0.331
	n_{50}	585	609	549	1743	3335	2985	3059	9379
	$n_{4_{50}}$	3	9	1	13	12	10	13	35
	PF_{50}	0.085	0.082	0.091	0.086	0.150	0.067	0.082	0.101
HFI	5860	6130	5490	5827	3336	7470	6126	4941	

Source: ILDOT

Chamber psi: 1150

Size: 1/2"

Tested by: Mark Bendok

Table C.7 X-41 Daily Data Sheet

Trial #	WHFT 94				WHFT 97			
	1	2	3	Total	1	2	3	Total
Date Treated	6/4/98	6/4/98	6/4/98	6/4/98	6/21/98			
initial m_0 , g	3060.0	3040.0	3040.0	9140.0	15964.5			15964.5
initial n_0	612	610	628	1850	3099			3099
Date Pressurized	6/5/98	6/5/98	6/5/98	6/5/98	6/22/98			
10 Cycles	m_{10} , g	3045.0	3018.0	3030.0	9093.0	15932.0		15932.0
	$m_{4_{10}}$, g	4.0	2.5	1.0	7.5	10.5		10.5
	PML_{10}	0.359	0.641	0.296	0.432	0.138		0.138
	n_{10}	609	610	631	1850	3094		3094
	$n_{4_{10}}$	9	8	2	19	27		27
	PF_{10}	0.245	0.656	0.637	0.514	0.274		0.274
Date Pressurized	6/6/98	6/6/98	6/6/98	6/6/98	6/23/98			
20 Cycles	m_{20} , g	3038.0	3010.0	3021.0	9069.0	15900.0		15900.0
	$m_{4_{20}}$, g	6.0	4.5	3.0	13.5	17.5		17.5
	PML_{20}	0.523	0.839	0.526	0.629	0.294		0.294
	n_{20}	611	610	631	1852	3092		3092
	$n_{4_{20}}$	13	13	7	33	39		39
	PF_{20}	0.899	1.066	1.035	1.000	0.403		0.403
Date Pressurized	6/7/98	6/7/98	6/7/98	6/7/98	6/24/98			
30 Cycles	m_{30} , g	3034.0	3007.0	3016.0	9057.0	15883.5		15883.5
	$m_{4_{30}}$, g	8.0	5.0	5.0	18.0	21.5		21.5
	PML_{30}	0.588	0.921	0.625	0.711	0.373		0.373
	n_{30}	609	611	630	1850	3093		3093
	$n_{4_{30}}$	18	15	12	45	49		49
	PF_{30}	0.980	1.393	1.274	1.216	0.597		0.597
Date Pressurized	6/8/98	6/8/98	6/8/98	6/8/98	6/25/98			
40 Cycles	m_{40} , g	3024.0	2997.0	3005.0	9026.0	15866.5		15866.5
	$m_{4_{40}}$, g	8.5	8.0	6.5	23.0	26.0		26.0
	PML_{40}	0.899	1.151	0.938	0.996	0.451		0.451
	n_{40}	609	611	629	1849	3089		3089
	$n_{4_{40}}$	20	19	17	56	59		59
	PF_{40}	1.144	1.721	1.513	1.459	0.629		0.629
Date Pressurized	6/9/98	6/9/98	6/9/98	6/9/98	6/26/98			
50 Cycles	m_{50} , g	3022.0	2995.0	3004.0	9021.0	15842.5		15842.5
	$m_{4_{50}}$, g	10.0	10.0	7.0	27.0	31.0		31.0
	PML_{50}	0.915	1.151	0.954	1.007	0.570		0.570
	n_{50}	608	609	629	1846	3090		3090
	$n_{4_{50}}$	22	24	18	64	66		66
	PF_{50}	1.144	1.803	1.592	1.514	0.774		0.774
HF1	437	277	314	330	646			646

Source: ILDOT

Chamber psi: 1150

Size: 1/2"

Tested by: Mark Bendok

Table C.8 X-42 Daily Data Sheet

Trial #	WHFT 94				WHFT 97				
	1	2	3	Total	1	2	3	Total	
Date Treated	6/10/98	6/10/98	6/10/98	6/10/98	6/21/98	9/27/98	9/27/98	9/27/98	
initial m_0 , g	3051.0	3035.0	3043.0	9129.0	16105.0	16073.0	16071.5	48249.5	
initial n_0	626	628	582	1836	3037	2840	2948	8825	
Date Pressurized	6/11/98	6/11/98	6/11/98	6/11/98	6/22/98	9/28/98	9/28/98	9/28/98	
10 Cycles	m_{10} , g	3045.0	3031.0	3039.0	9115.0	16078.5	16047.0	16053.5	48179.0
	$m_{4_{10}}$, g	2.0	0.0	1.0	3.0	5.5	4.0	1.5	11.0
	PML_{10}	0.131	0.132	0.099	0.121	0.130	0.137	0.103	0.123
	n_{10}	625	628	582	1835	3036	2837	2948	8821
	$n_{4_{10}}$	3	0	1	4	9	7	2	18
	PF_{10}	0.080	0.000	0.086	0.054	0.115	0.018	0.034	0.057
Date Pressurized	6/12/98	6/12/98	6/12/98	6/12/98	6/23/98	9/29/98	9/29/98	9/29/98	
20 Cycles	m_{20} , g	3043.0	3029.0	3035.0	9107.0	16055.5	16025.5	16036.0	48117.0
	$m_{4_{20}}$, g	3.0	0.0	1.5	4.5	10.5	7.0	3.5	21.0
	PML_{20}	0.164	0.198	0.214	0.192	0.242	0.252	0.199	0.231
	n_{20}	627	628	582	1837	3033	2838	2950	8821
	$n_{4_{20}}$	5	0	2	7	17	16	6	39
	PF_{20}	0.559	0.000	0.172	0.245	0.148	0.211	0.170	0.176
Date Pressurized	6/13/98	6/13/98	6/13/98	6/13/98	6/24/98	9/30/98	9/30/98	9/30/98	
30 Cycles	m_{30} , g	3036.0	3024.0	3031.0	9091.0	16034.0	16019.0	16019.5	48072.5
	$m_{4_{30}}$, g	3.0	0.0	1.0	4.0	13.5	8.0	4.0	25.5
	PML_{30}	0.393	0.362	0.361	0.372	0.357	0.286	0.299	0.314
	n_{30}	627	628	582	1837	3036	2839	2950	8825
	$n_{4_{30}}$	5	0	1	6	20	19	7	46
	PF_{30}	0.559	0.000	0.086	0.218	0.296	0.299	0.187	0.261
Date Pressurized	6/14/98	6/14/98	6/14/98	6/14/98	6/25/98	10/1/98	10/1/98	10/1/98	
40 Cycles	m_{40} , g	3031.0	3020.0	3028.0	9079.0	16021.0	15997.0	16010.5	48028.5
	$m_{4_{40}}$, g	4.5	0.5	1.5	6.5	14.0	8.5	4.0	26.5
	PML_{40}	0.508	0.478	0.444	0.477	0.435	0.420	0.355	0.403
	n_{40}	626	628	582	1836	3034	2839	2951	8824
	$n_{4_{40}}$	7	1	3	11	23	22	7	52
	PF_{40}	0.559	0.080	0.258	0.300	0.280	0.352	0.220	0.283
Date Pressurized	6/15/98	6/15/98	6/15/98	6/15/98	6/26/98	10/2/98	10/2/98	10/2/98	
50 Cycles	m_{50} , g	3031.0	3018.0	3025.0	9074.0	16010.0	15985.0	16003.5	47998.5
	$m_{4_{50}}$, g	5.0	2.5	3.5	11.0	14.0	8.5	7.5	30.0
	PML_{50}	0.492	0.478	0.477	0.482	0.503	0.495	0.376	0.458
	n_{50}	626	628	582	1836	3035	2839	2952	8826
	$n_{4_{50}}$	7	4	6	17	23	22	11	56
	PF_{50}	0.559	0.318	0.515	0.463	0.313	0.352	0.322	0.329
HF1	894	1570	970	1080	1598	1420	1552	1522	

Source: ILDOT

Chamber psi: 1150

Size: 1/2"

Tested by: Mark Bendok

Table C.9 X-98 Daily Data Sheet

Trial #	WHFT 94				WHFT 97				
	1	2	3	Total	1	2	3	Total	
Date Treated	6/10/98	6/10/98	6/10/98	6/10/98	9/13/98	10/11/98	10/11/98	10/11/98	
initial m_0 , g	3010.0	3020.0	3015.0	9045.0	16071.5	15919.0	16012.0	48002.5	
initial n_0	559	541	563	1663	2855	3228	3105	9188	
Date Pressurized	6/11/98	6/11/98	6/11/98	6/11/98	9/14/98	10/12/98	10/12/98	10/12/98	
10 Cycles	m_{10} , g	3008.0	3019.0	3013.0	9040.0	16060.5	15903.5	16003.5	47967.5
	$m_{4_{10}}$, g	0.0	0.0	0.0	0.0	0.5	4.0	0.0	4.5
	PML_{10}	0.066	0.033	0.066	0.055	0.065	0.072	0.053	0.064
	n_{10}	559	541	563	1663	2855	3228	3108	9191
	$n_{4_{10}}$	0	0	0	0	1	4	0	5
	PF_{10}	0.000	0.000	0.000	0.000	0.018	0.062	0.097	0.060
Date Pressurized	6/12/98	6/12/98	6/12/98	6/12/98	9/15/98	10/13/98	10/13/98	10/13/98	
20 Cycles	m_{20} , g	3006.0	3015.0	3010.0	9031.0	16054.0	15897.0	15998.0	47949.0
	$m_{4_{20}}$, g	0.0	0.0	0.0	0.0	0.5	4.5	0.0	5.0
	PML_{20}	0.133	0.166	0.166	0.155	0.106	0.110	0.087	0.101
	n_{20}	559	541	564	1664	2856	3228	3108	9192
	$n_{4_{20}}$	0	0	0	0	1	5	0	6
	PF_{20}	0.000	0.000	0.178	0.060	0.053	0.077	0.097	0.076
Date Pressurized	6/13/98	6/13/98	6/13/98	6/13/98	9/16/98	10/14/98	10/14/98	10/14/98	
30 Cycles	m_{30} , g	3004.0	3010.0	3006.0	9020.0	16045.0	15892.5	15992.5	47930.0
	$m_{4_{30}}$, g	0.5	1.5	0.0	2.0	0.5	4.5	0.0	5.0
	PML_{30}	0.183	0.281	0.299	0.254	0.162	0.138	0.122	0.141
	n_{30}	561	541	564	1666	2857	3228	3108	9193
	$n_{4_{30}}$	2	4	0	6	2	5	0	7
	PF_{30}	0.537	0.370	0.178	0.361	0.105	0.077	0.097	0.093
Date Pressurized	6/14/98	6/14/98	6/14/98	6/14/98	9/17/98	10/15/98	10/15/98	10/15/98	
40 Cycles	m_{40} , g	3001.0	3010.0	3005.0	9016.0	16036.5	15885.0	15986.0	47907.5
	$m_{4_{40}}$, g	0.5	2.0	1.0	3.5	0.5	4.5	0.0	5.0
	PML_{40}	0.282	0.265	0.299	0.282	0.215	0.185	0.162	0.187
	n_{40}	559	541	563	1663	2856	3228	3109	9193
	$n_{4_{40}}$	2	5	2	9	3	5	0	8
	PF_{40}	0.179	0.462	0.178	0.271	0.088	0.077	0.129	0.098
Date Pressurized	6/15/98	6/15/98	6/15/98	6/15/98	9/15/98	10/16/98	10/16/98	10/16/98	
50 Cycles	m_{50} , g	3000.0	3009.0	3005.0	9014.0	16027.5	15883.0	15977.0	47887.5
	$m_{4_{50}}$, g	1.0	2.0	1.0	4.0	1.5	5.0	0.0	6.5
	PML_{50}	0.299	0.298	0.299	0.299	0.264	0.195	0.219	0.226
	n_{50}	559	541	563	1663	2858	3229	3109	9196
	$n_{4_{50}}$	3	5	2	10	5	7	0	12
	PF_{50}	0.268	0.462	0.178	0.301	0.193	0.139	0.129	0.152
HFI	1863	1082	2815	1663	2595	3587	3881	3281	

Source: ILDOT

Chamber psi: 1150

Size: 1/2"

Tested by: Mark Bendok

Table C.10 X-167 Daily Data Sheet

Trial #	WHFT 94				WHFT 97				
	1	2	3	Total	1	2	3	Total	
Date Treated	6/15/98	7/12/98	9/13/98	9/13/98	6/15/98	9/20/98	9/20/98	9/20/98	
initial m_0 , g	3293.0	3269.0	3286.0	9848.0	16000.0	16032.5	16093.5	48126.0	
initial n_0	710	672	616	1998	3429	3099	3266	9794	
Date Pressurized	6/16/98	7/13/98	9/14/98	9/14/98	6/16/98	9/21/98	9/21/98	9/21/98	
10 Cycles	m_{10} , g	3275.0	3267.0	3281.0	9823.0	15992.5	16020.5	16075.0	48088.0
	$m_{4_{10}}$, g	8.0	0.0	0.5	8.5	7.0	1.0	6.5	14.5
	PML_{10}	0.304	0.061	0.137	0.168	0.003	0.069	0.075	0.049
	n_{10}	713	672	616	2001	3434	3098	3263	9795
	$n_{4_{10}}$	20	0	1	21	8	5	12	25
	PF_{10}	1.831	0.000	0.081	0.676	0.262	0.048	0.092	0.138
Date Pressurized	6/17/98	7/14/98	9/15/98	9/15/98	6/17/98	9/22/98	9/22/98	9/22/98	
20 Cycles	m_{20} , g	3268.5	3265.0	3279.5	9813.0	15986.5	16007.0	16056.5	48050.0
	$m_{4_{20}}$, g	10.0	1.0	0.5	11.5	8.0	4.5	13.0	25.5
	PML_{20}	0.440	0.092	0.183	0.239	0.034	0.131	0.149	0.105
	n_{20}	712	672	616	2000	3434	3098	3260	9792
	$n_{4_{20}}$	25	1	1	27	10	9	20	39
	PF_{20}	2.042	0.074	0.081	0.776	0.292	0.113	0.122	0.179
Date Pressurized	6/18/98	7/15/98	9/16/98	9/16/98	6/18/98	9/23/98	9/23/98	9/23/98	
30 Cycles	m_{30} , g	3264.5	3263.0	3278.5	9806.0	15980.0	15998.5	16050.0	48028.5
	$m_{4_{30}}$, g	13.0	1.5	0.5	15.0	9.0	8.5	13.0	30.5
	PML_{30}	0.471	0.138	0.213	0.274	0.069	0.159	0.190	0.139
	n_{30}	710	672	616	1998	3435	3097	3260	9792
	$n_{4_{30}}$	28	2	1	31	13	15	20	48
	PF_{30}	1.972	0.149	0.081	0.776	0.365	0.177	0.122	0.225
Date Pressurized	6/19/98	7/16/98	9/17/98	9/17/98	6/19/98	9/24/98	9/24/98	9/24/98	
40 Cycles	m_{40} , g	3260.5	3262.0	3277.5	9800.0	15967.5	15990.5	16043.0	48001.0
	$m_{4_{40}}$, g	13.0	1.5	0.5	15.0	14.5	9.5	13.0	37.0
	PML_{40}	0.592	0.168	0.243	0.335	0.113	0.203	0.233	0.183
	n_{40}	709	672	616	1997	3433	3098	3262	9793
	$n_{4_{40}}$	29	2	1	32	20	18	20	58
	PF_{40}	1.901	0.149	0.081	0.751	0.408	0.258	0.184	0.286
Date Pressurized	6/20/98	7/17/98	9/18/98	9/18/98	6/20/98	9/25/98	9/25/98	9/25/98	
50 Cycles	m_{50} , g	3259.0	3258.0	3276.5	9793.5	15963.0	15983.5	16037.5	47984.0
	$m_{4_{50}}$, g	13.0	4.5	1.0	18.5	14.5	11.0	14.0	39.5
	PML_{50}	0.638	0.199	0.259	0.366	0.141	0.237	0.261	0.213
	n_{50}	709	672	617	1998	3434	3099	3265	9798
	$n_{4_{50}}$	29	5	3	37	20	22	24	66
	PF_{50}	1.901	0.372	0.406	0.926	0.437	0.355	0.337	0.378
HFI	263	1344	1232	540	1143	1409	1485	1324	

Source: ILDOT

Chamber psi: 1150

Size: 1/2"

Tested by: Mark Bendok

Table C.11 X-262 Daily Data Sheet

Trial #	WHFT 94				WHFT 97				
	1	2	3	Total	1	2	3	Total	
Date Treated	6/15/98	6/15/98	10/26/98	6/15/98	6/15/98	10/4/98	10/4/98	10/4/98	
initial m_0 , g	3250.0	3030.0	3186.0	9466.0	16000.0	15988.0	15904.0	47892.0	
initial n_0	607	551	601	1759	2918	2798	2869	8585	
Date Pressurized	6/16/98	6/16/98	10/27/98	6/16/98	6/16/98	10/5/98	10/5/98	10/5/98	
10 Cycles	m_{10} , g	3248.0	3030.0	3184.0	9462.0	15995.5	15974.5	15892.0	47862.0
	$m_{4_{10}}$, g	0.0	0.0	0.0	0.0	0.5	0.5	1.0	2.0
	PML_{10}	0.062	0.000	0.063	0.042	0.025	0.081	0.069	0.058
	n_{10}	607	553	601	1761	2918	2798	2869	8585
	$n_{4_{10}}$	0	0	0	0	1	1	1	3
	PF_{10}	0.000	0.363	0.000	0.114	0.017	0.018	0.017	0.017
Date Pressurized	6/17/98	6/17/98	10/28/98	6/17/98	6/17/98	10/6/98	10/6/98	10/6/98	
20 Cycles	m_{20} , g	3243.5	3028.0	3182.5	9454.0	15984.0	15971.0	15884.5	47839.5
	$m_{4_{20}}$, g	1.0	0.5	0.0	1.5	0.5	0.5	1.0	2.0
	PML_{20}	0.169	0.050	0.110	0.111	0.097	0.103	0.116	0.105
	n_{20}	609	553	601	1763	2918	2799	2869	8586
	$n_{4_{20}}$	3	1	0	4	1	1	1	3
	PF_{20}	0.577	0.454	0.000	0.341	0.017	0.054	0.017	0.029
Date Pressurized	6/18/98	6/18/98	10/29/98	6/18/98	6/18/98	10/7/98	10/7/98	10/7/98	
30 Cycles	m_{30} , g	3241.5	3026.5	3181.5	9449.5	15975.5	15963.0	15877.0	47815.5
	$m_{4_{30}}$, g	1.0	0.5	0.0	1.5	1.0	0.5	1.0	2.5
	PML_{30}	0.231	0.099	0.141	0.158	0.147	0.153	0.163	0.155
	n_{30}	609	553	602	1764	2919	2799	2869	8587
	$n_{4_{30}}$	3	1	0	4	4	1	1	6
	PF_{30}	0.577	0.454	0.166	0.398	0.103	0.054	0.017	0.058
Date Pressurized	6/19/98	6/19/98	10/30/98	6/19/98	6/19/98	10/8/98	10/8/98	10/8/98	
40 Cycles	m_{40} , g	3238.5	3025.0	3180.5	9444.0	15964.0	15959.0	15870.0	47793.0
	$m_{4_{40}}$, g	3.0	0.5	0.0	3.5	1.5	0.5	1.0	3.0
	PML_{40}	0.262	0.149	0.173	0.195	0.216	0.178	0.207	0.200
	n_{40}	608	553	602	1763	2918	2800	2869	8587
	$n_{4_{40}}$	4	1	0	5	5	1	1	7
	PF_{40}	0.494	0.454	0.166	0.370	0.086	0.089	0.017	0.064
Date Pressurized	6/20/98	6/20/98	10/31/98	6/20/98	6/20/98	10/9/98	10/9/98	10/9/98	
50 Cycles	m_{50} , g	3235.5	3023.0	3180.0	9438.5	15954.5	15954.0	15867.5	47776.0
	$m_{4_{50}}$, g	3.0	0.5	0.5	4.0	2.5	0.5	1.5	4.5
	PML_{50}	0.354	0.215	0.173	0.248	0.269	0.210	0.220	0.233
	n_{50}	608	553	603	1764	2917	2800	2871	8588
	$n_{4_{50}}$	5	1	1	7	8	2	2	12
	PF_{50}	0.577	0.454	0.416	0.483	0.103	0.107	0.105	0.105
HFI	867	1102	1202	1035	4863	4663	4782	4769	

Source: ILLDOT

Chamber psi: 1150

Size: 1/2"

Tested by: Mark Bendok

Table C.12 X-263 Daily Data Sheet

Trial #	WHFT 94				WHFT 97			
	1	2	3	Total	1	2	3	Total
Date Treated	6/21/98	6/21/98	10/26/98	6/21/98	7/26/98			
initial m_0 , g	3233.0	3299.0	3210.0	9742.0	16129.0			16129.0
initial n_0	590	615	561	1766	2933			2933
Date Pressurized	6/22/98	6/22/98	10/27/98	6/22/98	7/27/98			
10 Cycles	m_{10} , g	3230.5	3297.0	3209.0	9736.5	16119.0		16119.0
	$m_{4_{10}}$, g	0.5	0.5	0.0	1.0	1.0		1.0
	PML_{10}	0.062	0.045	0.031	0.046	0.056		0.056
	n_{10}	590	616	561	1767	2938		2938
	$n_{4_{10}}$	1	1	0	2	4		4
	PF_{10}	0.085	0.244	0.000	0.113	0.239		0.239
Date Pressurized	6/23/98	6/23/98	10/28/98	6/23/98	7/28/98			
20 Cycles	m_{20} , g	3229.5	3296.0	3208.0	9733.5	16106.5		16106.5
	$m_{4_{20}}$, g	0.5	0.5	0.0	1.0	5.5		5.5
	PML_{20}	0.093	0.076	0.062	0.077	0.105		0.105
	n_{20}	591	616	561	1768	2938		2938
	$n_{4_{20}}$	1	1	0	2	14		14
	PF_{20}	0.254	0.244	0.000	0.170	0.409		0.409
Date Pressurized	6/24/98	6/24/98	10/29/98	6/24/98	7/29/98			
30 Cycles	m_{30} , g	3228.0	3295.0	3207.5	9730.5	16095.0		16095.0
	$m_{4_{30}}$, g	0.5	0.5	0.0	1.0	10.5		10.5
	PML_{30}	0.139	0.106	0.078	0.108	0.146		0.146
	n_{30}	591	616	561	1768	2938		2938
	$n_{4_{30}}$	1	1	0	2	23		23
	PF_{30}	0.254	0.244	0.000	0.170	0.563		0.563
Date Pressurized	6/25/98	6/21/98	10/30/98	6/25/98	7/30/98			
40 Cycles	m_{40} , g	3225.5	3294.5	3207.0	9727.0	16080.0		16080.0
	$m_{4_{40}}$, g	2.5	0.5	0.5	3.5	19.5		19.5
	PML_{40}	0.155	0.121	0.078	0.118	0.183		0.183
	n_{40}	591	616	562	1769	2934		2934
	$n_{4_{40}}$	3	1	1	5	30		30
	PF_{40}	0.424	0.244	0.267	0.311	0.546		0.546
Date Pressurized	6/26/98	6/26/98	10/31/98	6/26/98	7/31/98			
50 Cycles	m_{50} , g	3224.5	3291.5	3206.0	9722.0	16071.5		16071.5
	$m_{4_{50}}$, g	2.5	2.5	0.5	5.5	22.0		22.0
	PML_{50}	0.186	0.152	0.109	0.149	0.220		0.220
	n_{50}	591	615	563	1769	2934		2934
	$n_{4_{50}}$	3	6	1	10	35		35
	PF_{50}	0.424	0.488	0.446	0.453	0.631		0.631
HFI	1180	1025	1122	1104	793			793

Source: ILDOT

Chamber psi: 1150

Size: 1/2"

Tested by: Mark Bendok

Table C.13 X-264 Daily Data Sheet

Trial #	WHFT 94				WHFT 97				
	1	2	3	Total	1	2	3	Total	
Date Treated	6/21/98	6/21/98	6/21/98	6/21/98	7/26/98	9/27/98	9/27/98	9/27/98	
initial m_0 , g	2704.5	2924.0	2779.0	8407.5	13786.0	13270.0	13086.0	40142.0	
initial n_0	685	700	700	2085	3556	3160	3033	9749	
Date Pressurized	6/22/98	6/22/98	6/22/98	6/22/98	7/27/98	9/28/98	9/28/98	9/28/98	
10 Cycles	m_{10} , g	2694.5	2910.0	2766.0	8370.5	13754.0	13234.5	13048.5	40037.0
	$m_{4_{10}}$, g	4.0	5.5	5.5	15.0	4.0	1.0	5.0	10.0
	PML_{10}	0.222	0.291	0.270	0.262	0.203	0.260	0.248	0.237
	n_{10}	684	704	698	2086	3554	3160	3033	9747
	$n_{4_{10}}$	7	10	11	28	5	2	8	15
	PF_{10}	0.365	1.286	0.500	0.719	0.014	0.032	0.132	0.056
Date Pressurized	6/23/98	6/23/98	6/23/98	6/23/98	7/28/98	9/29/98	9/29/98	9/29/98	
20 Cycles	m_{20} , g	2684.0	2890.0	2750.0	8324.0	13726.0	13203.0	13019.0	39948.0
	$m_{4_{20}}$, g	9.5	7.5	17.5	34.5	5.0	1.0	6.0	12.0
	PML_{20}	0.407	0.906	0.414	0.583	0.399	0.497	0.466	0.453
	n_{20}	682	706	699	2087	3554	3160	3033	9747
	$n_{4_{20}}$	17	16	40	73	6	2	10	18
	PF_{20}	0.803	2.000	2.714	1.847	0.028	0.032	0.165	0.072
Date Pressurized	6/24/98	6/24/98	6/24/98	6/24/98	7/29/98	9/30/98	9/30/98	9/30/98	
30 Cycles	m_{30} , g	2672.0	2865.0	2729.5	8266.5	13702.5	13194.0	12997.0	39893.5
	$m_{4_{30}}$, g	10.0	27.0	25.0	62.0	5.0	3.0	6.5	14.5
	PML_{30}	0.832	1.094	0.882	0.940	0.569	0.550	0.630	0.583
	n_{30}	683	712	697	2092	3554	3160	3033	9747
	$n_{4_{30}}$	21	55	53	129	6	7	11	24
	PF_{30}	1.241	5.643	3.357	3.429	0.028	0.111	0.181	0.103
Date Pressurized	6/25/98	6/25/98	6/25/98	6/25/98	7/30/98	10/1/98	10/1/98	10/1/98	
40 Cycles	m_{40} , g	2665.5	2856.0	2721.0	8242.5	13680.5	13174.0	12974.0	39828.5
	$m_{4_{40}}$, g	10.5	28.5	27.5	66.5	5.0	3.5	7.5	16.0
	PML_{40}	1.054	1.351	1.098	1.172	0.729	0.697	0.799	0.741
	n_{40}	684	715	697	2096	3554	3160	3033	9747
	$n_{4_{40}}$	22	60	56	138	6	8	13	27
	PF_{40}	1.460	6.429	3.571	3.837	0.028	0.127	0.214	0.118
Date Pressurized	6/26/98	6/26/98	6/26/98	6/26/98	7/31/98	10/2/98	10/2/98	10/2/98	
50 Cycles	m_{50} , g	2657.5	2845.0	2712.0	8214.5	13652.5	13155.0	12956.0	39763.5
	$m_{4_{50}}$, g	13.5	32.5	31.5	77.5	7.0	5.0	8.0	20.0
	PML_{50}	1.239	1.590	1.277	1.374	0.918	0.829	0.932	0.893
	n_{50}	685	714	697	2096	3554	3164	3034	9752
	$n_{4_{50}}$	32	68	65	165	9	11	16	36
	PF_{50}	2.336	6.857	4.214	4.484	0.070	0.301	0.297	0.215
HFI	214	73	119	111	7112	1663	1685	2321	

Source: ILDOT

Chamber psi: 1150

Size: 1/2"

Tested by: Mark Bendok

Table C.14 X-275 Daily Data Sheet

Trial #	WHFT 94				WHFT 97				
	1	2	3	Total	1	2	3	Total	
Date Treated	12/6/98	7/19/98	10/26/98	12/6/98	7/19/98	10/11/98	10/11/98	10/11/98	
initial m_0	2968.0	3209.5	3205.0	9382.5	16168.5	16015.5	16022.0	48206.0	
initial n_0	561	613	601	1775	3144	2816	2844	8804	
Date Pressurized	12/7/98	7/20/98	10/27/98	12/7/98	7/20/98	10/12/98	10/12/98	10/12/98	
10 Cycles	m_{10} , g	2964.0	3208.0	3203.0	9375.0	16151.5	15997.0	16006.0	48154.5
	$m_{4_{10}}$, g	0.0	0.0	0.0	0.0	6.0	6.5	7.0	19.5
	PML_{10}	0.135	0.047	0.062	0.080	0.068	0.075	0.056	0.066
	n_{10}	561	613	601	1775	3141	2816	2843	8800
	$n_{4_{10}}$	0	0	0	0	9	6	6	21
	PF_{10}	0.000	0.000	0.000	0.000	0.048	0.107	0.070	0.074
Date Pressurized	12/8/98	7/21/98	10/28/98	12/8/98	7/21/98	10/13/98	10/13/98	10/13/98	
20 Cycles	m_{20} , g	2960.0	3207.5	3202.0	9369.5	16144.0	15982.5	16001.5	48128.0
	$m_{4_{20}}$, g	2.5	2.0	1.0	5.5	7.5	10.5	7.5	25.5
	PML_{20}	0.185	0.000	0.062	0.080	0.105	0.140	0.081	0.109
	n_{20}	560	612	601	1773	3142	2813	2847	8802
	$n_{4_{20}}$	3	2	2	7	12	13	7	32
	PF_{20}	0.089	0.000	0.166	0.085	0.127	0.124	0.229	0.159
Date Pressurized	12/9/98	7/22/98	10/29/98	12/9/98	7/22/98	10/14/98	10/14/98	10/14/98	
30 Cycles	m_{30} , g	2956.5	3207.0	3201.0	9364.5	16135.0	15973.0	15993.5	48101.5
	$m_{4_{30}}$, g	3.5	2.0	1.0	6.5	10.0	10.5	11.0	31.5
	PML_{30}	0.270	0.016	0.094	0.123	0.145	0.200	0.109	0.151
	n_{30}	560	612	601	1773	3142	2813	2846	8801
	$n_{4_{30}}$	6	2	2	10	17	13	11	41
	PF_{30}	0.357	0.000	0.166	0.169	0.207	0.124	0.264	0.199
Date Pressurized	12/10/98	7/23/98	10/30/98	12/10/98	7/23/98	10/15/98	10/15/98	10/15/98	
40 Cycles	m_{40} , g	2952.0	3207.0	3200.0	9359.0	16127.5	15967.5	15988.0	48083.0
	$m_{4_{40}}$, g	5.5	2.0	1.5	9.0	12.5	15.5	12.5	40.5
	PML_{40}	0.354	0.016	0.109	0.155	0.176	0.203	0.134	0.171
	n_{40}	560	614	601	1775	3142	2813	2846	8801
	$n_{4_{40}}$	7	2	2	11	21	20	13	54
	PF_{40}	0.446	0.326	0.166	0.310	0.270	0.249	0.299	0.273
Date Pressurized	12/11/98	7/24/98	10/31/98	12/11/98	7/25/98	10/16/98	10/16/98	10/16/98	
50 Cycles	m_{50} , g	2949.5	3205.5	3198.5	9353.5	16118.5	15964.5	15982.5	48065.5
	$m_{4_{50}}$, g	7.0	2.0	2.0	11.0	13.0	16.0	14.5	43.5
	PML_{50}	0.387	0.062	0.140	0.192	0.229	0.219	0.156	0.201
	n_{50}	560	615	602	1777	3143	2813	2846	8802
	$n_{4_{50}}$	8	2	3	13	24	23	15	62
	PF_{50}	0.535	0.489	0.416	0.479	0.350	0.302	0.334	0.329
HFI	935	1022	1202	1044	1429	1656	1497	1518	

Source: ILDOT

Chamber psi: 1150

Size: 1/2"

Tested by: Mark Bendok

Table C.15 X-277 Daily Data Sheet

Trial #	WHFT 94				WHFT 97				
	1	2	3	Total	1	2	3	Total	
Date Treated	6/30/98	7/19/98	8/2/98	8/2/98	10/4/98	10/4/98	12/6/98	12/6/98	
initial m_0 , g	3245.0	3236.5	3215.5	9697.0	15994.5	16019.5	16063.5	48077.5	
initial n_0	583	641	655	1879	3035	2979	3056	9070	
Date Pressurized	7/1/98	7/20/98	8/3/98	8/3/98	10/5/98	10/5/98	12/7/98	12/7/98	
10 Cycles	m_{10} , g	3243.0	3232.5	3213.5	9689.0	15989.0	16011.0	16051.0	48051.0
	$m_{4_{10}}$, g	0.0	0.5	0.0	0.5	0.0	0.0	0.0	0.0
	PML_{10}	0.062	0.108	0.062	0.077	0.034	0.053	0.078	0.055
	n_{10}	584	641	655	1880	3036	2979	3056	9071
	$n_{4_{10}}$	0	1	0	1	0	0	0	0
	PF_{10}	0.172	0.078	0.000	0.080	0.033	0.000	0.000	0.011
Date Pressurized	7/2/98	7/21/98	8/4/98	8/4/98	10/6/98	10/6/98	12/8/98	12/8/98	
20 Cycles	m_{20} , g	3237.0	3226.5	3207.5	9671.0	15983.0	16002.5	16043.0	48028.5
	$m_{4_{20}}$, g	3.0	5.0	0.0	8.0	0.0	0.0	0.0	0.0
	PML_{20}	0.154	0.154	0.249	0.186	0.072	0.106	0.128	0.102
	n_{20}	586	638	655	1879	3038	2980	3056	9074
	$n_{4_{20}}$	5	6	0	11	0	0	0	0
	PF_{20}	0.943	0.000	0.000	0.293	0.099	0.034	0.000	0.044
Date Pressurized	7/3/98	7/22/98	8/5/98	8/5/98	10/7/98	10/7/98	12/9/98	12/9/98	
30 Cycles	m_{30} , g	3233.0	3225.0	3205.5	9663.5	15974.0	15993.0	16038.0	48005.0
	$m_{4_{30}}$, g	3.5	5.0	0.5	9.0	1.5	0.0	0.5	2.0
	PML_{30}	0.262	0.201	0.295	0.253	0.119	0.165	0.156	0.147
	n_{30}	586	638	655	1879	3038	2980	3057	9075
	$n_{4_{30}}$	7	6	1	14	3	0	1	4
	PF_{30}	1.115	0.000	0.076	0.373	0.148	0.034	0.049	0.077
Date Pressurized	7/4/98	7/23/98	8/6/98	8/6/98	10/8/98	10/8/98	12/10/98	12/10/98	
40 Cycles	m_{40} , g	3232.0	3223.5	3204.0	9659.5	15970.0	15991.0	16032.0	47993.0
	$m_{4_{40}}$, g	3.5	5.5	0.5	9.5	2.0	0.5	1.0	3.5
	PML_{40}	0.293	0.232	0.342	0.289	0.141	0.175	0.190	0.168
	n_{40}	586	638	656	1880	3038	2981	3057	9076
	$n_{4_{40}}$	7	7	2	16	4	1	2	7
	PF_{40}	1.115	0.078	0.305	0.479	0.165	0.084	0.065	0.105
Date Pressurized	7/5/98	7/24/98	8/7/98	8/7/98	10/9/98	10/9/98	12/11/98	12/11/98	
50 Cycles	m_{50} , g	3229.5	3222.0	3203.0	9654.5	15963.5	15990.0	16029.0	47982.5
	$m_{4_{50}}$, g	4.5	5.5	0.5	10.5	2.0	1.0	2.0	5.0
	PML_{50}	0.339	0.278	0.373	0.330	0.181	0.178	0.202	0.187
	n_{50}	586	638	656	1880	3039	2982	3058	9079
	$n_{4_{50}}$	11	7	2	20	4	3	4	11
	PF_{50}	1.458	0.078	0.305	0.585	0.198	0.151	0.131	0.160
HFI	343	6410	1638	854	2529	3310	3820	3128	

Source: ILDOT

Chamber psi: 1150

Size: 1/2"

Tested by: Mark Bendok

Table C.16 X-281 Daily Data Sheet

Trial #	WHFT 94				WHFT 97				
	1	2	3	Total	1	2	3	Total	
Date Treated	6/30/98	8/2/98	10/26/98	8/2/98	6/30/98	10/11/98	10/11/98	10/11/98	
initial m_0 , g	3295.0	3226.0	3205.0	9726.0	16156.0	16052.5	15952.5	48161.0	
initial n_0	588	613	578	1779	3030	2821	2825	8676	
Date Pressurized	7/1/98	8/3/98	10/27/98	8/3/98	7/1/98	10/12/98	10/12/98	10/12/98	
10 Cycles	m_{10} , g	3292.5	3223.0	3203.0	9718.5	16138.0	16035.0	15940.0	48113.0
	$m_{4_{10}}$, g	1.0	0.0	0.5	1.5	4.0	1.5	0.5	6.0
	PML_{10}	0.046	0.093	0.047	0.062	0.087	0.100	0.075	0.087
	n_{10}	588	613	578	1779	3029	2821	2825	8675
	$n_{4_{10}}$	1	0	1	2	5	2	1	8
	PF_{10}	0.085	0.000	0.087	0.056	0.050	0.035	0.018	0.035
Date Pressurized	7/2/98	8/4/98	10/28/98	8/4/98	7/2/98	10/13/98	10/13/98	10/13/98	
20 Cycles	m_{20} , g	3289.5	3218.0	3201.0	9708.5	16123.5	16024.5	15930.0	48078.0
	$m_{4_{20}}$, g	1.0	2.0	0.5	3.5	4.5	4.0	1.5	10.0
	PML_{20}	0.137	0.186	0.109	0.144	0.173	0.150	0.132	0.152
	n_{20}	588	613	578	1779	3030	2821	2826	8677
	$n_{4_{20}}$	1	2	1	4	6	5	2	13
	PF_{20}	0.085	0.163	0.087	0.112	0.099	0.089	0.071	0.086
Date Pressurized	7/3/98	8/5/98	10/29/98	8/5/98	7/3/98	10/14/98	10/14/98	10/14/98	
30 Cycles	m_{30} , g	3286.0	3215.5	3199.0	9700.5	16106.0	16019.0	15925.0	48050.0
	$m_{4_{30}}$, g	2.0	2.5	1.0	5.5	8.5	4.0	1.5	14.0
	PML_{30}	0.212	0.248	0.156	0.206	0.257	0.184	0.163	0.201
	n_{30}	588	613	578	1779	3030	2821	2826	8677
	$n_{4_{30}}$	2	3	2	7	9	5	2	16
	PF_{30}	0.170	0.245	0.173	0.197	0.149	0.089	0.071	0.104
Date Pressurized	7/4/98	8/6/98	10/30/98	8/6/98	7/4/98	10/15/98	10/15/98	10/15/98	
40 Cycles	m_{40} , g	3283.5	3213.0	3198.0	9694.5	16093.0	16010.0	15922.0	48025.0
	$m_{4_{40}}$, g	2.5	2.5	1.0	6.0	9.5	4.0	1.5	15.0
	PML_{40}	0.273	0.325	0.187	0.262	0.331	0.240	0.182	0.251
	n_{40}	588	613	579	1780	3030	2822	2826	8678
	$n_{4_{40}}$	4	3	2	9	11	5	2	18
	PF_{40}	0.340	0.245	0.346	0.309	0.182	0.124	0.071	0.127
Date Pressurized	7/5/98	8/7/98	10/31/98	8/7/98	7/5/98	10/16/98	10/16/98	10/16/98	
50 Cycles	m_{50} , g	3279.5	3211.0	3196.0	9686.5	16084.5	16001.5	15914.5	48000.5
	$m_{4_{50}}$, g	4.0	3.0	1.5	8.5	9.5	4.0	2.5	16.0
	PML_{50}	0.349	0.372	0.234	0.319	0.384	0.293	0.223	0.300
	n_{50}	588	614	579	1781	3030	2823	2827	8680
	$n_{4_{50}}$	7	4	3	14	11	5	4	20
	PF_{50}	0.595	0.489	0.433	0.506	0.182	0.160	0.142	0.161
HFI	840	1022	1156	988	2755	3134	3531	3099	

Source: ILDOT

Chamber psi: 1150

Size: 1/2"

Tested by: Mark Bendok

Table C.17 X-282 Daily Data Sheet

Trial #	WHFT 94				WHFT 97				
	1	2	3	Total	1	2	3	Total	
Date Treated	6/30/98	9/13/98	9/13/98	9/13/98	6/30/98	10/11/98	10/11/98	10/11/98	
initial m_0 , g	3280.0	3271.5	3282.0	9833.5	16034.5	15939.0	16049.0	48022.5	
initial n_0	627	588	565	1780	3147	2978	3052	9177	
Date Pressurized	7/1/98	9/14/98	9/14/98	9/14/98	7/1/98	10/12/98	10/12/98	10/12/98	
10 Cycles	m_{10} , g	3276.5	3269.0	3278.5	9824.0	16010.0	15928.0	16034.5	47972.5
	$m_{4_{10}}$, g	1.0	0.0	0.0	1.0	4.0	1.5	0.0	5.5
	PML_{10}	0.076	0.076	0.107	0.086	0.128	0.060	0.090	0.093
	n_{10}	627	588	565	1780	3150	2978	3055	9183
	$n_{4_{10}}$	1	0	0	1	5	3	0	8
	PF_{10}	0.080	0.000	0.000	0.028	0.175	0.050	0.098	0.109
Date Pressurized	7/2/98	9/15/98	9/15/98	9/15/98	7/2/98	10/13/98	10/13/98	10/13/98	
20 Cycles	m_{20} , g	3271.0	3269.0	3276.0	9816.0	15993.0	15920.0	16019.0	47932.0
	$m_{4_{20}}$, g	3.5	0.5	0.0	4.0	6.5	2.0	2.0	10.5
	PML_{20}	0.168	0.061	0.183	0.137	0.218	0.107	0.174	0.167
	n_{20}	626	588	566	1780	3148	2978	3055	9181
	$n_{4_{20}}$	3	1	0	4	9	4	2	15
	PF_{20}	0.080	0.085	0.177	0.112	0.175	0.067	0.131	0.125
Date Pressurized	7/3/98	9/16/98	9/16/98	9/16/98	7/3/98	10/14/98	10/14/98	10/14/98	
30 Cycles	m_{30} , g	3268.5	3268.0	3274.0	9810.5	15979.5	15916.0	16010.0	47905.5
	$m_{4_{30}}$, g	4.0	0.5	0.0	4.5	7.5	2.0	2.5	12.0
	PML_{30}	0.229	0.092	0.244	0.188	0.296	0.132	0.227	0.219
	n_{30}	626	590	566	1782	3148	2978	3055	9181
	$n_{4_{30}}$	5	1	0	6	11	4	3	18
	PF_{30}	0.239	0.425	0.177	0.281	0.207	0.067	0.147	0.142
Date Pressurized	7/4/98	9/17/98	9/17/98	9/17/98	7/4/98	10/15/98	10/15/98	10/15/98	
40 Cycles	m_{40} , g	3262.5	3266.0	3272.0	9800.5	15959.5	15902.5	16000.5	47862.5
	$m_{4_{40}}$, g	6.5	0.5	0.5	7.5	14.5	2.5	2.5	19.5
	PML_{40}	0.335	0.153	0.289	0.259	0.377	0.213	0.287	0.293
	n_{40}	627	590	566	1783	3147	2978	3055	9180
	$n_{4_{40}}$	8	1	1	10	22	6	3	31
	PF_{40}	0.638	0.425	0.265	0.449	0.350	0.101	0.147	0.202
Date Pressurized	7/5/98	9/18/98	9/18/98	9/18/98	7/5/98	10/16/98	10/16/98	10/16/98	
50 Cycles	m_{50} , g	3258.5	3262.5	3269.0	9790.0	15947.0	15894.5	15999.0	47840.5
	$m_{4_{50}}$, g	10.5	1.0	1.0	12.5	15.0	2.5	3.0	20.5
	PML_{50}	0.335	0.245	0.366	0.315	0.452	0.264	0.293	0.336
	n_{50}	626	590	566	1782	3147	2979	3055	9181
	$n_{4_{50}}$	11	1	3	15	23	6	4	33
	PF_{50}	0.718	0.425	0.442	0.534	0.365	0.134	0.164	0.223
HFI	697	1176	1130	937	1368	3723	3052	2238	

Source: ILDOT

Chamber psi: 1150

Size: 1/2"

Tested by: Mark Bendok

Table C.18 X-285 Daily Data Sheet

Trial #	WHFT 94				WHFT 97			
	1	2	3	Total	1	2	3	Total
Date Treated	6/30/98	7/26/98	12/6/98	12/6/98	7/19/98			
initial m_0 , g	3011.5	3218.0	3222.0	9451.5	16162.5			16162.5
initial n_0	690	618	604	1912	3228			3228
Date Pressurized	7/1/98	7/27/98	12/7/98	12/7/98	7/20/98			
10 Cycles	m_{10} , g	3009.5	3215.0	3213.5	9438.0	16149.0		16149.0
	$m_{4_{10}}$, g	0.0	0.0	0.0	0.0	2.5		2.5
	PML_{10}	0.066	0.093	0.264	0.143	0.068		0.068
	n_{10}	690	618	604	1912	3228		3228
	$n_{4_{10}}$	0	0	0	0	3		3
	PF_{10}	0.000	0.000	0.000	0.000	0.046		0.046
Date Pressurized	7/2/98	7/28/98	12/8/98	12/8/98	7/21/98			
20 Cycles	m_{20} , g	3007.5	3213.0	3210.5	9431.0	16139.0		16139.0
	$m_{4_{20}}$, g	0.5	0.0	0.0	0.5	2.5		2.5
	PML_{20}	0.116	0.155	0.357	0.212	0.130		0.130
	n_{20}	690	618	604	1912	3228		3228
	$n_{4_{20}}$	1	0	0	1	3		3
	PF_{20}	0.072	0.000	0.000	0.026	0.046		0.046
Date Pressurized	7/3/98	7/29/98	12/9/98	12/9/98	7/22/98			
30 Cycles	m_{30} , g	3006.0	3211.5	3209.0	9426.5	16130.0		16130.0
	$m_{4_{30}}$, g	0.5	0.0	0.0	0.5	2.5		2.5
	PML_{30}	0.166	0.202	0.403	0.259	0.186		0.186
	n_{30}	690	618	604	1912	3228		3228
	$n_{4_{30}}$	1	0	0	1	3		3
	PF_{30}	0.072	0.000	0.000	0.026	0.046		0.046
Date Pressurized	7/4/98	7/30/98	12/10/98	12/10/98	7/23/98			
40 Cycles	m_{40} , g	3005.0	3209.5	3207.5	9422.0	16121.0		16121.0
	$m_{4_{40}}$, g	0.5	0.0	0.0	0.5	2.5		2.5
	PML_{40}	0.199	0.264	0.450	0.307	0.241		0.241
	n_{40}	690	618	605	1913	3229		3229
	$n_{4_{40}}$	1	0	0	1	3		3
	PF_{40}	0.072	0.000	0.166	0.078	0.077		0.077
Date Pressurized	7/5/98	7/31/98	12/11/98	12/11/98	7/24/98			
50 Cycles	m_{50} , g	3004.0	3208.0	3206.0	9418.0	16112.5		16112.5
	$m_{4_{50}}$, g	0.5	1.0	0.5	2.0	3.5		3.5
	PML_{50}	0.232	0.280	0.481	0.333	0.288		0.288
	n_{50}	690	618	604	1912	3229		3229
	$n_{4_{50}}$	1	1	1	3	5		5
	PF_{50}	0.072	0.081	0.083	0.078	0.108		0.108
HFI	6900	6180	6040	6373	4611			4611

Source: ILDOT

Chamber psi: 1150

Size: 1/2"

Tested by: Mark Bendok

Table C.19 X-290 Daily Data Sheet

Trial #	WHFT 94				WHFT 97			
	1	2	3	Total	1	2	3	Total
Date Treated	6/30/98	7/12/98	12/6/98	12/6/98	9/27/98	9/27/98		9/27/98
initial m_0 , g	3051.5	3178.5	3199.0	9429.0	15628.0	15809.0		31437.0
initial n_0	679	700	642	2021	3388	3422		6810
Date Pressurized	7/1/98	7/13/98	12/7/98	12/7/98	9/28/98	9/28/98		
10 Cycles	m_{10} , g	3048.0	3173.5	3194.5	9416.0	15612.5	15794.5	31407.0
	$m_{4_{10}}$, g	1.5	2.0	0.0	3.5	5.5	2.5	8.0
	PML_{10}	0.066	0.094	0.141	0.101	0.064	0.076	0.070
	n_{10}	679	699	642	2020	3386	3422	6808
	$n_{4_{10}}$	1	2	0	3	7	5	12
	PF_{10}	0.074	0.000	0.000	0.025	0.044	0.073	0.059
Date Pressurized	7/2/98	7/14/98	12/8/98	12/8/98	9/29/98	9/29/98		
20 Cycles	m_{20} , g	3045.5	3170.5	3191.5	9407.5	15594.5	15783.5	31378.0
	$m_{4_{20}}$, g	2.0	3.0	0.5	5.5	15.0	5.5	20.5
	PML_{20}	0.131	0.157	0.219	0.170	0.118	0.127	0.122
	n_{20}	679	700	642	2021	3385	3422	6807
	$n_{4_{20}}$	2	3	1	6	18	11	29
	PF_{20}	0.147	0.214	0.078	0.148	0.177	0.161	0.169
Date Pressurized	7/3/98	7/15/98	12/9/98	12/9/98	9/30/98	9/30/98		
30 Cycles	m_{30} , g	3044.0	3167.5	3189.5	9401.0	15582.0	15779.0	31361.0
	$m_{4_{30}}$, g	2.0	5.0	0.5	7.5	18.5	9.0	27.5
	PML_{30}	0.180	0.189	0.281	0.217	0.176	0.133	0.154
	n_{30}	679	699	642	2020	3384	3422	6806
	$n_{4_{30}}$	2	6	1	9	26	16	42
	PF_{30}	0.147	0.286	0.078	0.173	0.266	0.234	0.250
Date Pressurized	7/4/98	7/16/98	12/10/98	12/10/98	10/1/98	10/1/98		
40 Cycles	m_{40} , g	3042.5	3166.0	3187.0	9395.5	15572.0	15767.5	31339.5
	$m_{4_{40}}$, g	2.5	5.0	1.0	8.5	21.0	9.0	30.0
	PML_{40}	0.213	0.236	0.344	0.265	0.224	0.206	0.215
	n_{40}	679	699	642	2020	3384	3422	6806
	$n_{4_{40}}$	3	6	2	11	29	16	45
	PF_{40}	0.221	0.286	0.156	0.223	0.310	0.234	0.272
Date Pressurized	7/5/98	7/17/98	12/11/98	12/11/98	10/2/98	10/2/98		
50 Cycles	m_{50} , g	3041.0	3163.0	3183.5	9387.5	15555.5	15764.0	31319.5
	$m_{4_{50}}$, g	2.5	6.0	1.5	10.0	28.0	9.0	37.0
	PML_{50}	0.262	0.299	0.438	0.334	0.285	0.228	0.256
	n_{50}	679	698	642	2019	3380	3422	6802
	$n_{4_{50}}$	3	7	3	13	35	16	51
	PF_{50}	0.221	0.214	0.234	0.223	0.280	0.234	0.257
HFI	2263	2333	2140	2246	1783	2139		1946

Source: ILDOT

Chamber psi: 1150

Size: 1/2"

Tested by: Mark Bendok

Table C.20 X-305 Daily Data Sheet

Trial #	WHFT 94				WHFT 97				
	1	2	3	Total	1	2	3	Total	
Date Treated	6/30/98	7/26/98	9/13/98	9/13/98	7/26/98	9/27/98	9/27/98	9/27/98	
initial m_0 , g	3190.0	3246.5	3273.5	9710.0	16065.5	16025.5	16054.0	48145.0	
initial n_0	614	634	560	1808	3138	2775	2919	8832	
Date Pressurized	7/1/98	7/27/98	9/14/98	9/14/98	7/27/98	9/28/98	9/28/98	9/28/98	
10 Cycles	m_{10} , g	3185.0	3244.5	3270.0	9699.5	16053.0	16011.5	16038.0	48102.5
	$m_{4_{10}}$, g	2.0	0.0	1.5	3.5	4.5	2.0	5.0	11.5
	PML_{10}	0.094	0.062	0.061	0.072	0.050	0.075	0.069	0.064
	n_{10}	614	634	560	1808	3138	2773	2919	8830
	$n_{4_{10}}$	1	0	1	2	5	4	6	15
	PF_{10}	0.081	0.000	0.089	0.055	0.080	0.000	0.103	0.062
Date Pressurized	7/2/98	7/28/98	9/15/98	9/15/98	7/28/98	9/29/98	9/29/98	9/29/98	
20 Cycles	m_{20} , g	3181.0	3241.5	3262.0	9684.5	16034.0	16003.0	16026.5	48063.5
	$m_{4_{20}}$, g	3.5	0.5	2.0	6.0	13.0	2.5	7.5	23.0
	PML_{20}	0.172	0.139	0.290	0.201	0.115	0.125	0.125	0.122
	n_{20}	613	634	559	1806	3132	2773	2919	8824
	$n_{4_{20}}$	2	1	3	6	12	5	10	27
	PF_{20}	0.000	0.079	0.089	0.055	0.000	0.018	0.171	0.062
Date Pressurized	7/3/98	7/29/98	9/16/98	9/16/98	7/29/98	9/30/98	9/30/98	9/30/98	
30 Cycles	m_{30} , g	3179.0	3240.0	3261.0	9680.0	16022.5	15996.5	16016.0	48035.0
	$m_{4_{30}}$, g	4.0	0.5	2.0	6.5	15.5	3.5	9.0	28.0
	PML_{30}	0.219	0.185	0.321	0.242	0.171	0.159	0.181	0.170
	n_{30}	613	634	559	1806	3133	2773	2919	8825
	$n_{4_{30}}$	3	1	3	7	15	8	12	35
	PF_{30}	0.081	0.079	0.089	0.083	0.080	0.072	0.206	0.119
Date Pressurized	7/4/98	7/30/98	9/17/98	9/17/98	7/30/98	10/1/98	10/1/98	10/1/98	
40 Cycles	m_{40} , g	3179.0	3238.0	3260.0	9677.0	16014.5	15988.5	16008.0	48011.0
	$m_{4_{40}}$, g	5.0	0.5	2.0	7.5	16.0	5.5	10.5	32.0
	PML_{40}	0.188	0.246	0.351	0.263	0.218	0.197	0.221	0.212
	n_{40}	613	634	559	1806	3133	2773	2918	8824
	$n_{4_{40}}$	5	2	3	10	16	10	14	40
	PF_{40}	0.244	0.158	0.089	0.166	0.096	0.108	0.206	0.136
Date Pressurized	7/5/98	7/31/98	9/18/98	9/18/98	7/31/98	10/2/98	10/2/98	10/2/98	
50 Cycles	m_{50} , g	3179.0	3236.5	3258.0	9673.5	16005.5	15975.5	15999.5	47980.5
	$m_{4_{50}}$, g	5.0	0.5	4.0	9.5	17.0	8.0	11.5	36.5
	PML_{50}	0.188	0.293	0.351	0.278	0.268	0.262	0.268	0.266
	n_{50}	613	634	558	1805	3133	2772	2916	8821
	$n_{4_{50}}$	5	2	7	14	18	14	17	49
	PF_{50}	0.244	0.158	0.268	0.221	0.127	0.144	0.188	0.153
HFI	2047	3170	1867	2260	3923	3469	2654	3271	

Source: ILDOT

Chamber psi: 1150

Size: 1/2"

Tested by: Mark Bendok

Table C.21 X-309 Daily Data Sheet

Trial #	WHFT 94				WHFT 97				
	1	2	3	Total	1	2	3	Total	
Date Treated	6/30/98	8/2/98	10/26/98	8/2/98	6/30/98	10/4/98	10/4/98	10/4/98	
initial m_0 , g	2846.5	3258.5	3204.0	9309.0	16162.0	15894.0	15980.0	48036.0	
initial n_0	680	688	654	2022	3299	3044	3069	9412	
Date Pressurized	7/1/98	8/3/98	10/27/98	8/3/98	7/1/98	10/5/98	10/5/98	10/5/98	
10 Cycles	m_{10} , g	2841.5	3253.5	3202.0	9297.0	16146.5	15878.0	15975.0	47999.5
	$m_{4_{10}}$, g	2.0	3.0	0.0	5.0	2.5	5.5	2.0	10.0
	PML_{10}	0.105	0.061	0.062	0.075	0.080	0.066	0.019	0.055
	n_{10}	680	688	654	2022	3298	3043	3069	9410
	$n_{4_{10}}$	1	2	0	3	3	5	2	10
	PF_{10}	0.074	0.145	0.000	0.074	0.015	0.049	0.033	0.032
Date Pressurized	7/2/98	8/4/98	10/28/98	8/4/98	7/2/98	10/6/98	10/6/98	10/6/98	
20 Cycles	m_{20} , g	2840.0	3249.5	3201.0	9290.5	16135.5	15872.5	15968.0	47976.0
	$m_{4_{20}}$, g	2.0	4.5	0.0	6.5	4.5	5.5	2.0	12.0
	PML_{20}	0.158	0.138	0.094	0.129	0.136	0.101	0.063	0.100
	n_{20}	680	687	654	2021	3298	3043	3069	9410
	$n_{4_{20}}$	1	3	0	4	6	5	2	13
	PF_{20}	0.074	0.073	0.000	0.049	0.061	0.049	0.033	0.048
Date Pressurized	7/3/98	8/5/98	10/29/98	8/5/98	7/3/98	10/7/98	10/7/98	10/7/98	
30 Cycles	m_{30} , g	2838.5	3247.5	3199.5	9285.5	16119.5	15865.0	15961.5	47946.0
	$m_{4_{30}}$, g	2.0	4.5	0.0	6.5	6.5	6.5	2.0	15.0
	PML_{30}	0.211	0.199	0.140	0.183	0.223	0.142	0.103	0.156
	n_{30}	680	687	654	2021	3295	3042	3069	9406
	$n_{4_{30}}$	1	3	0	4	8	8	2	18
	PF_{30}	0.074	0.073	0.000	0.049	0.000	0.066	0.033	0.032
Date Pressurized	7/4/98	8/6/98	10/30/98	8/6/98	7/4/98	10/8/98	10/8/98	10/8/98	
40 Cycles	m_{40} , g	2834.0	3244.5	3198.5	9277.0	16111.5	15855.5	15954.0	47921.0
	$m_{4_{40}}$, g	5.0	6.0	0.0	11.0	8.0	7.5	3.0	18.5
	PML_{40}	0.263	0.246	0.172	0.226	0.263	0.195	0.144	0.201
	n_{40}	679	686	654	2019	3295	3042	3068	9405
	$n_{4_{40}}$	3	4	0	7	10	9	4	23
	PF_{40}	0.074	0.000	0.000	0.025	0.030	0.082	0.033	0.048
Date Pressurized	7/5/98	8/7/98	10/31/98	8/7/98	7/5/98	10/9/98	10/9/98	10/9/98	
50 Cycles	m_{50} , g	2833.0	3241.0	3197.0	9271.0	16103.5	15853.0	15944.0	47900.5
	$m_{4_{50}}$, g	5.0	7.5	0.5	13.0	8.5	7.5	4.5	20.5
	PML_{50}	0.299	0.307	0.203	0.269	0.309	0.211	0.197	0.239
	n_{50}	679	686	654	2019	3296	3042	3068	9406
	$n_{4_{50}}$	3	5	1	9	11	9	7	27
	PF_{50}	0.074	0.073	0.076	0.074	0.076	0.082	0.081	0.080
HFI	6800	6880	6540	6740	6598	6088	6138	6275	

Source: ILDOT

Chamber psi: 1150

Size: 1/2"

Tested by: Mark Bendok

